von KARMAN INSTITUTE FOR FLUID DYNAMICS

September 26-27, 2016 – Measurement, simulation and control of subsonic and supersonic jet noise

Subsonic and supersonic jet noise

Christophe Bailly, Christophe Bogey & Thomas Castelain

Université de Lyon, Ecole Centrale de Lyon & LMFA - UMR CNRS 5509

http://acoustique.ec-lyon.fr

Introduction

Jet mixing noise

- Experimental observations
- Mean flow effects
- Steady CFD & statistical models
- Direct computation of jet mixing noise
- Installation effects

Supersonic jet noise

- Experimental observations
- Mach waves
- Broadband shock-associated noise (BBSAN) & Screech

Concluding remarks

- Jet noise reduction

First jet flight with fare-paying passengers

- **De Havilland DH 106 Comet 1 G-ALYP**

  2 May 1952 leaving London to Johannesburg

Heathrow – British Overseas Airways Corporation (BOAC)

http://www.bamuseum.com/

- By way of Rome, Beirut, Khartoum, Entebbe & Livingston

5 stops, 36 passengers, return fare 315 £, 6663-mile journey of 23 hours 33' (about 33 hours with a piston-engine)

BOAC - Handley Page Hermes 4 G-ALDI

- De Havilland DH 106 Comet 1

- Note received by a predecessor of United Air Lines in 1926 !

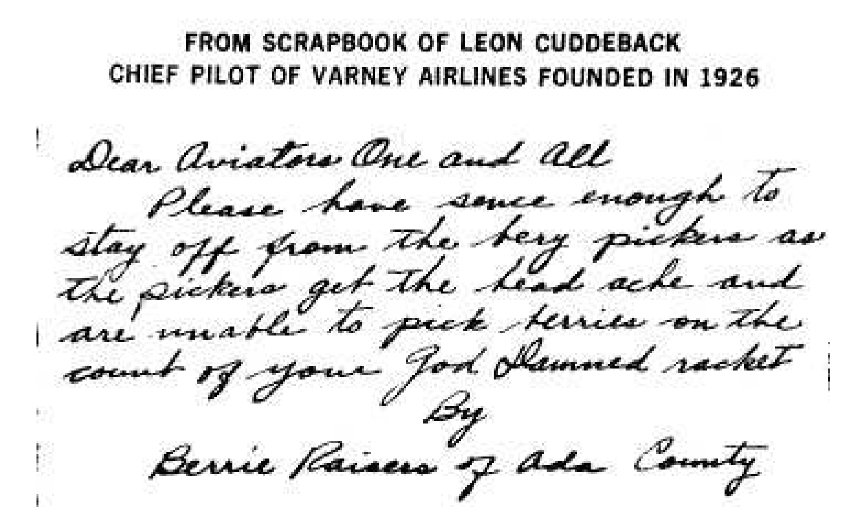
FROM SCRAPBOOK OF LEON CUDDEBACK
CHIEF PILOT OF VARNEY AIRLINES FOUNDED IN 1926

Dear Aviators One and All
Please have sence enough to
stay off from the bery pickers as
the pickers get the head ache and
are unable to pick berries on the
count of your God Damned racket
By
Berrie Raisers of Ada County

Dear Aviators One and All,
Please have sence enough to stay off from over the berry pickers as the pickers get the headhache and are unable to pick berries on the count of yours God damned racket,
by Berrie Raisers of Ada Country (vicinity Boise, Idaho)

- **2013 Top 10 world airports** (Airports Council International)

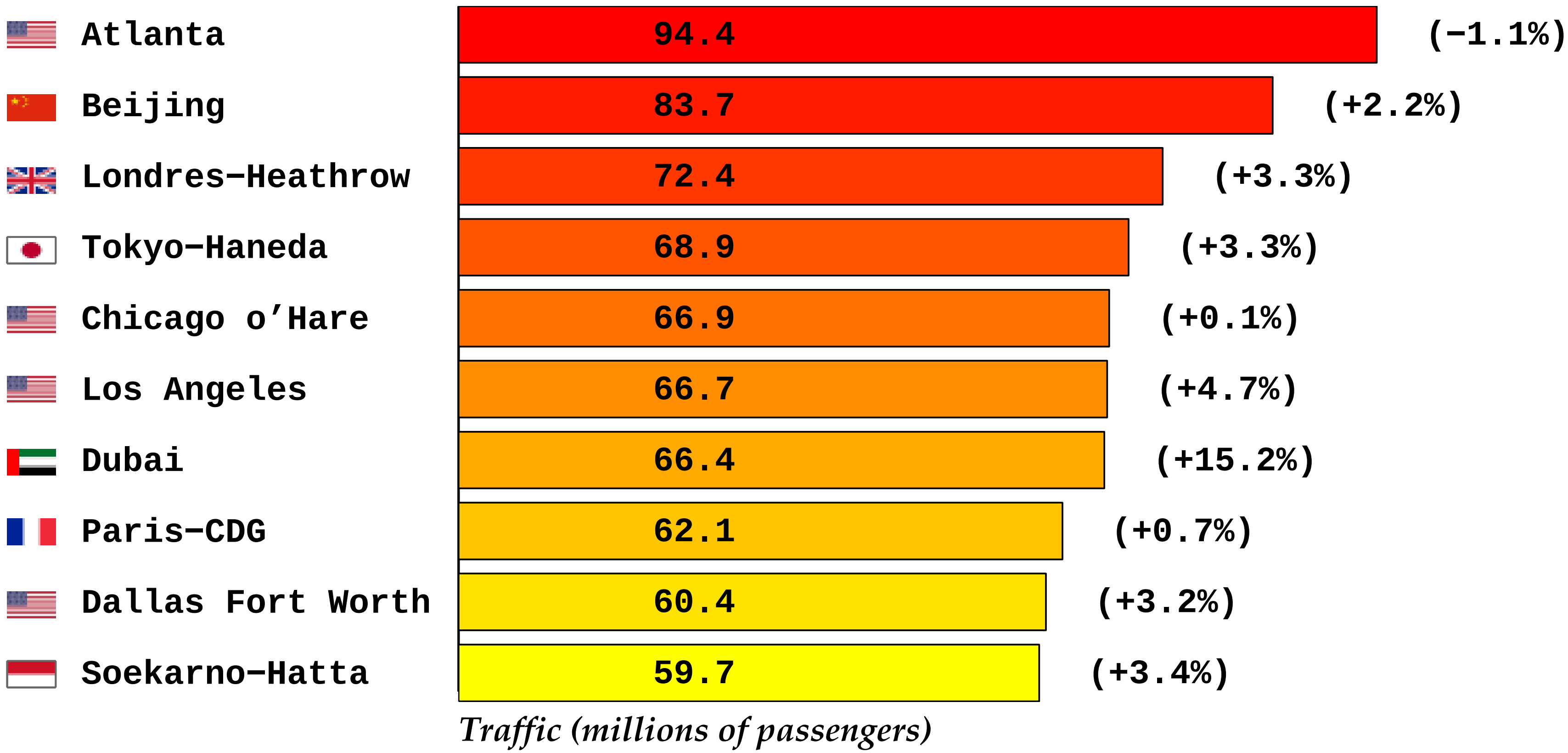

long-term traffic forecasts predict that the number of passengers will double in the next 15 years

AirTraffic Worldwide 2008
http://radar.zhaw.ch/

Roissy-CDG versus Orly

1974, 23 km from Paris

$\sim$ 1952 for civil, 14 km from Paris

Aircraft noise is a major inhibitor of the growth of air transport
(airports in key locations are operating at full capacity)

Traffic growth must be compensated for by quieter aircrafts

- Three noise certification reference points

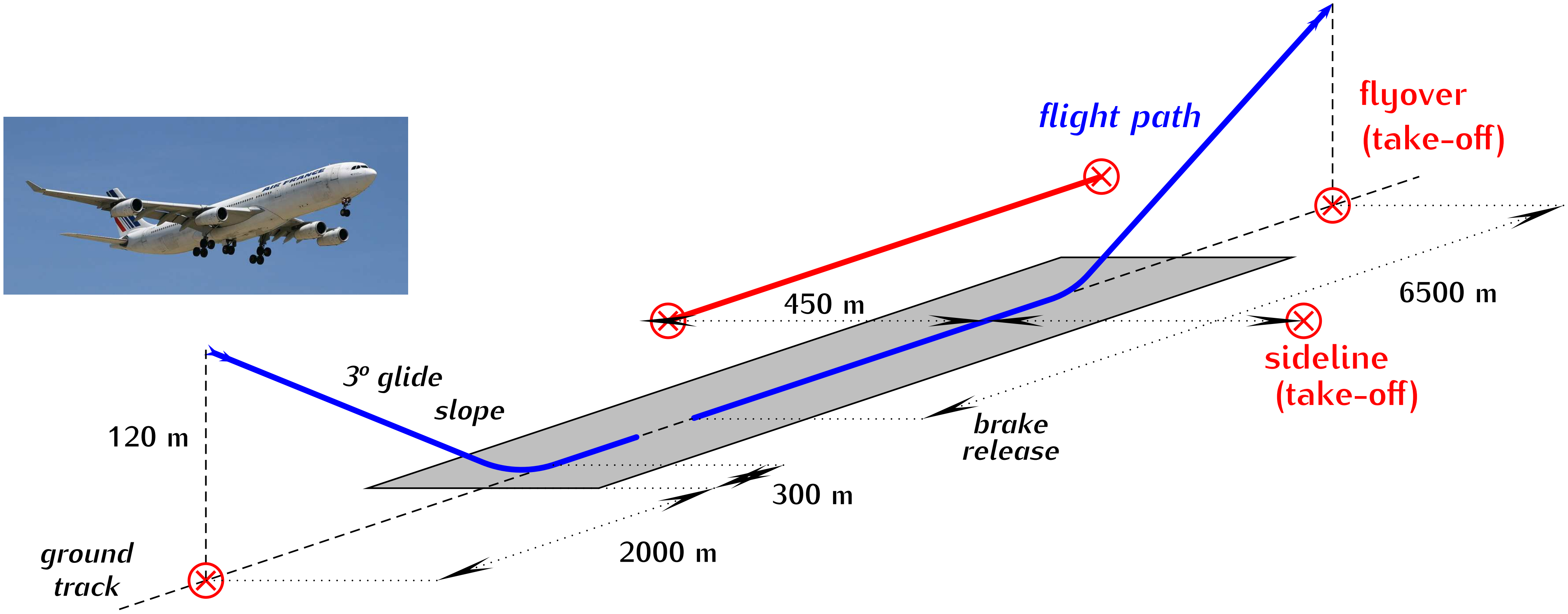

Sideline noise level

(Federal Aviation Administration FAA-AC-36-1H & FAA-AC-36-2H)

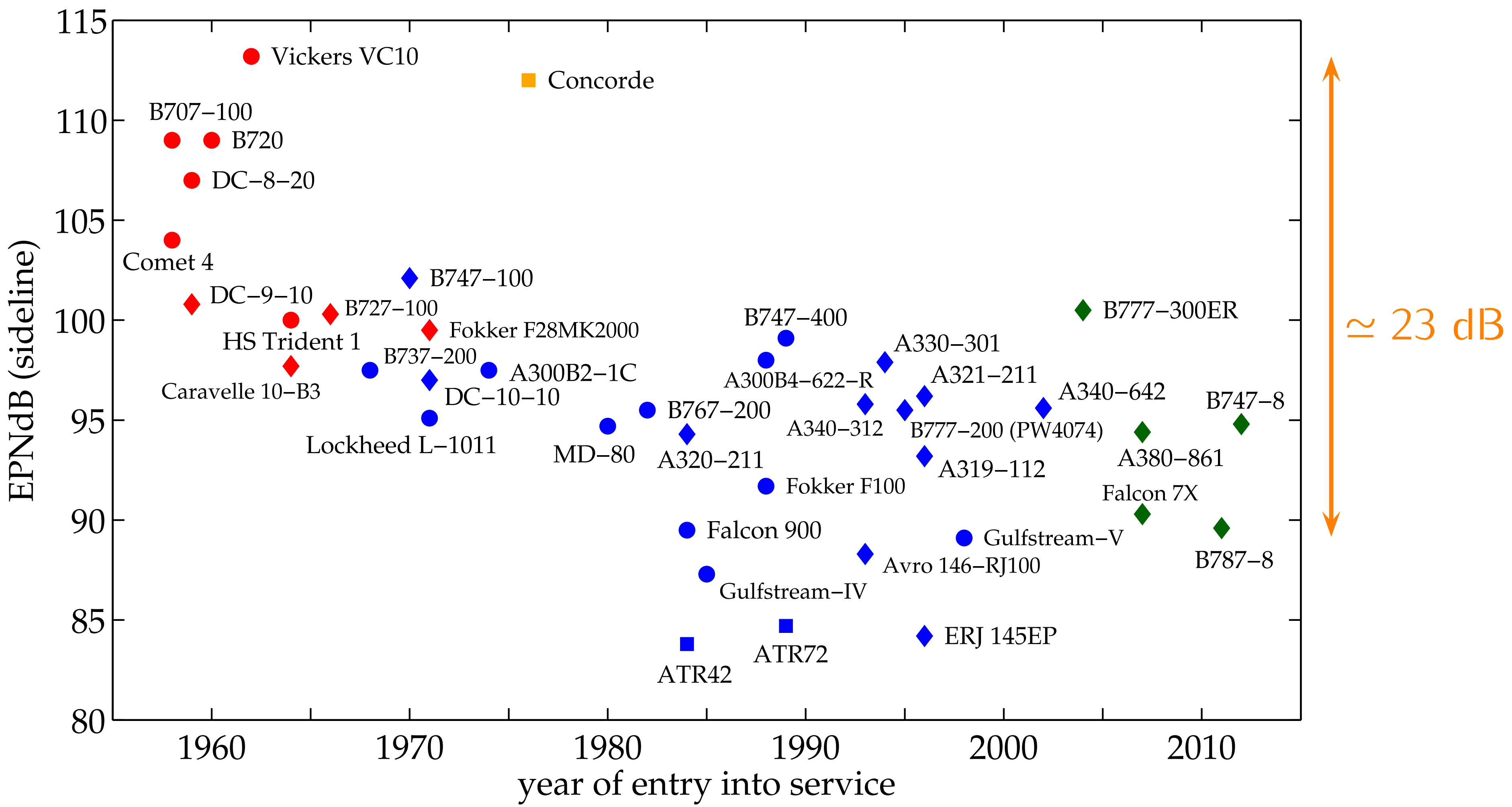

- **Sideline noise level (normalized by thrust, $T = 10^5$ lbs)**
  (Federal Aviation Administration FAA-AC-36-1H & FAA-AC-36-2H)

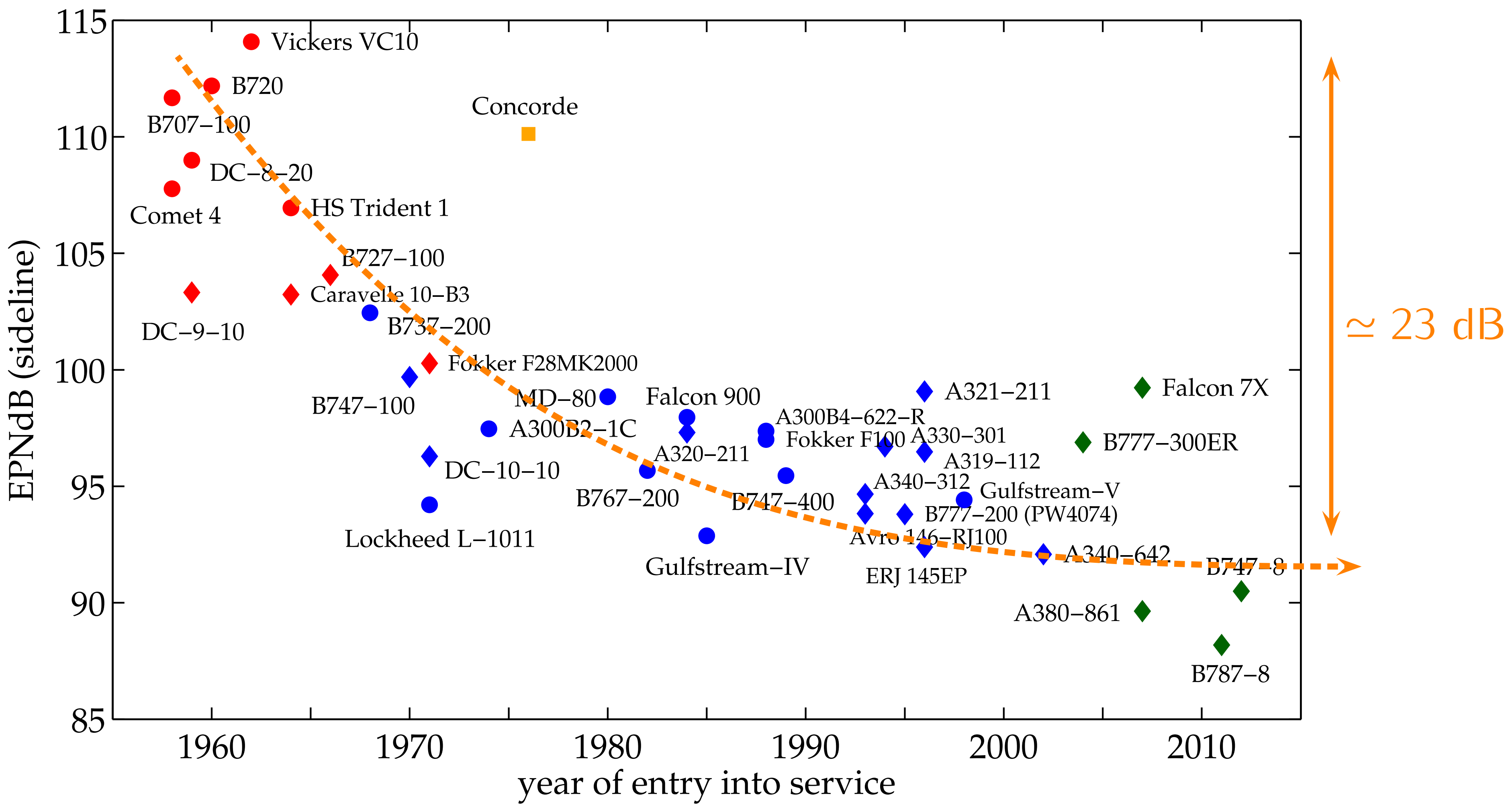

- **Engine Alliance GP7200** (A380, BPR = 8.7, $D_{\text{fan}} = 2.95$ m)

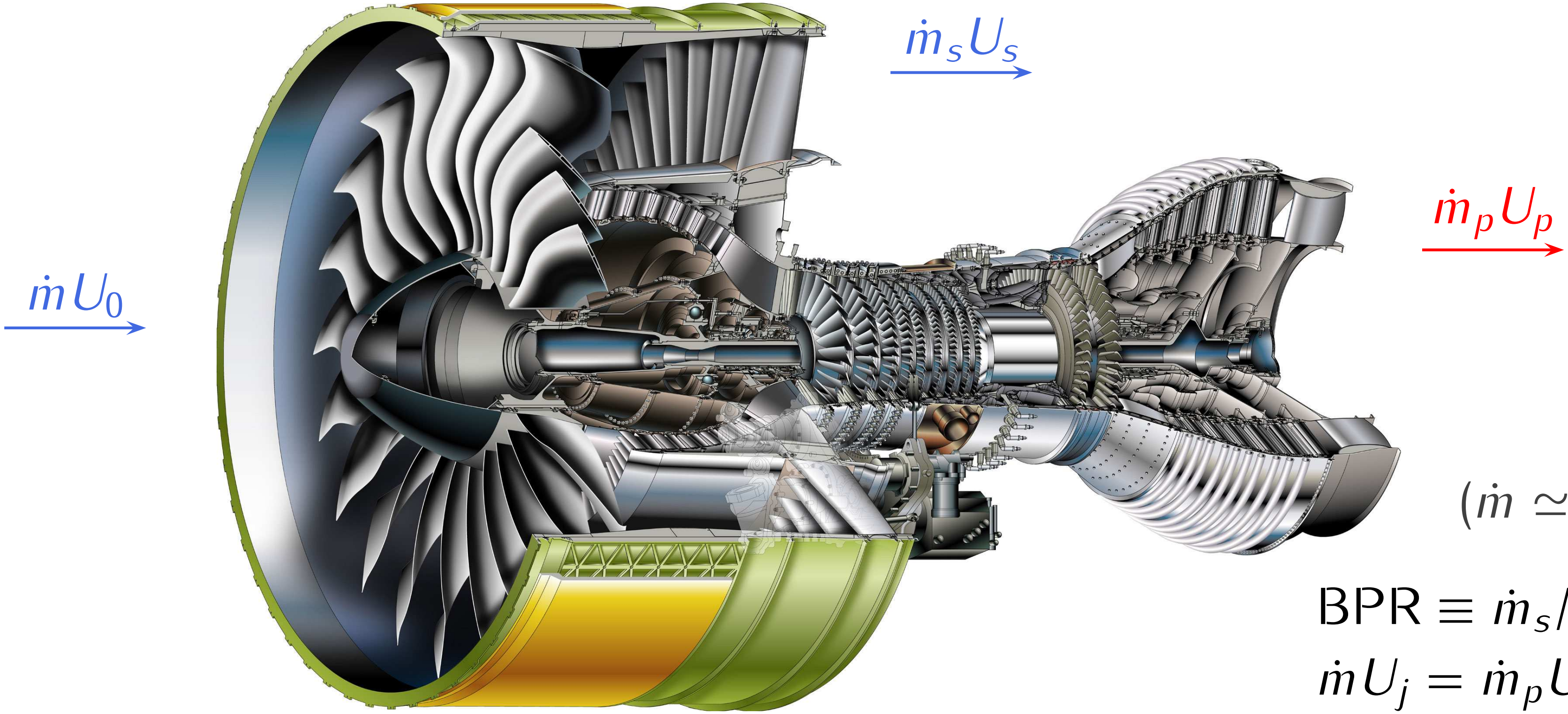

$(\dot{m} \simeq \dot{m}_p + \dot{m}_s)$

$$\text{BPR} \equiv \dot{m}_s / \dot{m}_p$$
$$\dot{m} U_j = \dot{m}_p U_p + \dot{m}_s U_s$$
$$\delta U = U_j - U_0$$

Thrust $T = \dot{m}\,\delta U$ Propulsive efficiency $\eta_p = \dfrac{1}{1 + \delta U/(2U_0)}$

$\eta_p \nearrow \quad \Longrightarrow \quad \delta U \searrow \quad \Longrightarrow \quad \dot{m}_s, \text{BPR} \nearrow$

Jet mixing noise
(subsonic convection velocity)

- Reynolds number $Re_D = u_j D/\nu$

Prasad & Sreenivasan (1989)
$Re_D \simeq 4000$

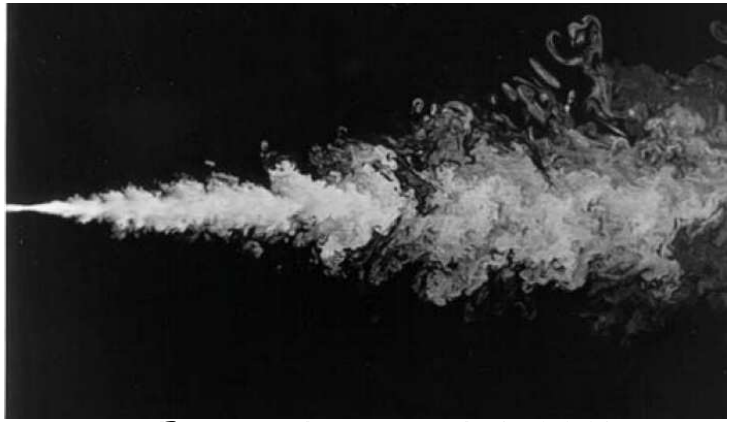

Dimotakis *et al.* (1983)
$Re_D \simeq 10^4$

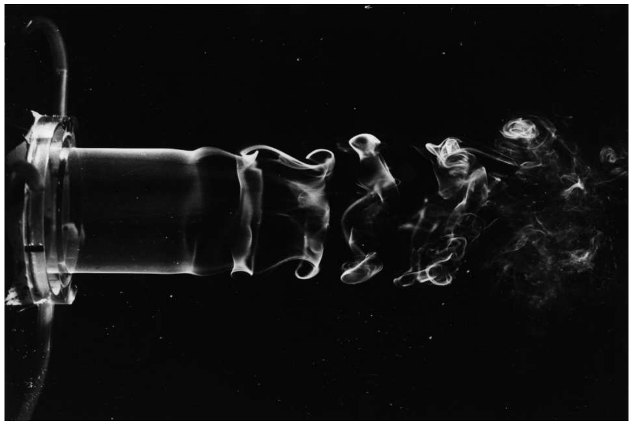

Kurima, Kasagi & Hirata (1983)
$Re_D \simeq 5.6 \times 10^3$

Ayrault, Balint & Schon (1981)
$Re_D \simeq 1.1 \times 10^4$

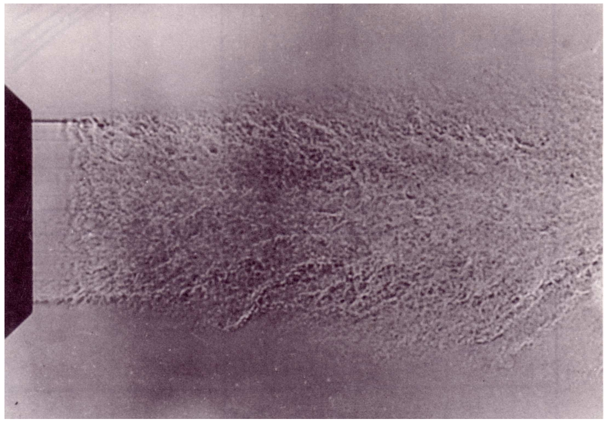

Mollo-Christensen (1963)
$Re_D = 4.6 \times 10^5$

Von Braun (1912 - 1977) / Saturn V

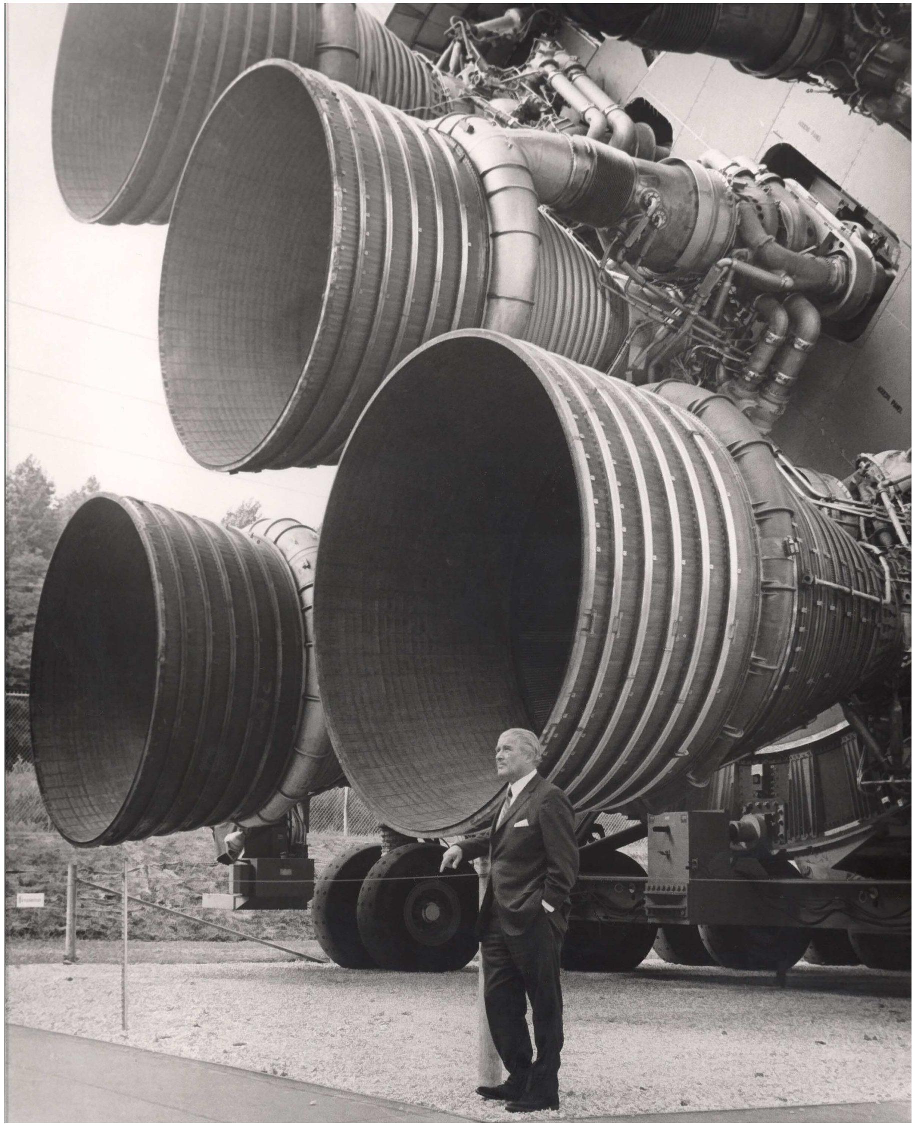

- Acoustic Mach number M_a

$$M_a = \frac{U_j}{c_\infty} \qquad \text{noise} \propto M_a^n$$

- Reynolds number Re_D

$$\mathrm{Re}_D = \frac{U_j D}{\nu} = \frac{D^2/\nu}{D/U_j} \sim \frac{\text{viscous time}}{\text{convective time}}$$

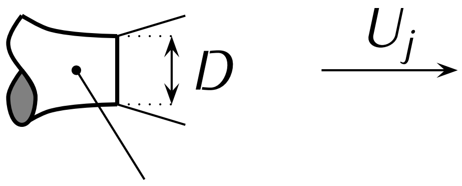

- Strouhal number St

$$St = \frac{fD}{U_j} = \frac{f}{U_j/D} \qquad \text{non-dimension frequency}$$

- **Initial conditions at the nozzle exit**

(visualizations by T. Castelain & B. André, ECL)

$\mathrm{Re}_D \sim 3 \times 10^7$

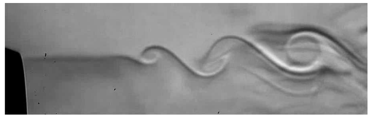

$\mathrm{Re}_D \sim 3.3 \times 10^4$

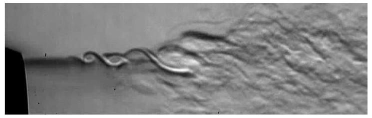

$\mathrm{Re}_D \sim 1.2 \times 10^5$

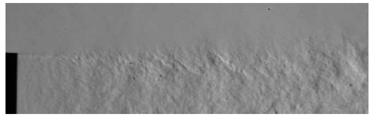

$\mathrm{Re}_D \sim 8.7 \times 10^5$

nominally laminar
$u'_e/U_j \sim 1\%$

nominally turbulent
$u'_e/U_j \sim 10\%$

fully laminar
$u'_e/U_j < 1\%$

transitional jets

fully turbulent

Re_D

$\mathrm{Re}_D \sim 10^5$
$(\mathrm{Re}_{\delta_\theta} \simeq 300)$

$\mathrm{Re}_D \sim 3 \times 10^5$

$$\mathrm{Re}_D = U_j D/\nu \qquad \mathrm{Re}_{\delta_\theta} = U_j \delta_\theta/\nu \qquad \sigma_{u_e} = u'_e/U_j$$

Sound levels

At standard conditions ($T = 20^{\circ}$C, atmospheric pressure),
$\rho_\infty = 1.21$ kg.m^{-3}, $c_\infty = 343$ m.s^{-1}, $Z_\infty = \rho_\infty c_\infty = 415$ rayls

- Sound Pressure Level (SPL) in a 1 Hz frequency band centered at f is called the spectral density $S_{pp}(f)$,

$$p_{\mathrm{rms}}^2 = \overline{p'} = \int_0^\infty S_{pp}(f)df \qquad \mathrm{SPL\ (dB)} = 20\log_{10}(p_{\mathrm{rms}}/p_{\mathrm{ref}})$$

$$\mathrm{PSD\ (dB/Hz)} = 10\log_{10}(S_{pp}(f)/p_{\mathrm{ref}}^2)$$

- The average SPL in a band with bandwidth Δf is called the Pressure Band Level (PBL), PSD (dB/Hz) $=$ PBL $- 10\log_{10}(\Delta f)$

- PSD in dB per Strouhal, PSD (dB/St) $=$ PSD (dB/Hz) $+ 10\log_{10}(U_j/D)$

- **Experimental directivity** $M = 0.9$ $T_j/T_\infty = 1$ $r/D = 53$

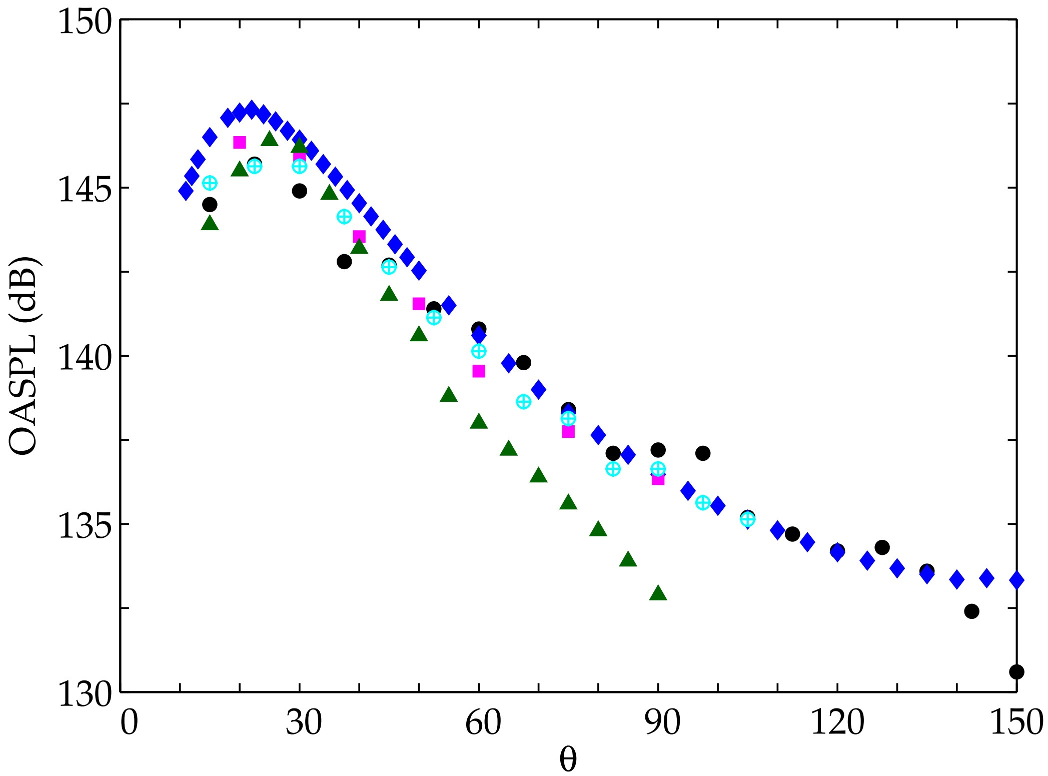

◆ Barré & Fleury (ECLyon, 2003) $\mathrm{Re}_D = 7.8 \times 10^5$

▲ Stromberg *et al.* (1980) $\mathrm{Re}_D = 3600$

⊕ Lush (1971) $\mathrm{Re}_D = 5 \times 10^5$

■ Mollo-Christensen *et al.* (1964) $\mathrm{Re}_D = 5.4 \times 10^5$

● Tanna (1976) $\mathrm{Re}_D = 10^6$

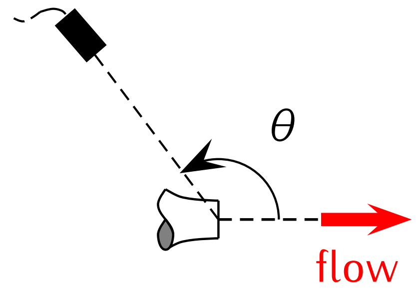

Experiments in the high-speed anechoic wind-tunnel of ECL

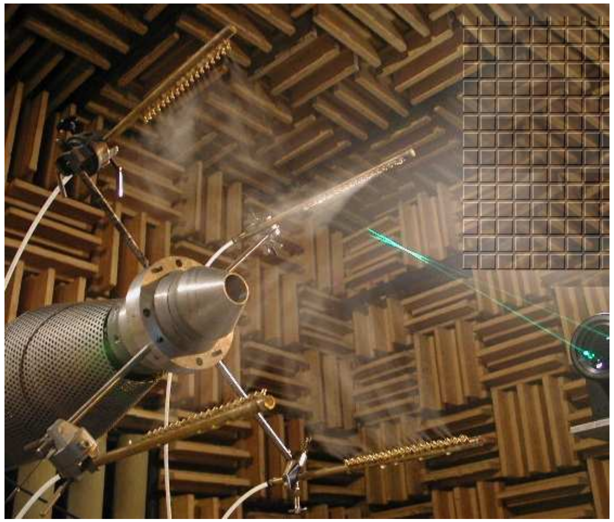

Barré & Fleury (2003 & 2004)

Experimental directivity

Free-field loss-less data scaled to a nozzle exit area A of 1 m^2, $T_j/T_\infty = 1$

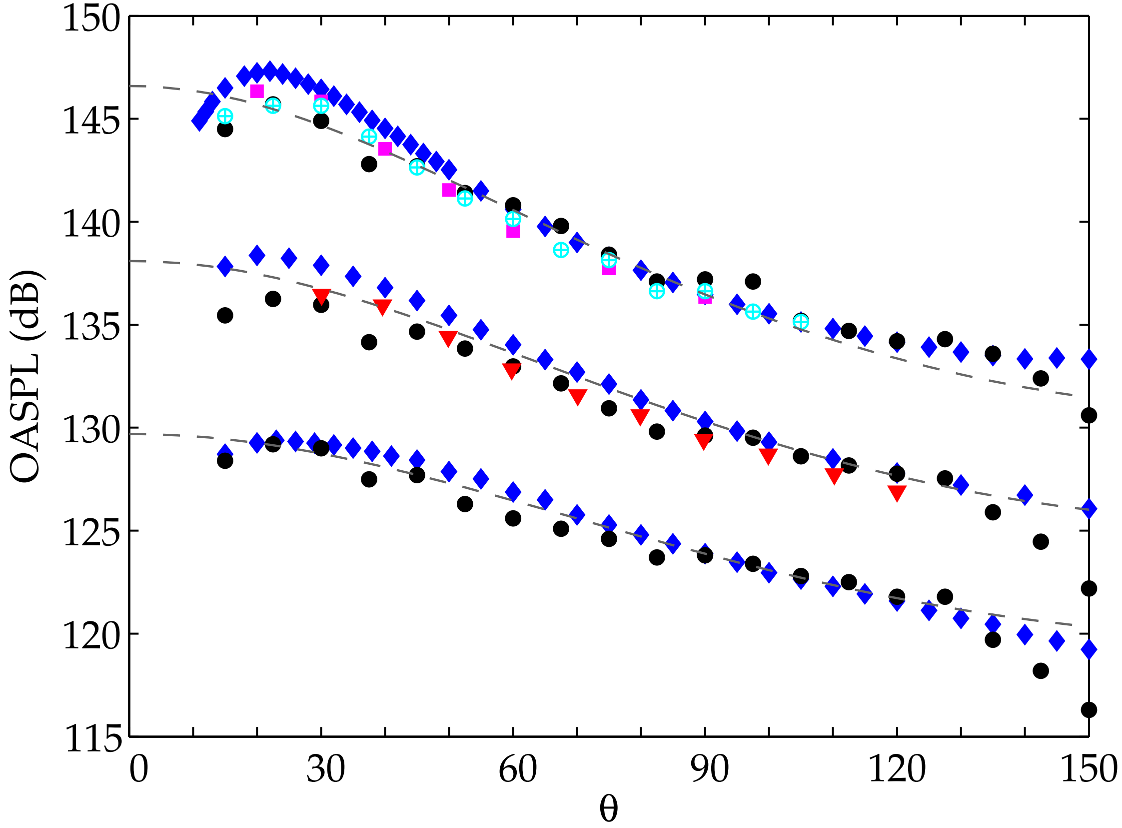

$\mathrm{M} = 0.6, 0.75, 0.9$

– – – directivity factor $(1 - \mathrm{M}_c \cos\theta)^{-3}$ with $\mathrm{M}_c \propto \mathrm{M}_a$

♦ Bogey *et al.* (2007), • Tanna (1977), ⊕ Lush (1971), ▼ Pinker *et al.* (2003), ■ Mollo-Christensen *et al.* (1964)

Narrow-band spectra in dB/St

$M = 0.75 \qquad T_j/T_\infty = 1$

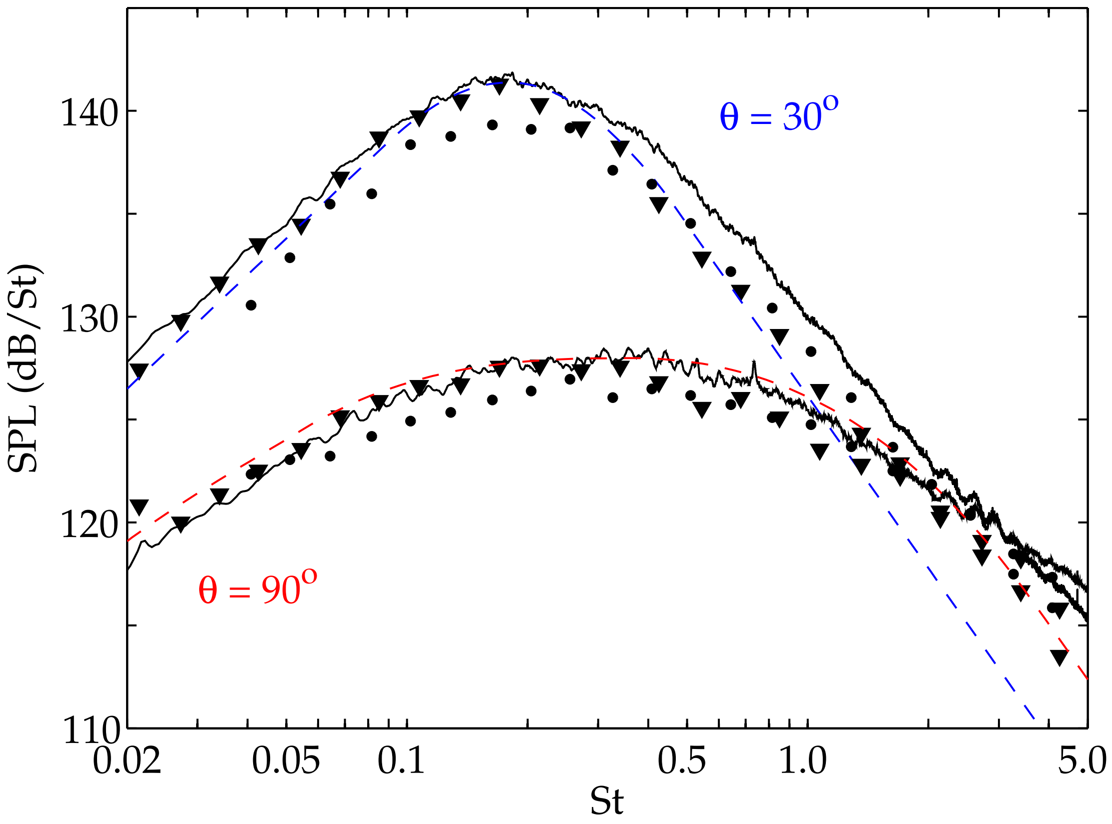

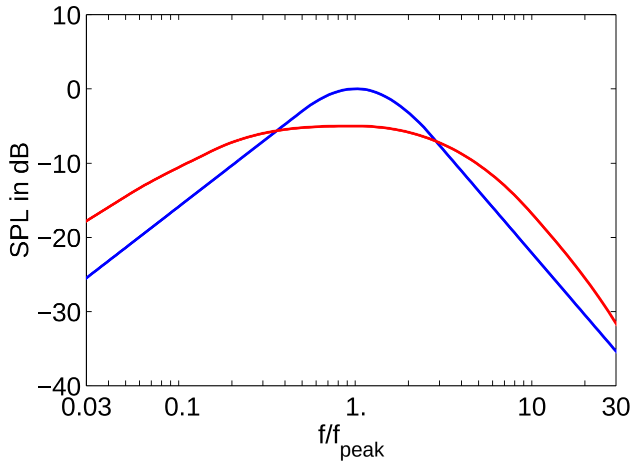

Semi-empirical model of
Tam, Golebiowski & Seiner (1996)

—— $Re = 6.4 \times 10^5$ (Bogey *et al.*, 2007),
• $Re = 8.4 \times 10^5$ (Tanna, 1977), ▾ $Re = 1.4 \times 10^6$ (Pinker *et al.*, 2003)

- **Narrow-band spectra in dB/St**

$M = 0.9 \quad T_j/T_\infty = 1 \quad r/D = 53 \quad Re_D = 7.8 \times 10^5$ Barré & Fleury (ECLyon, 2003)

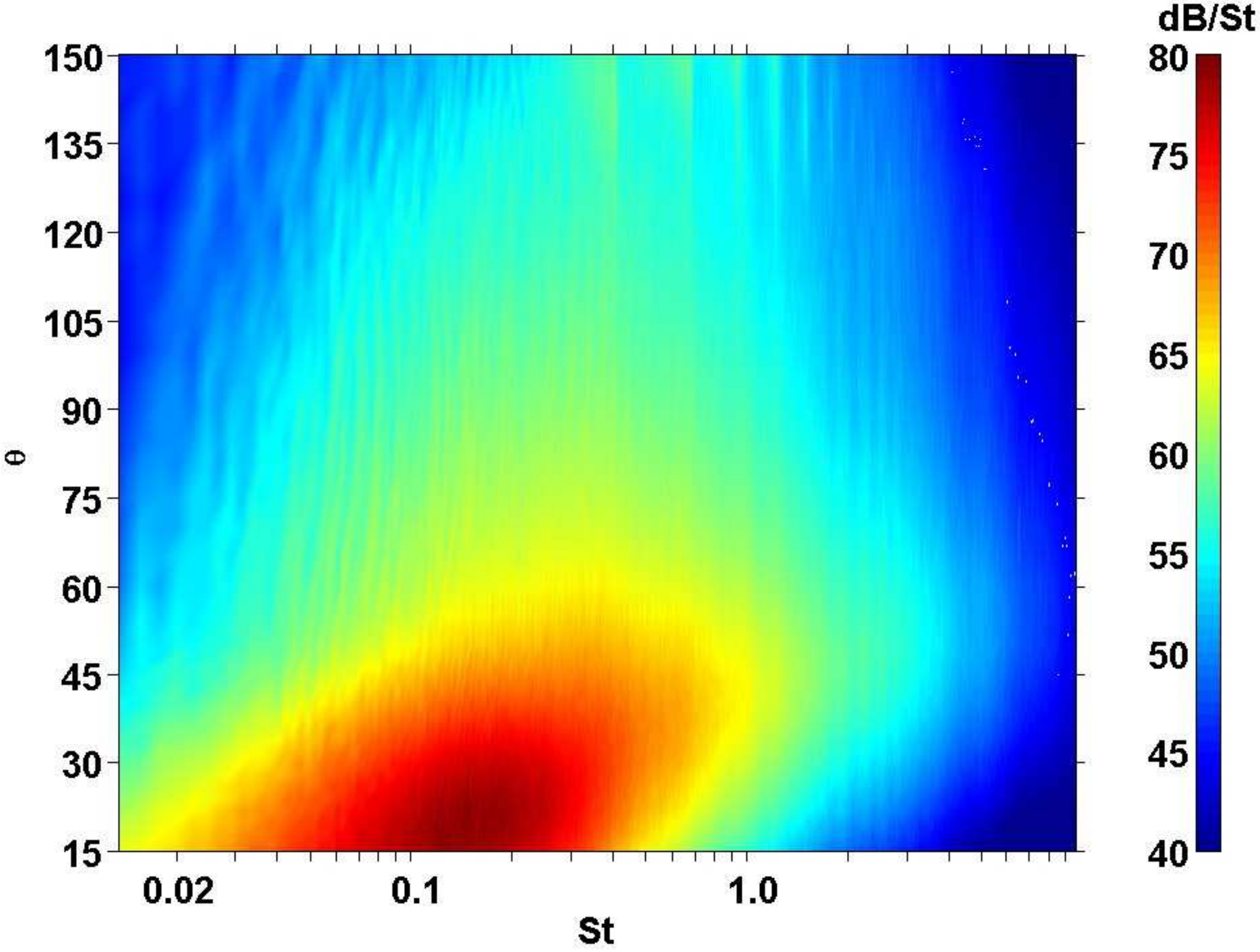

Narrow-band spectra in dB/St

$\theta = 30^o$, M = 0.6, 0.7, 0.9, 0.98 $(T_j/T_\infty = 1)$

Bogey *et al. IJA* (2007)

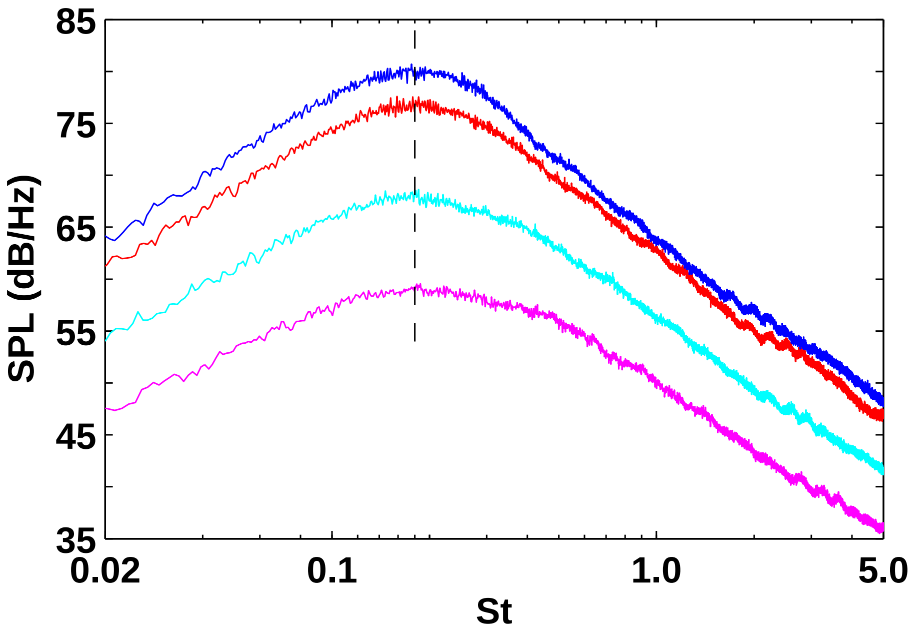

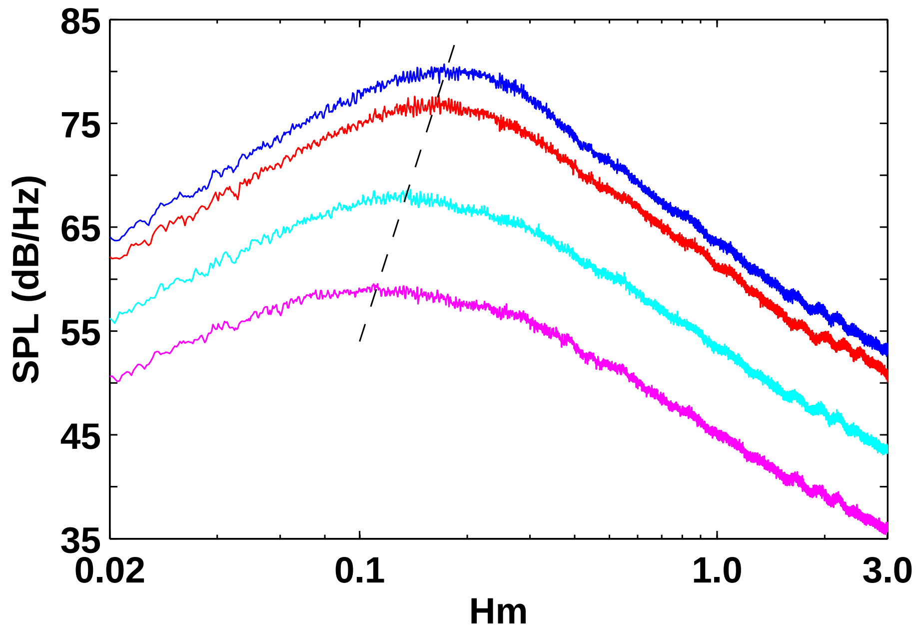

f_{peak} scales as St $= fD/U_j \quad (\neq \text{Hm} = fD/c_\infty)$

$\sim (u_j/c_\infty)^{11}$ scaling law

- Narrow-band spectra in dB/St : temperature effects

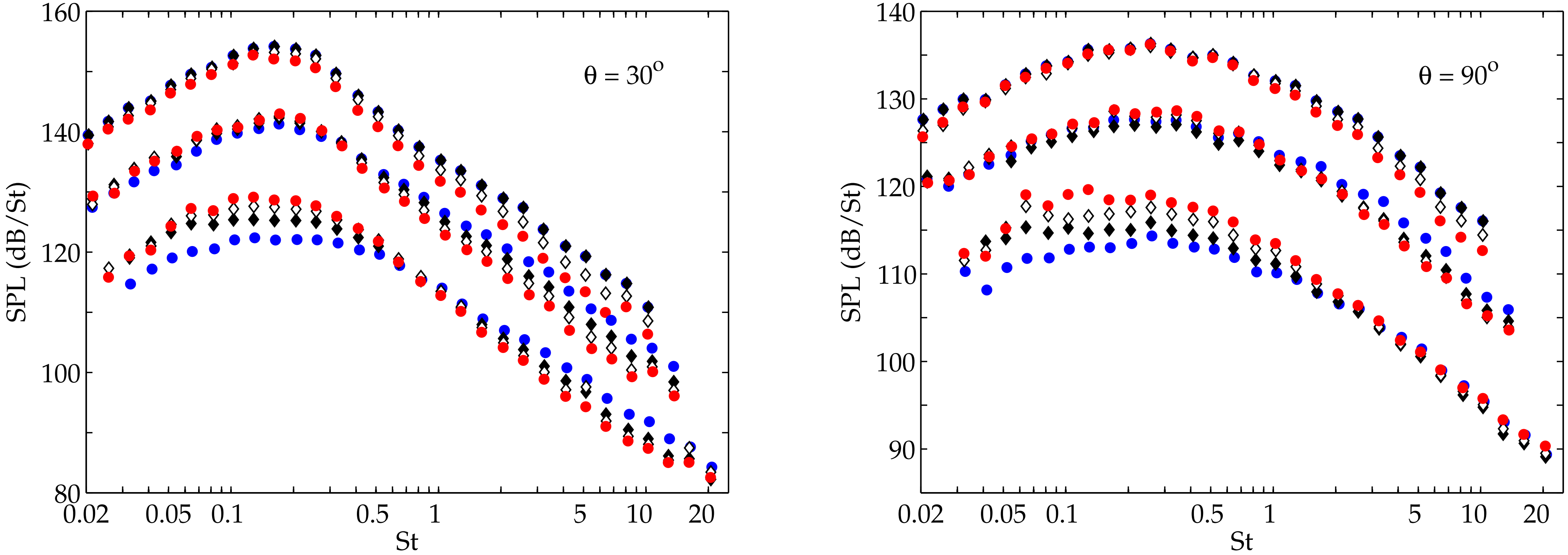

Pinker *et al.* (2003) $\quad M = 0.5, 0.75, 1.0$

● $T_j/T_\infty = 1.0$, ♦ $T_j/T_\infty = 1.5$, ◊ $T_j/T_\infty = 2.0$, ● $T_j/T_\infty = 2.5$

It should be observed that $\mathrm{Re}_D = \mathrm{Re}_D(T_j)$

- **Formulation :** The simplest wave equation from the conservation of mass and Navier-Stokes equations :

$$\frac{\partial \rho}{\partial t} + \frac{\partial (\rho u_i)}{\partial x_i} = 0 \qquad (1)$$

$$\frac{\partial (\rho u_i)}{\partial t} + \frac{\partial \left(\rho u_i u_j\right)}{\partial x_j} = -\frac{\partial p}{\partial x_i} + \frac{\partial \tau_{ij}}{\partial x_j} \qquad (2)$$

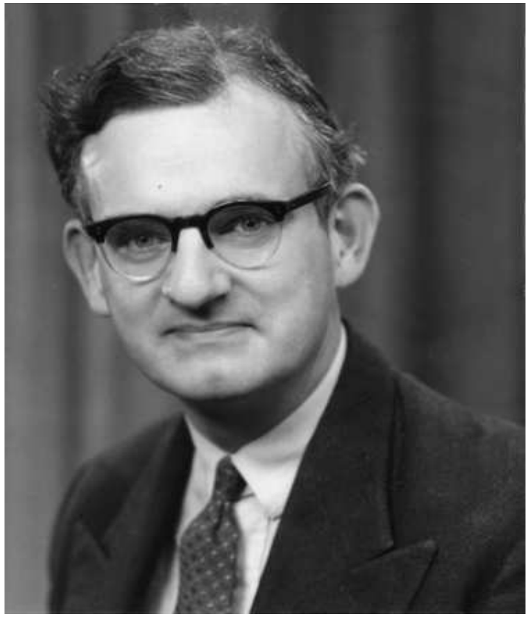

Sir James Lighthill (1924-1998)

$$\frac{\partial}{\partial t}(1) - \frac{\partial}{\partial x_i}(2) \qquad \text{and} \qquad c_\infty^2 \nabla^2 \rho = c_\infty^2 \frac{\partial^2}{\partial x_i \partial x_j}(\rho \delta_{ij})$$

$$\frac{\partial^2 \rho}{\partial t^2} - c_\infty^2 \nabla^2 \rho = \frac{\partial^2 T_{ij}}{\partial x_i \partial x_j} \qquad \text{with} \qquad T_{ij} = \rho u_i u_j + \left(p - c_\infty^2 \rho\right) \delta_{ij} - \tau_{ij}$$

Lighthill's tensor

Lighthill, *Proc. Roy. Soc. London* (1952) & *AIAA Journal* (1982)

- **Interpretation of Lighthill's equation $\Box \rho = \Lambda$**
  $\Box \equiv \partial_{tt} - c_\infty^2 \nabla^2 \quad \Lambda = \nabla \cdot \nabla \cdot T$

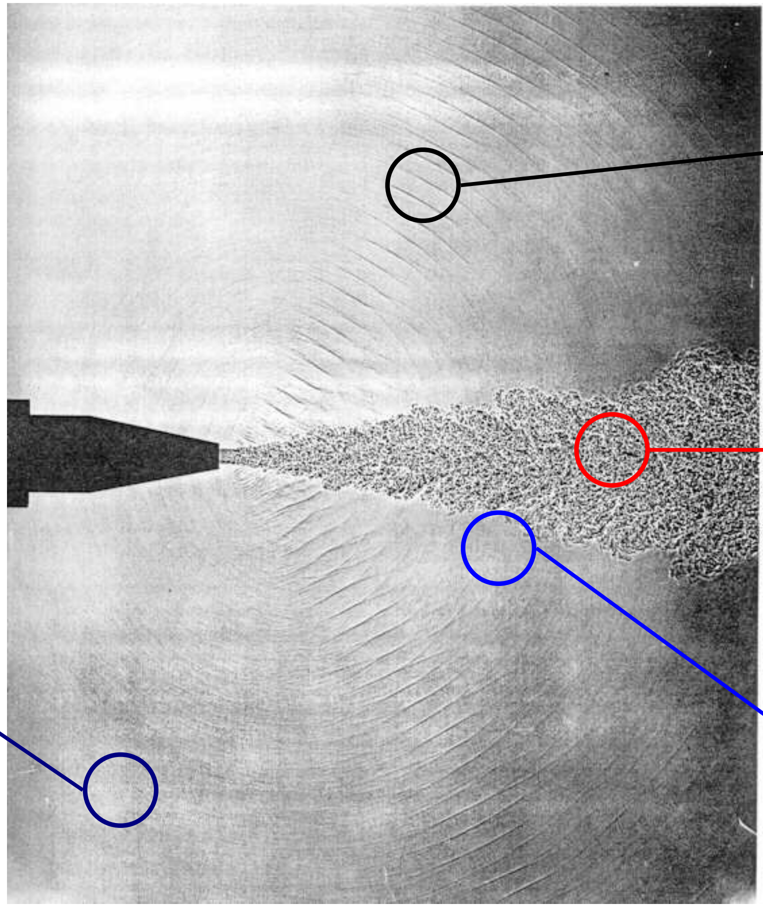

$\Box \rho \simeq \Lambda_{\text{nonlinear effects}}$

$\Box \rho \simeq \Lambda_{\text{turbulence}}$

In a uniform medium
at rest
$\rho_\infty, p_\infty, c_\infty$

$\Box \rho = 0$

$\Box \rho \simeq \Lambda_{\text{mean flow effects}}$

Retarded-time solution of Lighthill's equation

$$\rho\,(\boldsymbol{x},t) = \frac{1}{4\pi c_\infty^4}\int_V \frac{\partial^2 T_{ij}}{\partial y_i \partial y_j}\left(\boldsymbol{y}, t - \frac{r}{c_\infty}\right)\frac{d\boldsymbol{y}}{r}$$

By using

$$r = |\boldsymbol{x}-\boldsymbol{y}| \simeq x - \frac{\boldsymbol{x}\cdot\boldsymbol{y}}{x} + \mathcal{O}\left(\frac{y^2}{x}\right) \qquad x \gg y$$

$$\frac{\partial}{\partial y_i} \rightsquigarrow -\frac{1}{c_\infty}\frac{x_i}{x}\frac{\partial}{\partial t} \qquad x \gg y$$

$$\rho'\,(\boldsymbol{x},t) \simeq \frac{1}{4\pi c_\infty^4 x}\frac{x_i x_j}{x^2}\int_V \frac{\partial^2 T_{ij}}{\partial t^2}\left(\boldsymbol{y}, t - \frac{r}{c_\infty}\right) d\boldsymbol{y}$$

in the far-field approximation

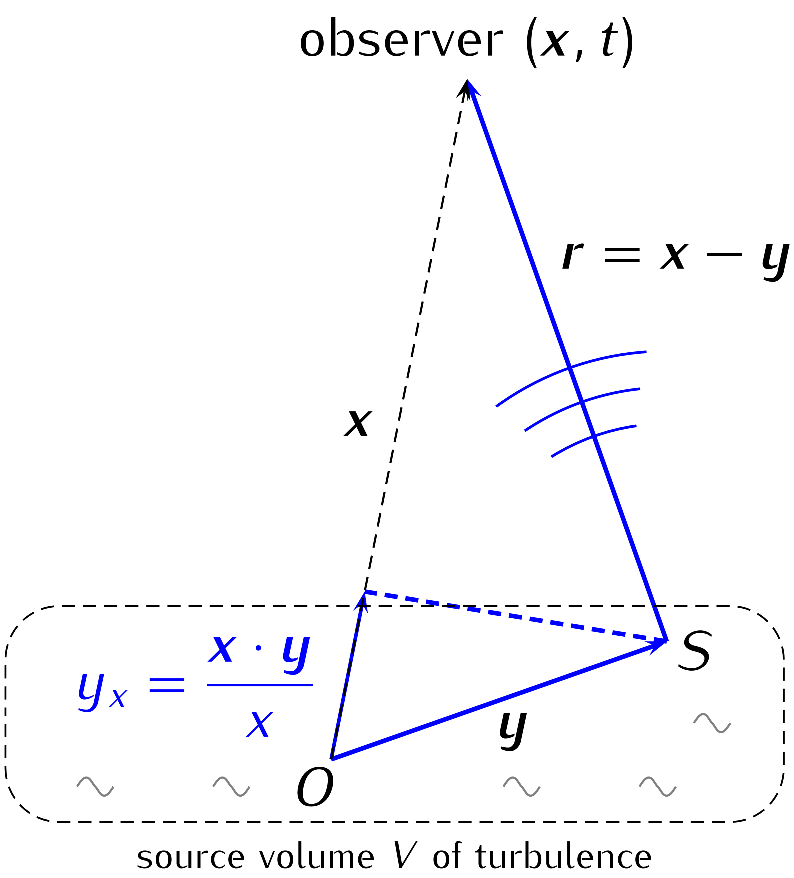

Retarded-time solution of Lighthill's equation

$$\mathcal{L} = \partial^2_{tt} - c_\infty^2 \nabla^2 \qquad S = \partial^2_{x_i x_j} T_{ij} \qquad G_\infty(\boldsymbol{x}, t) = 1/(4\pi c_\infty^2 x)\ \delta(t - x/c_\infty)$$

$$\rho' = \rho' * \delta = \rho' * \mathcal{L}(G_\infty) = \mathcal{L}(\rho') * G_\infty = S * G_\infty \qquad \text{(in free space)}$$

$$\rho(\boldsymbol{x}, t) = S * G_\infty = \frac{\partial^2 T_{ij}}{\partial x_i \partial x_j} * \frac{1}{4\pi c_\infty^2 x}\,\delta\left(t - \frac{x}{c_\infty}\right)$$

$$\simeq \frac{1}{4\pi c_\infty^2 x}\frac{\partial T_{ij}}{\partial x_j} * \frac{\partial}{\partial x_i}\delta\left(t - \frac{x}{c_\infty}\right) \simeq \frac{1}{4\pi c_\infty^2 x}\frac{\partial T_{ij}}{\partial x_j} * \left(-\frac{1}{c_\infty}\frac{x_i}{x}\right)\frac{\partial}{\partial t}\delta\left(t - \frac{x}{c_\infty}\right)$$

as $x \to \infty$

- **Some remarks about these subtle integral formulations**

  Crighton (1975), Ffowcs Williams (1992)

  May we neglect the retarded time differences in the integral solutions ?

$$t - \frac{r}{c_\infty} = t - \frac{|\boldsymbol{x} - \boldsymbol{y}|}{c_\infty} \simeq t - \frac{x}{c_\infty} + \frac{\boldsymbol{x} \cdot \boldsymbol{y}}{x c_\infty} + \cdots$$

difference in time emission $\quad \dfrac{\boldsymbol{x} \cdot \boldsymbol{y}}{x c_\infty} \sim \dfrac{l_s}{c_\infty}$

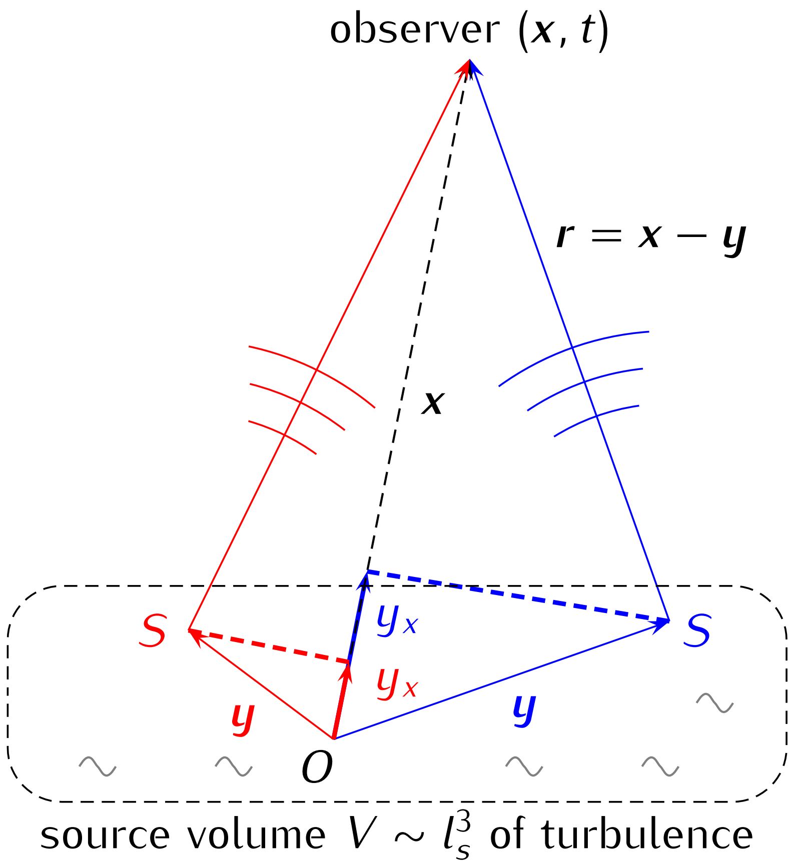

$$\frac{\text{difference in time emission}}{\text{source turbulent time}} \sim \frac{l_s / c_\infty}{l_s / u'} \sim M_t$$

$\leadsto$ Yes if $M_t \ll 1$, compact sources

(M_t turbulent Mach number)

Simplification of the source term T'_{ij}

Viscous effects as a possible noise source are negligible, $T_{ij} \simeq \rho u_i u_j + (p - c_\infty^2 \rho)\delta_{ij}$. Moreover, $p' = c_\infty^2 \rho' + (p_\infty / c_v)\, s'$ for a perfect gas. Hence, $T_{ij} \simeq \rho u_i u_j$ for flows nearly isentropic.

For low Mach number isothermal flows $T_{ij} \simeq \bar{\rho} u_i u_j \simeq \rho_\infty u_i u_j$
…but acoustic - mean flow interactions are definitively lost

- Mean flow effects are contained in the linear **compressible** part of the Lighthill tensor T_{ij}
- Aerodynamic noise source term $\equiv$ non-linear part of T_{ij}

- **Crudest approximation for jet noise scaling**

In the far field and for $M_t \leq 1$ (compact sources)

$$\rho'(\mathbf{x},t) \simeq \frac{1}{4\pi c_\infty^4 x}\frac{x_i x_j}{x^2}\int_V \frac{\partial^2 T_{ij}}{\partial t^2}\left(\mathbf{y}, t-\frac{x}{c_\infty}\right) d\mathbf{y}$$

$$\sim \frac{1}{c_\infty^4 x}\frac{\rho_j U_j^2}{(D/U_j)^2} D^3 \qquad \begin{cases}\text{jet nozzle diameter } D\\ \text{jet exit velocity } U_j\end{cases}$$

Hence,

$$W_a \sim \frac{\rho_j}{\rho_\infty}\frac{U_j^5}{c_\infty^5} A\rho_j U_j^3 \qquad (A = \pi D^2/4)$$

Lighthill's eigth power law (1952)

$$\overline{p'^2}\Big|_{\theta=90^o} = K\rho_\infty^2 c_\infty^4 \frac{A}{r^2}\left(\frac{\rho_j}{\rho_\infty}\right)^2 \mathrm{M}^{7.5} \qquad K \simeq 1.9\times 10^{-6}$$

Jet noise scaling – acoustic efficiency η

$$\eta = W_{\mathrm{acoustic}}/W_{\mathrm{mechanical}} \simeq 1.2 \times 10^{-4}\ (\rho_j/\rho_\infty)\ \mathrm{M}^5$$

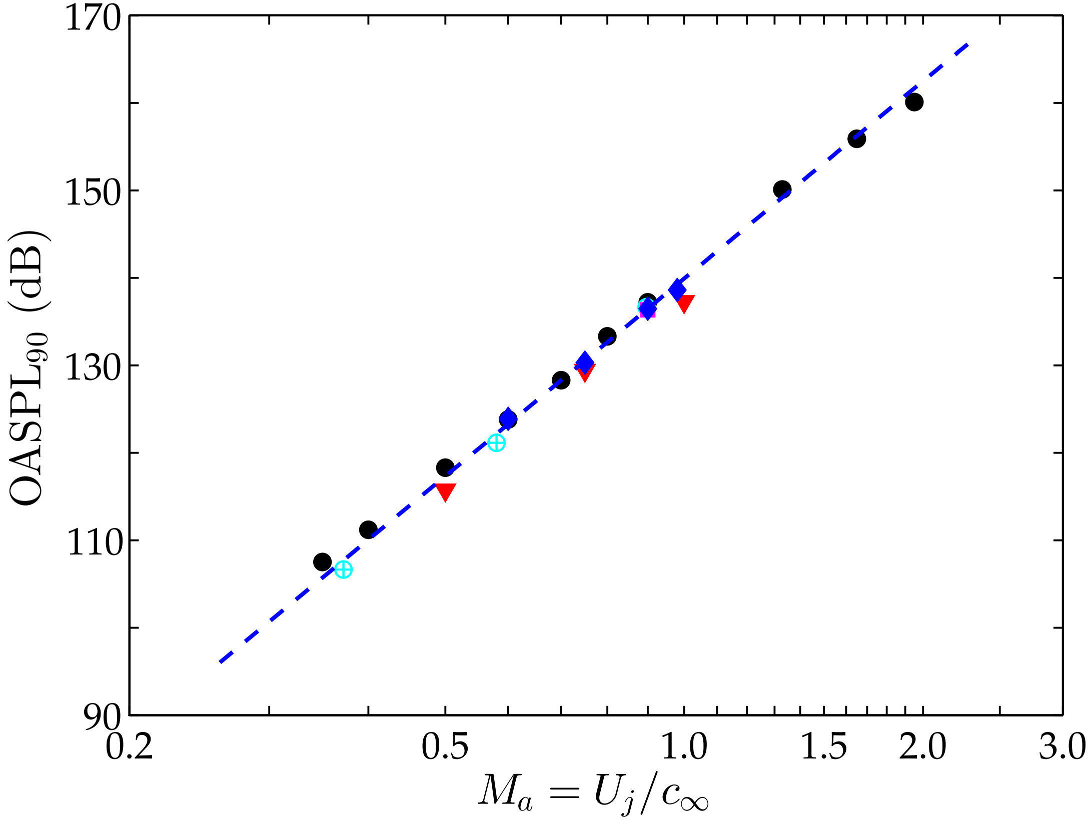

$$W_{\mathrm{acoustic}} \sim A U_j^8$$

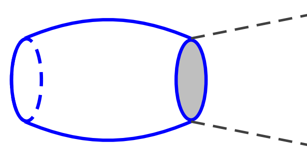

$$\text{thrust} = \dot{m}_j U_j$$
$$= A \rho_j U_j^2$$

$$W_{\mathrm{mechanical}} = A \rho_j U_j^3/2$$

♦ Bogey *et al.* (2007), • Tanna (1977), ⊕ Lush (1971), ▼ QinetiQ 1983 NTF data, ■ MolloChristensen (1964)

(free-field loss-less data scaled to a nozzle exit area A of 1 m^2, $T_j/T_\infty = 1$)

Jet noise scaling

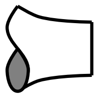 D $\xrightarrow{U_j}$

$T = \dot{m} U_j \propto \rho D^2 U_j^2$

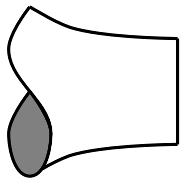 $2D$ $\xrightarrow{U_j/2}$

same thrust T, -18 dB !

The Linearized Euler Equations (LEE)

Small perturbations arround a steady mean flow $(\bar{\rho}, \bar{\boldsymbol{u}}, \bar{p})$ (no gravity)

$$\begin{cases} \partial_t \rho' + \nabla \cdot \left(\rho' \bar{\boldsymbol{u}} + \bar{\rho} \boldsymbol{u}' \right) = 0 \\ \partial_t \left(\bar{\rho} \boldsymbol{u}' \right) + \nabla \cdot \left(\bar{\rho} \bar{\boldsymbol{u}} \boldsymbol{u}' \right) + \nabla p' + \left(\bar{\rho} \boldsymbol{u}' + \rho' \bar{\boldsymbol{u}} \right) \cdot \nabla \bar{\boldsymbol{u}} = 0 \\ \partial_t p' + \nabla \cdot \left[p' \bar{\boldsymbol{u}} + \gamma \bar{p} \boldsymbol{u}' \right] + (\gamma - 1)\, p' \nabla \cdot \bar{\boldsymbol{u}} - (\gamma - 1)\, \boldsymbol{u}' \cdot \nabla \bar{p} = 0 \end{cases}$$

- Acoustic propagation in the presence of a flow (atmosphere, ocean, turbulent flow, ...) is governed by LEE
- In the general case, this system cannot be reduced exactly to a **single wave equation**.

Blokhintzev (1946)
Pridmore-Brown (1958), Lilley (1972), Goldstein (1976, 2001, 2003)

The Linearized Euler Equations (LEE)

For a parallel base flow $\bar{u}_i = \bar{u}_1(x_2, x_3)\delta_{1i}$, $\bar{\rho} = \bar{\rho}(x_2, x_3)$ (and thus $\bar{p} = p_\infty = \text{cst}$), the LEE can be recast into a wave equation based on the pressure, $\mathcal{L}_0[\boldsymbol{p'}] = \mathbf{0}$

$$\mathcal{L}_0 \equiv \frac{\bar{D}}{\bar{D}t}\left[\frac{\bar{D}^2}{\bar{D}t^2} - \nabla\cdot\left(\bar{c}^2\nabla\right)\right] + 2\bar{c}^2\frac{\partial \bar{u}_1}{\partial x_i}\frac{\partial^2}{\partial x_1 \partial x_i} \qquad i = 2,3 \quad \bar{D} \equiv \partial_t + \bar{u}_1\partial_{x_1}$$

From the (exact) Navier-Stokes equations, we can also form an inhomogeneous wave equation based on $\mathcal{L} \rightarrow \mathcal{L}_0$ at leading order, $\mathcal{L}[\boldsymbol{p'}] = \Lambda$ Lilley (1972)

Sir Geoffrey Lilley (1919-2015)

$$\frac{d}{dt}\left\{\frac{d^2\pi}{dt^2} - \frac{\partial}{\partial x_i}\left(c^2\frac{\partial \pi}{\partial x_i}\right)\right\} + 2\frac{\partial u_i}{\partial x_j}\frac{\partial}{\partial x_i}\left(c^2\frac{\partial \pi}{\partial x_j}\right) = -2\frac{\partial u_i}{\partial x_j}\frac{\partial u_j}{\partial x_k}\frac{\partial u_k}{\partial x_i}$$

$$+2\frac{\partial u_i}{\partial x_j}\frac{\partial}{\partial x_i}\left(\frac{1}{\rho}\frac{\partial \tau_{ij}}{\partial x_i}\right) + \frac{d^2}{dt^2}\left(\frac{1}{c_p}\frac{ds}{dt}\right) - \frac{d}{dt}\left\{\frac{\partial}{\partial x_i}\left(\frac{1}{\rho}\frac{\partial \tau_{ij}}{\partial x_j}\right)\right\}$$

$\boldsymbol{\pi = \ln p}$

$\boldsymbol{\pi' \simeq (1/\gamma)p'/p_\infty}$

- **Linearized Lilley Equation $\mathcal{L}_0[p'] = \Lambda$**

Seek a solution of the form $p'(\mathbf{x}, t) = \varphi(x_2)\, e^{i(k_1 x_1 - \omega t)} = \varphi(x_2)\, e^{ik(\nu_1 x_1 - c_\infty t)}$

$k = \omega / c_\infty$, $\nu_1 = k_1/k = \cos\theta$, $M = \bar{u}_1 / c_\infty$

shear-layer thickness δ

$$\varphi'' + \frac{2\nu_1}{1 - \nu_1 M}\frac{dM}{dx_2}\varphi' + k^2\left[(1 - \nu_1 M)^2 - \nu_1^2\right]\varphi = 0$$

$$\sim k^2 \qquad \sim k/\delta \qquad \sim k^2$$

High-frequency approximation, $k\delta \gg 1$

$\varphi'' + q(x_2)\varphi = 0$ with $q(x_2) = (1 - \nu_1 M)^2 - \nu_1^2$

$$\begin{cases} q(x_2) < 0 \ \text{ exponential decrease} \\ q(x_2) > 0 \ \text{ periodic oscillations} \\ \text{Turning point given by } q(x_2^\star) = 0, \ \cos\theta^\star = 1/(M+1) \end{cases}$$

... propagation effects are now intrinsically contained in the wave operator $\mathcal{L}_0$ (and not in the source term, as in Lighthill's wave equation)

Linearized Lilley Equation

Harmonic source in a Bickley jet $\quad \dfrac{\bar{u}_1}{u_j} = \dfrac{1}{\cosh^2(\beta y/\delta)} \quad \beta = \ln(1+\sqrt{2})$

$\mathrm{St} = 4.4 \quad \mathrm{M} = 0.5 \quad \lambda \sim \delta$

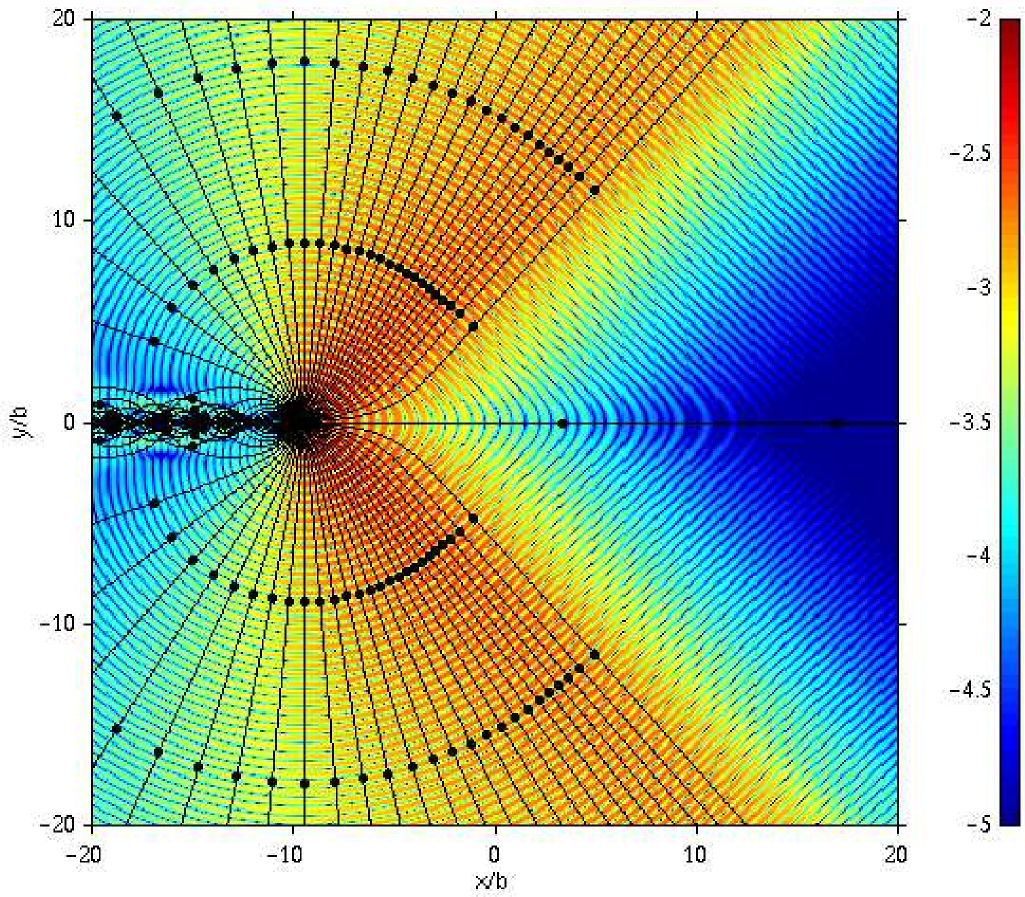

LEE ($\log_{10}(|p'| + \epsilon)$) and ray-tracing

high-frequency noise is diverting away from the jet axis

shadow zone at angles close to the jet axis, $\theta^\star \simeq 48.2^{\mathrm{o}}$ (edge of the silence cone)

High-frequency solution

Wavelength matching at the interface,

$$\frac{c_1}{f}\left(\frac{1}{\cos\theta_1}+M_1\right)=\frac{c_2}{f}\frac{1}{\cos\theta_2}$$

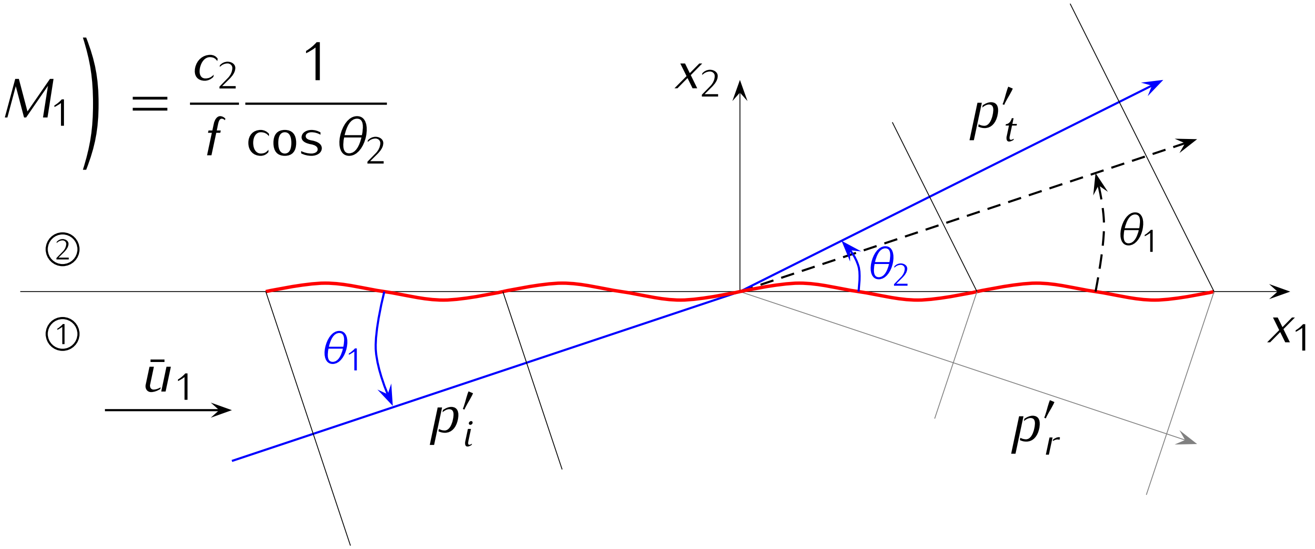

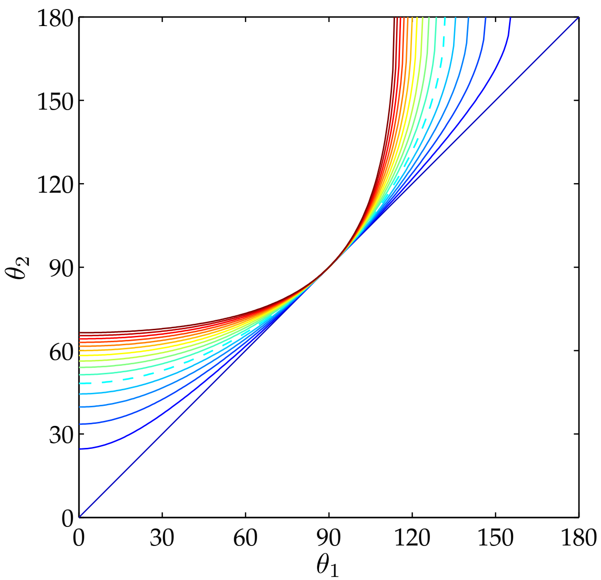

$$\cos\theta_2=\frac{\cos\theta_1}{1+M_1\cos\theta_1}\quad(0\leq\theta_1\leq\pi)$$

$$\theta_{2\mathrm{min}}=\theta_2^\star=\frac{1}{1+M_1}\text{ for }\theta_1=0^{\mathrm{o}}\text{ (grazing incidence)}$$

$$\theta_2=f(\theta_1)\text{ for }M_1=0:0.1:1.5$$

Ray tracing

The dispersion relation $\omega = \boldsymbol{k} \cdot \boldsymbol{u}_0 + c_0 k$ (obtained by the eikonal method from LEE) can be solved by the method of characteristics, commonly called **rays** and defined as the solution of

$$\dot{\boldsymbol{x}} = \boldsymbol{v}_g = c_0 \boldsymbol{\nu} + \boldsymbol{u}_0 = c_0 \left(\boldsymbol{\nu} + \boldsymbol{M}_0 \right)$$

$\rightsquigarrow$ rays : curves $\boldsymbol{x} = \boldsymbol{x}(t)$ tangent to the group velocity at each point, and not perpendicular to wavefronts in a moving medium.

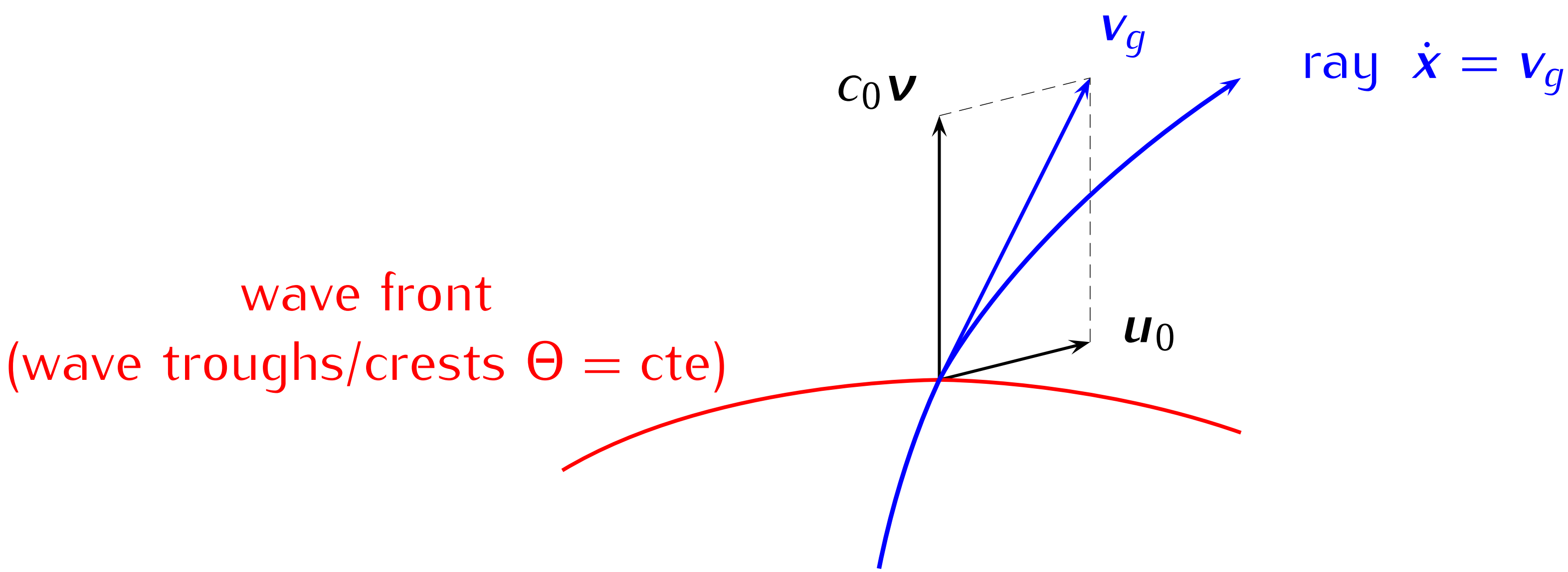

Ray tracing equations

Hayes (*Proc. Roy. Soc. Lond.* 1970), Candel (*J. Fluid Mech.*, 1977)

system of differential equations to solve

$$\begin{cases} \dfrac{dx_i}{dt} = c_0 \dfrac{k_i}{k} + u_{0i} \\[2ex] \dfrac{dk_i}{dt} = -k \dfrac{\partial c_0}{\partial x_i} - k_j \dfrac{\partial u_{0j}}{\partial x_i} \end{cases}$$

The system requires 3 initial conditions in 2-D,

- Source position S
- Orientation of the wavefront, with shooting angle θ_0

$$\cos\theta_0 = \frac{M_0 + \cos\phi_0}{\sqrt{(M_0+\cos\phi_0)^2 + \sin^2\phi_0}}$$

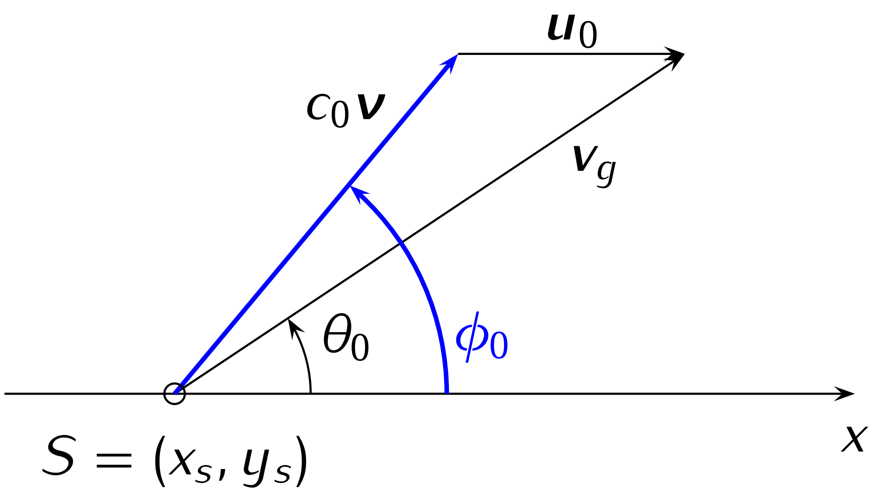

Ray tracing equations

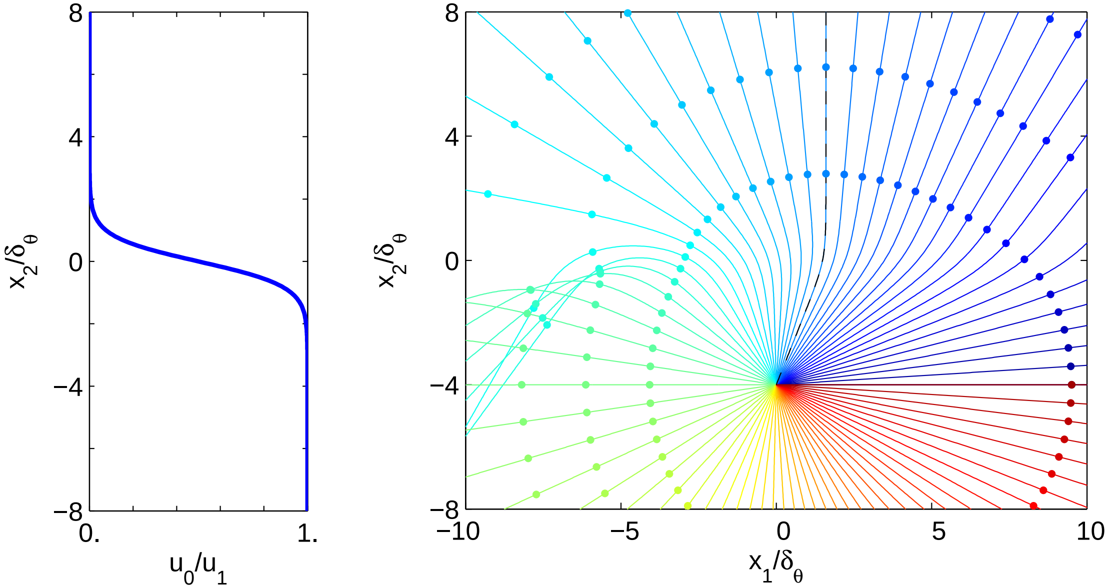

$M_1 = 0.4$

source at $y_s = -4\delta_\theta$

ray every $\Delta\phi_0 = 5^{\mathrm{o}}$

$- - -$ $\phi_1 = \phi_2 = 90^{\mathrm{o}}$

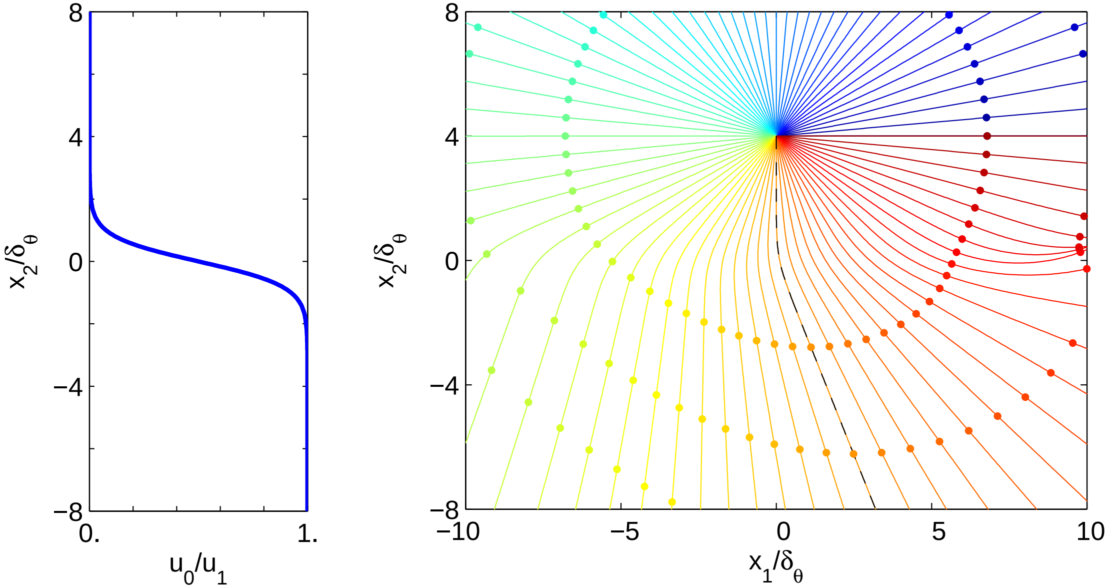

$M_1 = 0.4$

source at $y_s = 4\delta_\theta$

ray every $\Delta\phi_0 = 5^{\mathrm{o}}$

$- - -$ $\phi_1 = \phi_2 = 90^{\mathrm{o}}$

Ray tracing : amplitude of the acoustic mode

Conservation of the **acoustic flux** in a ray tube

$$\int_S E\,\boldsymbol{v}_g \cdot \boldsymbol{n}\, dS = 0 \qquad \boldsymbol{n} = \frac{\boldsymbol{v}_g}{v_g} \qquad E c_0 \left|\boldsymbol{M}_0 + \boldsymbol{\nu}\right| dS = \text{cte}$$

The calculation of the surface element dS allows to determine the local amplitude of the acoustic field, not always easy to implement in practice.

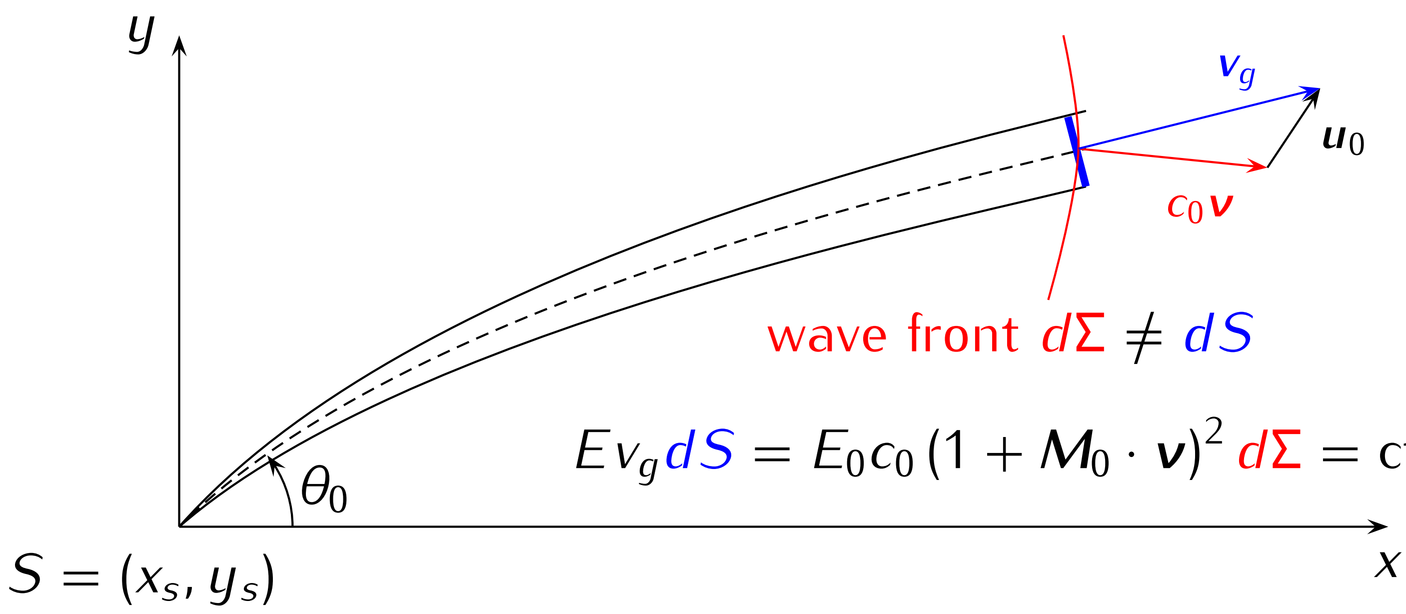

$$E v_g dS = E_0 c_0 \left(1 + \boldsymbol{M}_0 \cdot \boldsymbol{\nu}\right)^2 d\Sigma = \text{cte}$$

- Different levels of representation/modelling in aeroacoustics

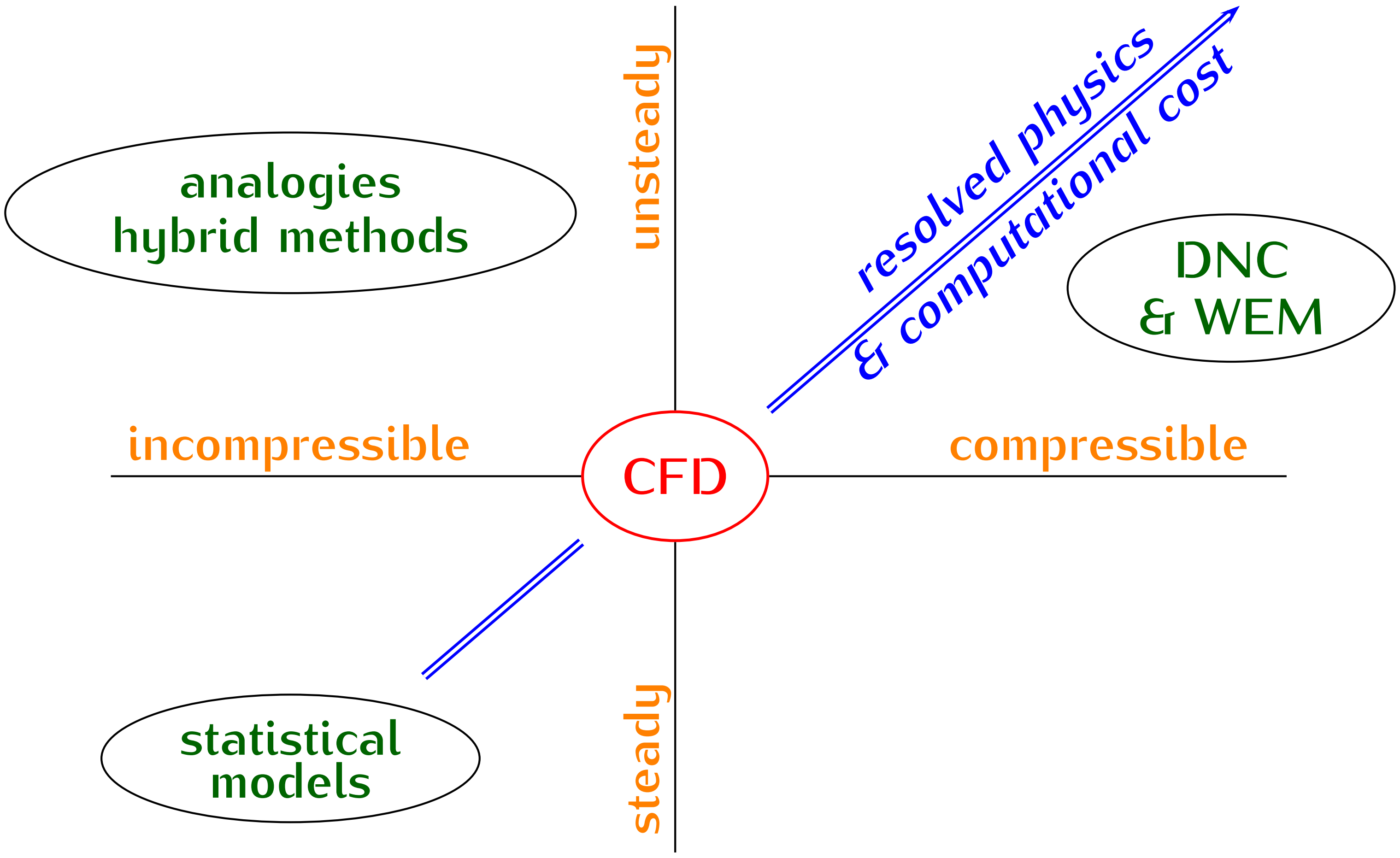

DNC = Direct Noise Computation

WEM = Wave Extrapolation Methods

What could be a philosophy to use (often heavy) aeroacoustics simulations ?

real life

- predict aerodynamic noise in pratical / realistic configurations
- provide the bounds of achievable noise reduction
- use CAA as diagnostic tool for studying specific (small) problems
- known-how : industrial softwares, hpc, reduced-order models
- understand physics of aerodynamic noise generation

concepts
theory

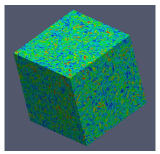

Lightill's theory

When a time-dependent solution of T_{ij} is not available, an alternative approach is to estimate the autocorrelation function of the acoustic pressure defined as,

$$R_a(\mathbf{x},\tau) = \overline{p'(\mathbf{x},t)p'(\mathbf{x},t+\tau)}/(\rho_\infty c_\infty)$$

- Acoustic intensity, $I(\mathbf{x}) = R(\mathbf{x},\tau=0)$
- Power spectral density,

$$S_a(\mathbf{x},\omega) = \frac{1}{2\pi}\int_{-\infty}^{+\infty} R_a(\mathbf{x},\tau)e^{i\omega\tau}d\tau$$

Turbulence statistically stationary,

$$R_a(\mathbf{x},\tau) = \frac{1}{16\pi^2\rho_\infty c_\infty^5 x^2}\frac{x_i x_j x_k x_l}{x^4}\int_V\int_V \frac{\partial^4}{\partial\tau^4}\overline{T_{ij}[\mathbf{y}_A,t]\;T_{kl}[\mathbf{y}_B,t+\tau]}\,d\mathbf{y}_A\,d\mathbf{y}_B$$

$\equiv R_{ijkl}\left(\mathbf{y},\boldsymbol{\eta},\tau+\tau_\eta\right)$ fourth-order two-point two-time correlation tensor

$$\mathbf{y}=\mathbf{y}_A \qquad \boldsymbol{\eta}=\mathbf{y}_B-\mathbf{y}_A \qquad \tau_\eta = \mathbf{x}\cdot\boldsymbol{\eta}/(xc_\infty)$$

Modelling

$$R_a(\boldsymbol{x},\tau) = \frac{1}{16\pi^2\rho_\infty c_\infty^5 x^2}\frac{x_i x_j x_k x_l}{x^4}\int_V \left\{ \int_V \frac{\partial^4}{\partial\tau^4} R_{ijkl}\left(\boldsymbol{y},\boldsymbol{\eta},\tau+\tau_\eta\right) d\boldsymbol{\eta} \right\} d\boldsymbol{y}$$

- moving frame to separate the convective amplification from the evolution of the turbulence itself (Doppler or convection factor)
- isotropic turbulence locally over the $\boldsymbol{\eta}$ integration
- only two turbulence scales ($k_t - \epsilon$ model, $k_t - \omega - SST$ model, ...)

$$L \sim \frac{k_t^{3/2}}{\epsilon} \qquad \tau \sim \frac{k_t}{\epsilon}$$

two-point time correlation function ?

Ref. MGB model (Mani, Gliebe, Balsa) & Kharavan, *AIAA J.*, 37(7), 1999
Bailly, Lafon & Candel, *J. Sound Vib.*, 194(2), 1996 & *AIAA J.*, 35(11), 1997

Tam & Auriault *AIAA J.*, 37(2), 1999 & *AIAA J.* 42(1), 2004
Morris & Farassat *AIAA J.*, 40(4), 2002

Modelling

A key result : to radiate sound, turbulence must have a sonic phase velocity in the observer direction

- Wavenumber frequency spectrum

$$H_{ijkl}(\boldsymbol{y},\boldsymbol{k},\omega)=\frac{1}{(2\pi)^4}\int_V\int_{-\infty}^{+\infty}R_{ijkl}(\boldsymbol{y},\boldsymbol{\eta},\tau)\,e^{i(\omega\tau-\boldsymbol{k}\cdot\boldsymbol{\eta})}d\boldsymbol{\eta}d\tau$$

- Power spectral density

$$S_a(\boldsymbol{x},\omega)=\frac{\pi}{2}\frac{\omega^4}{\rho_\infty c_\infty^5 x^2}\frac{x_i x_j x_k x_l}{x^4}\int_V H_{ijkl}\left(\boldsymbol{y},\frac{\omega}{c_\infty}\frac{\boldsymbol{x}}{x},\omega\right)d\boldsymbol{y}$$

Condition for sound radiation,

$$\boldsymbol{k}_{\text{turbulence}}=\frac{\omega}{c_\infty}\frac{\boldsymbol{x}}{x}$$

- **Subsonic round jets**

  JEAN European program, Bodard / SNECMA (2009)

RANS with a $k_t - \epsilon$ turbulence model

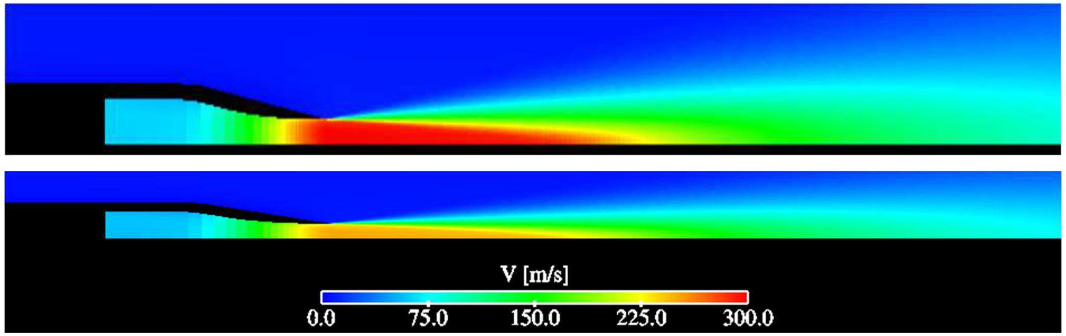

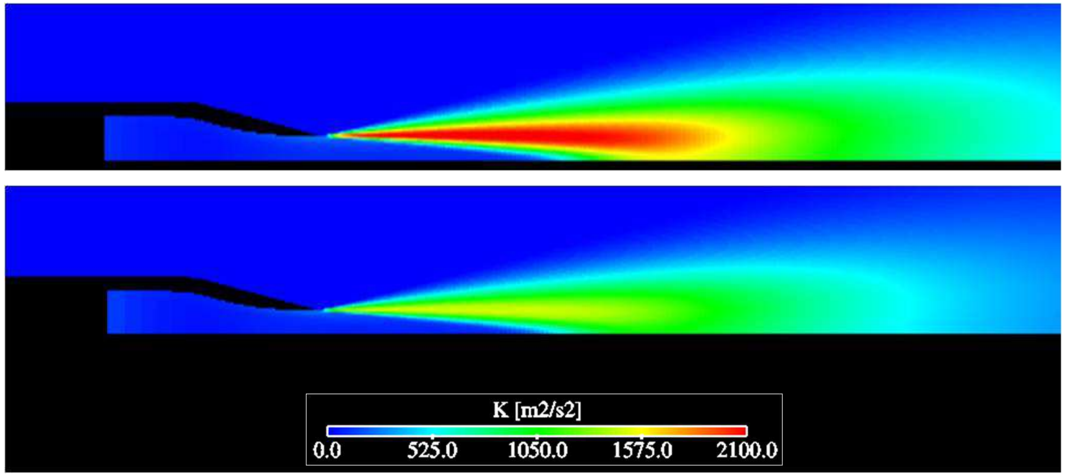

Isothermal jets
at $M = 0.75$ and $M = 0.9$

Cedre solver (ONERA), 45800 nodes, structured hexahedral mesh

Subsonic round jets

JEAN European program, Bodard / SNECMA (2009)

Acoustic spectra at $r = 30D$

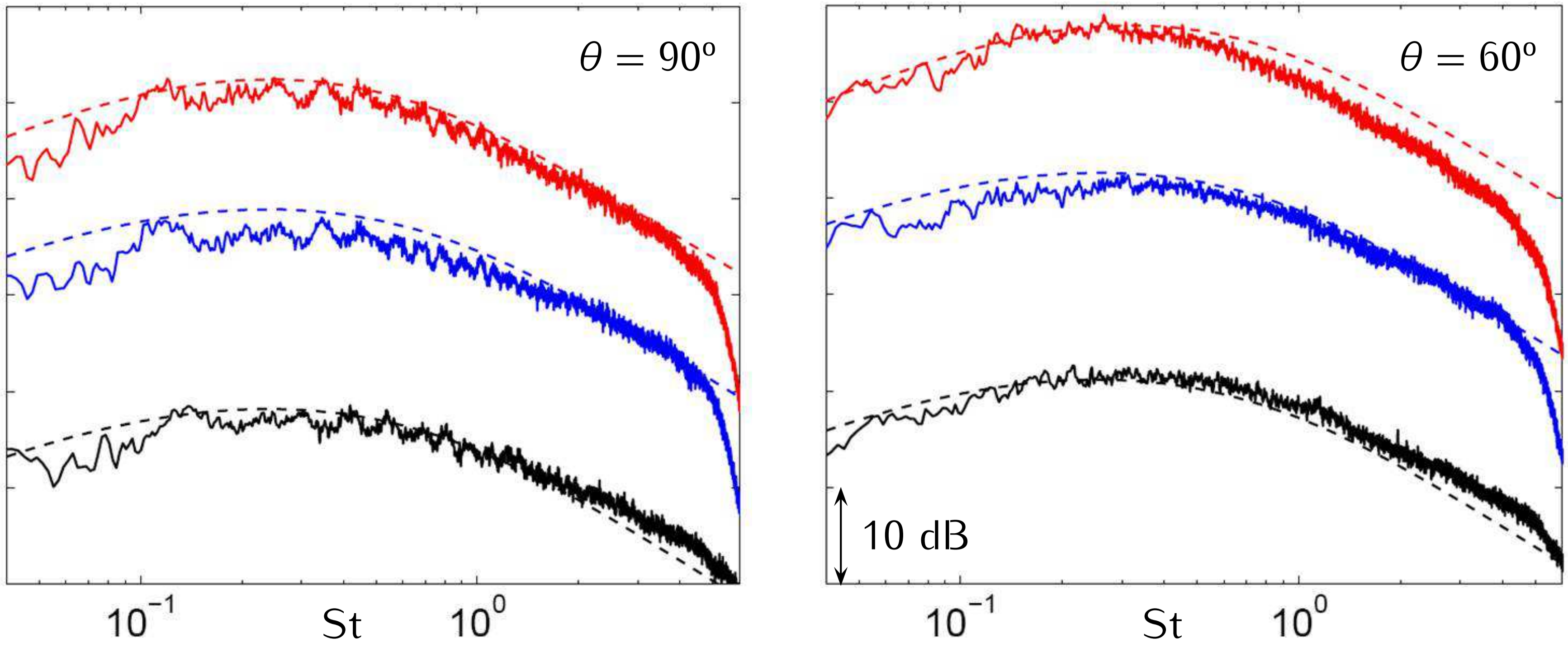

— $M = 0.75$, $T_j/T_\infty = 1$ — $M = 0.9$, $T_j/T_\infty = 1$ — $M = 0.9$, $T_j/T_\infty = 2$

- - - simplified Tam & Auriault model

- The $k_t - \omega -$ SST (shear-stress transport) model

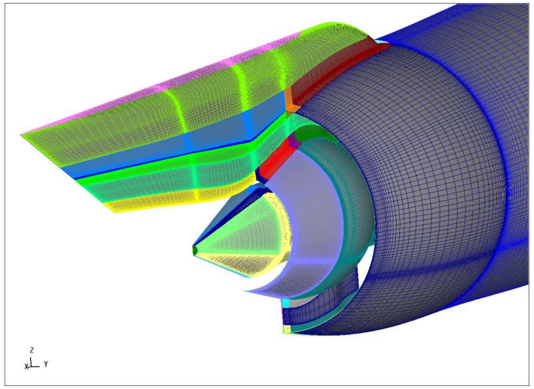

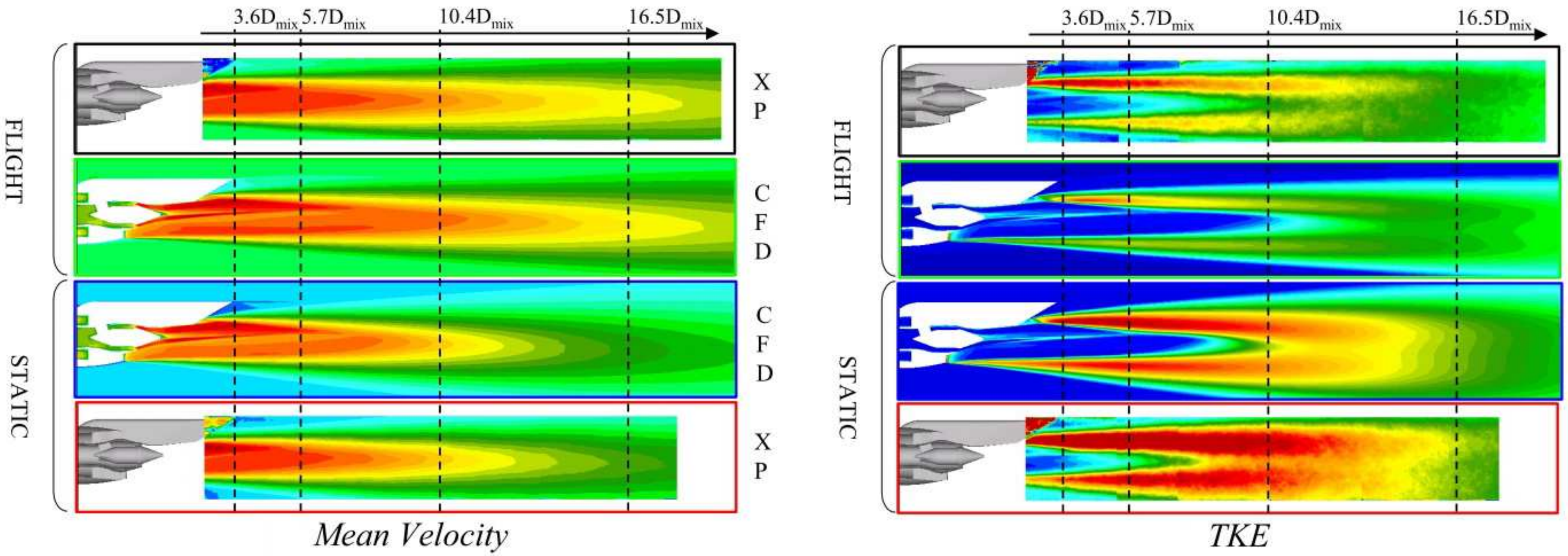

Dezitter *et al.*, AIAA Paper 2009-3370 (VITAL project)

- The $k_t - \omega - SST$ (shear-stress transport) model

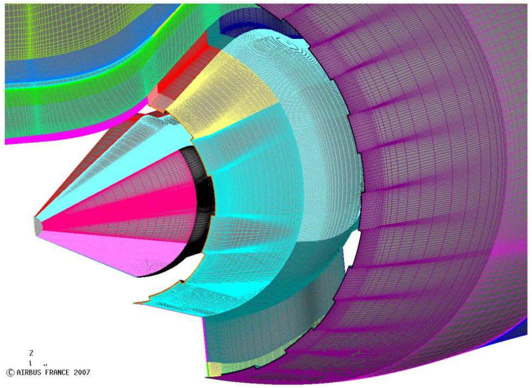

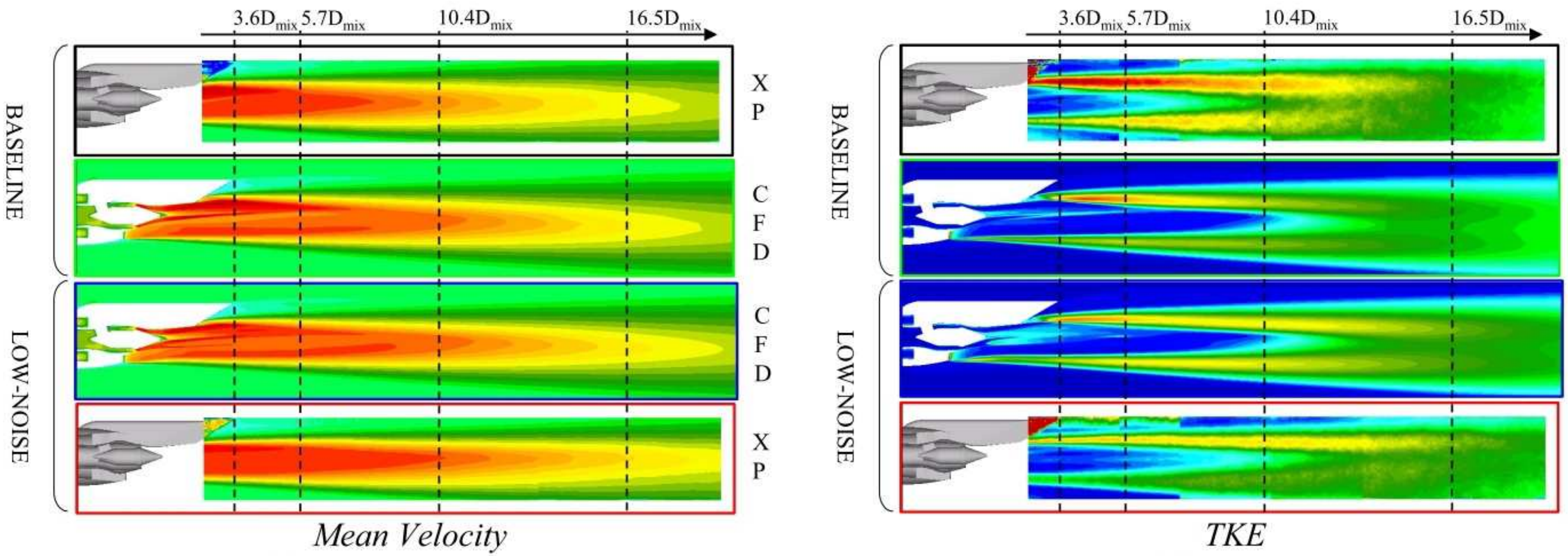

Dezitter *et al.*, AIAA Paper 2009-3370 (VITAL project)

Critical analysis : the devil is in the details !

Mean flow effects :
numerical computation of the Green function

Generalization to more complex flow :
co-axial jets, flight effects, noise reduction devices, ...

Fidelity of RANS turbulence models, calibration of the acoustic model,
correlation tensor $R_{ijkl}(\boldsymbol{y}, \boldsymbol{\eta}, \tau)$

Miller, 2014, *AIAA Journal*, **52**(10), 2143-2164
Miller, 2014, *J. Sound Vib.*, **333**, 1193-1207
Depuru Mohan *et al.*, 2015, *AIAA Journal*, **53**(9), 2421-2436

Space-time velocity correlations by dual-PIV

(Fleury *et al.*, *AIAA Journal*, 2008)

$Re_D = 7.5 \times 10^5$, $M = 0.9$, $D = 3.8$ cm, $\delta_\theta / D|_{\text{init}} \simeq 3 \times 10^{-3}$
At $x = 5D$, $L_{11}^{(1)} \simeq 0.27D$, Kolmogorov scale $l_\eta \simeq 10^{-4} D$

Space-time second-order correlation functions $R_{11}(\boldsymbol{x}, \boldsymbol{\xi}, \tau)$ and $R_{22}(\boldsymbol{x}, \boldsymbol{\xi}, \tau)$ measured at $\boldsymbol{x} = (6.5D, 0.5D)$

$L_{11}^{(1)} \simeq 2\delta_\theta \quad L_{22}^{(1)} \simeq \delta_\theta$

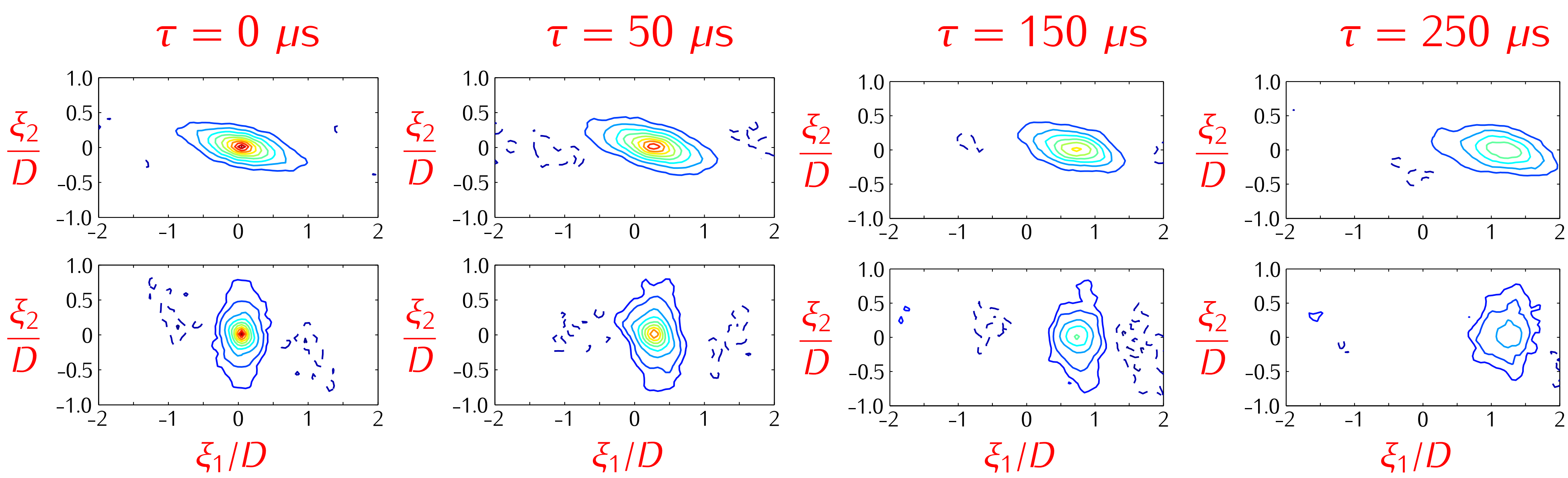

- High fidelity flow/noise simulation in a physically and numerically controlled environment

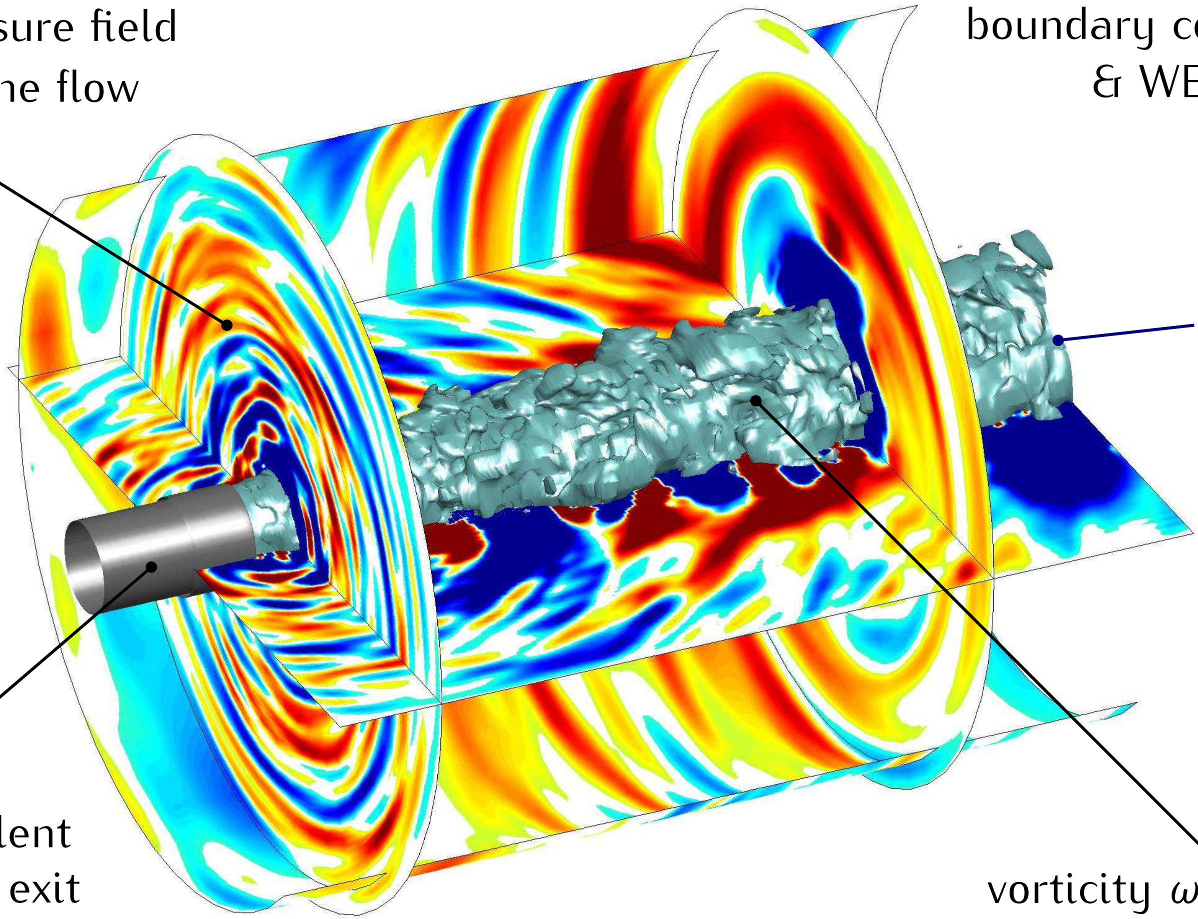

Barré *et al., Int. J. AeroAcous.* (2006)
Bogey & Bailly, *J. Fluid Mech.* (2007)

Direct Noise Computation of coplanar coaxial hot jets (CoJen)

- Velocities $V_p = 404.5$ m.s^{-1} and $V_s = 306.8$ m.s^{-1}
- Temperatures $T_{sp} = 775.6$ K and $T_{ss} = 288.1$ K
- AR = 3, VR = 0.759
- Reynolds number $\mathrm{Re}_{D_2} = V_s D_2/\nu = 10^6$ $D_2 = 4.9$cm
- Grid of 14×10^6 points & 400,000 time steps, $T = 0.03$s
  1800h CPU Nec-SX5

Bogey *et al.*, 2009, *Phys. Fluids*, 21

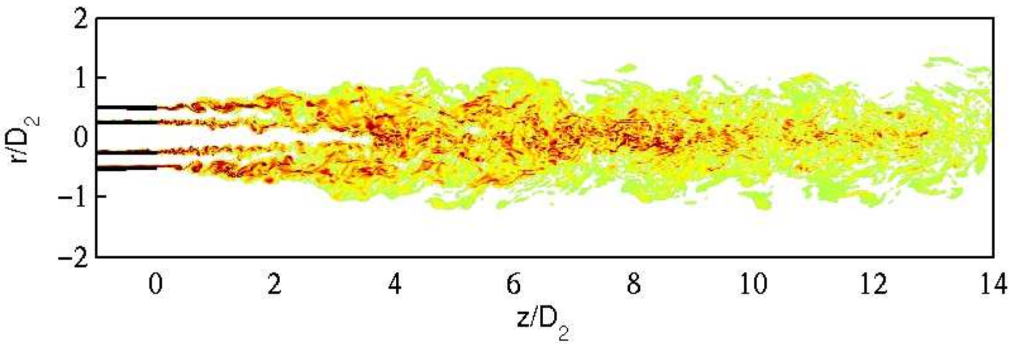

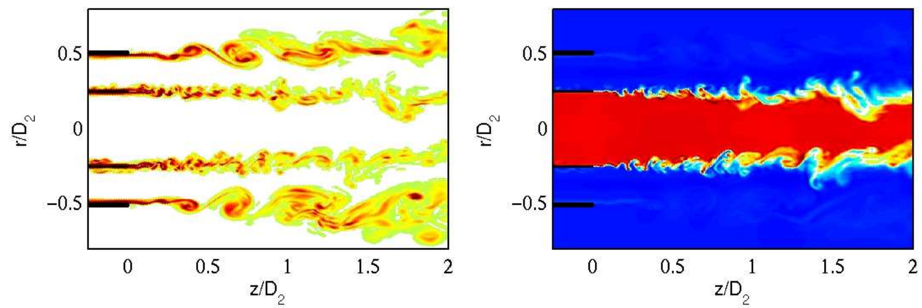

snapshot of vorticity norm & temperature

WEM at $60D_2$ from LES results (LEE, 102×10^6 pts)

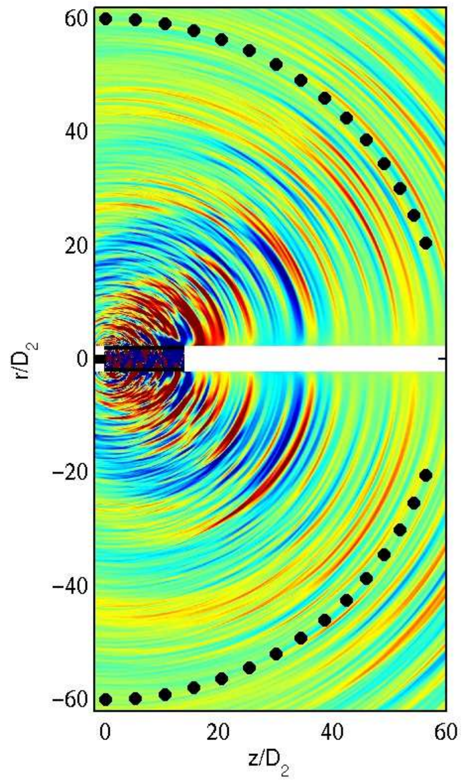

Pressure spectra at $\theta = 30°$

— experimental data (QinetiQ, UK)

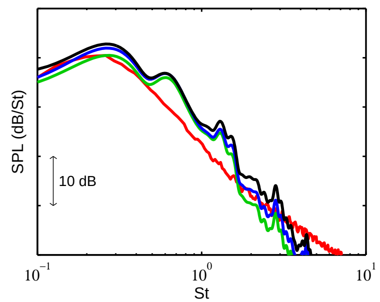

$r = 2D_2$

$r = 3D_2$

$r = 4D_2$

Influence of exit boundary-layer thickness

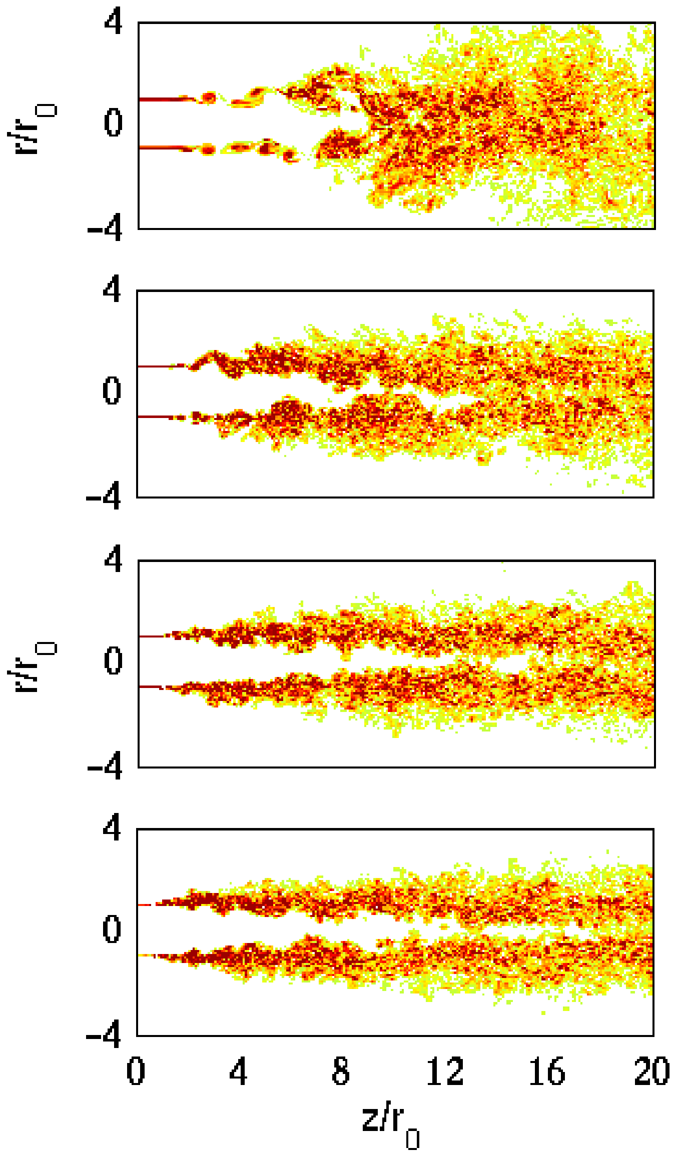

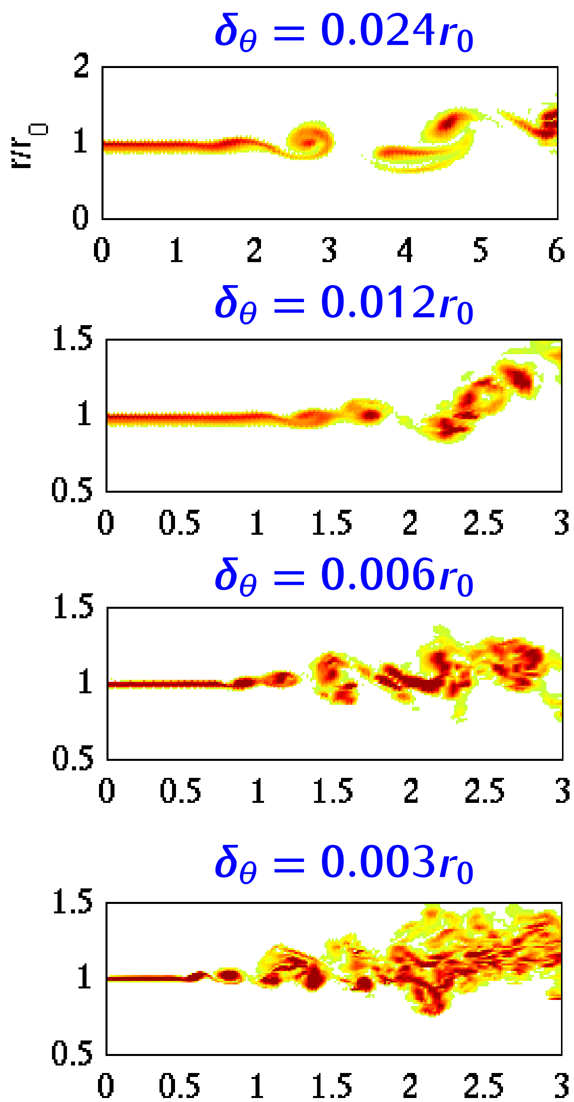

$M = 0.9 \quad Re_D = 10^5$

$\sigma_{u_e} \leq 1\%$

- Smaller shear-layer thickness results in delayed jet development and longer potential core
- All transitions are characterized by shear-layer rolling-up and a first stage of strong vortex pairings

Bogey & Bailly,
J. Fluid Mech., 2010, **663**

Influence of the initial turbulence levels

$M = 0.9 \quad \mathrm{Re}_D = 10^5 \quad \delta_\theta / r_0 = 1.8\%$

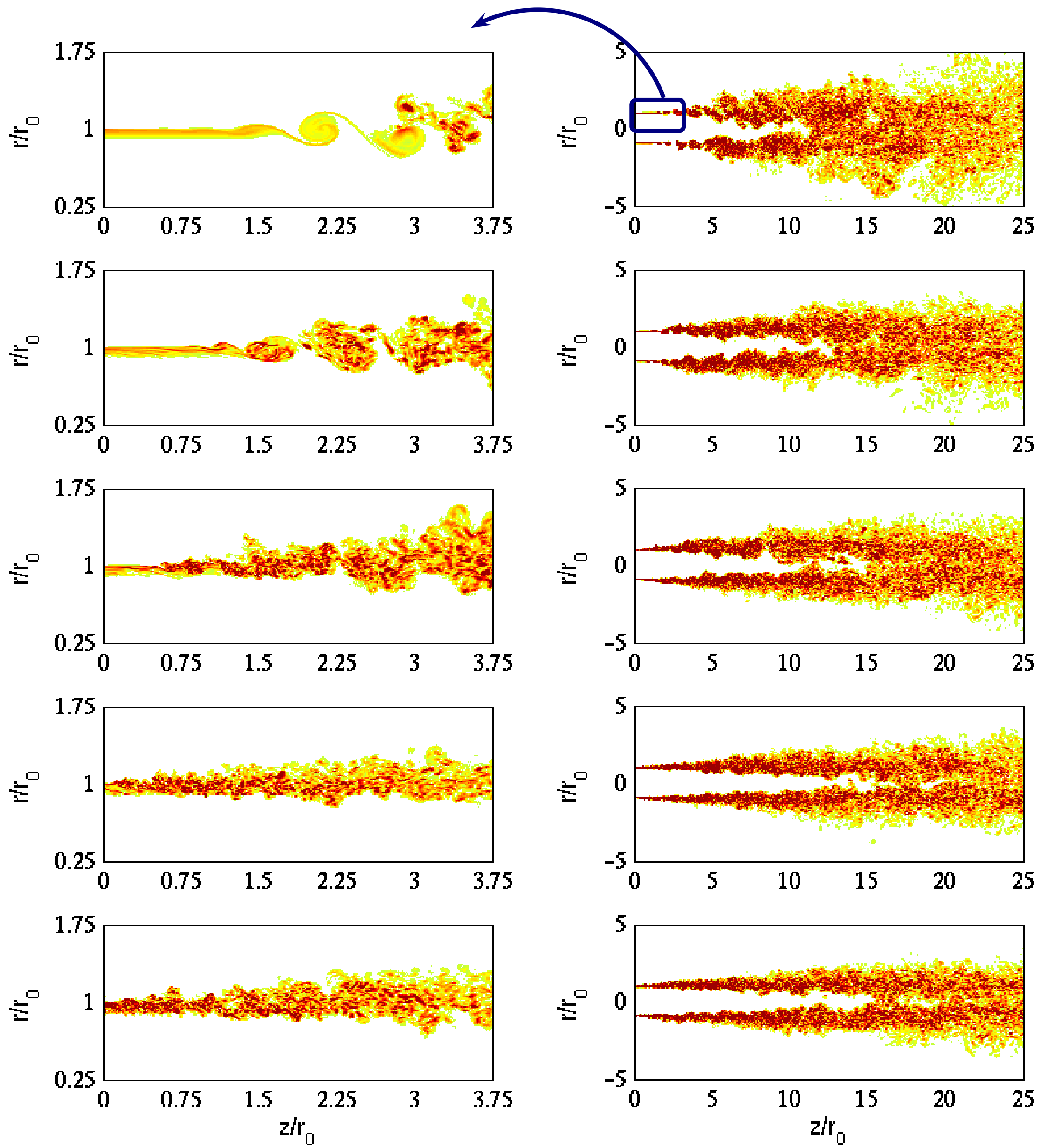

$$\sigma_{u_e} = 0\%,\ 3\%,\ 6\%,\ 9\%,\ 12\%$$

$$n_r \times n_\theta = n_z = 256 \times 1024 \times 962$$
$$= 252 \text{ million pts}$$

- as the exit turbulence level increases, coherent structures (and consequently vortex rolling-ups and pairings) gradually disappear
- higher initial turbulence levels lead to longer potential cores

  from $L_c = 9.3 r_0$ for $\sigma_{u_e} = 0\%$
  to $17 r_0$ for $\sigma_{u_e} = 12\%$

Influence of the initial turbulence levels

$M = 0.9$ $\mathrm{Re}_D = 10^5$ $\delta_\theta / r_0 = 1.8\%$

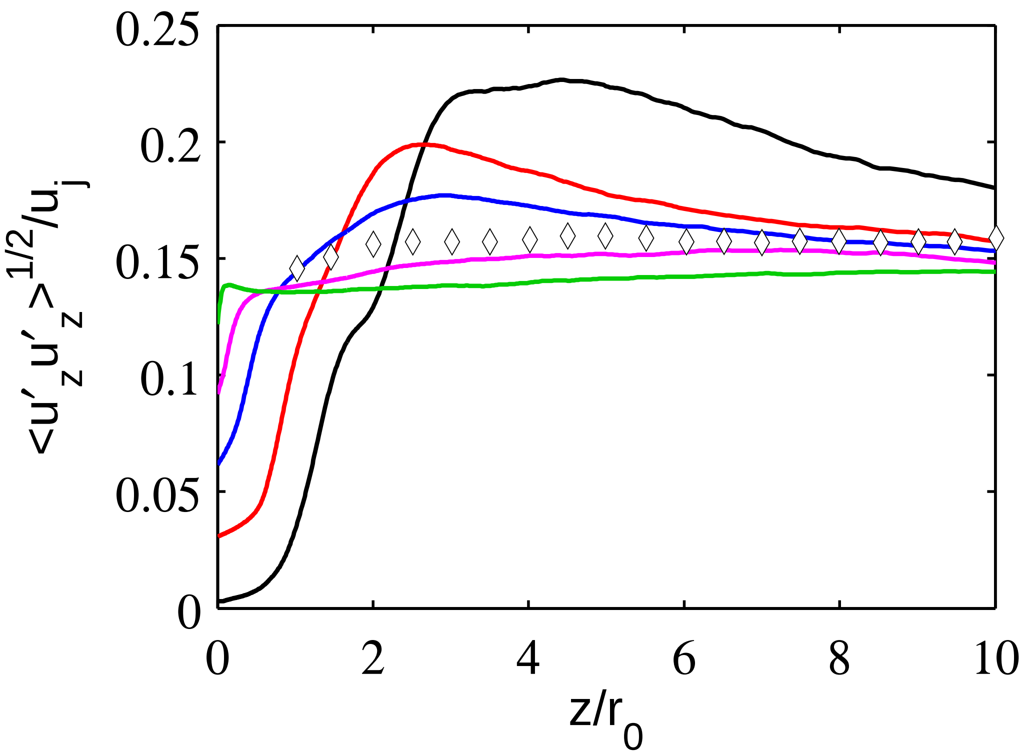

u'_z / u_j along $r = r_0$

$\sigma_{u_e} = 0\%$
$\sigma_{u_e} = 3\%$
$\sigma_{u_e} = 6\%$
$\sigma_{u_e} = 9\%$
$\sigma_{u_e} = 12\%$

$\diamond$ Fleury *et al.*, *AIAA Journal* (2008), $M = 0.9$ & $\mathrm{Re}_D = 7.7 \times 10^5$

- as the initial turbulence level increases, the shear layers develop more slowly with lower rms velocity peaks (from 22.6% to 14.5% of u_j)

Computing initially fully turbulent jets is still a challenge

$M = 0.9 \quad \mathrm{Re}_D = 10^5 \quad \delta_\theta / r_0 = 1.8\% \quad Re_{\delta_\theta} = 900 \quad \sigma_{u_e} = 9\%$

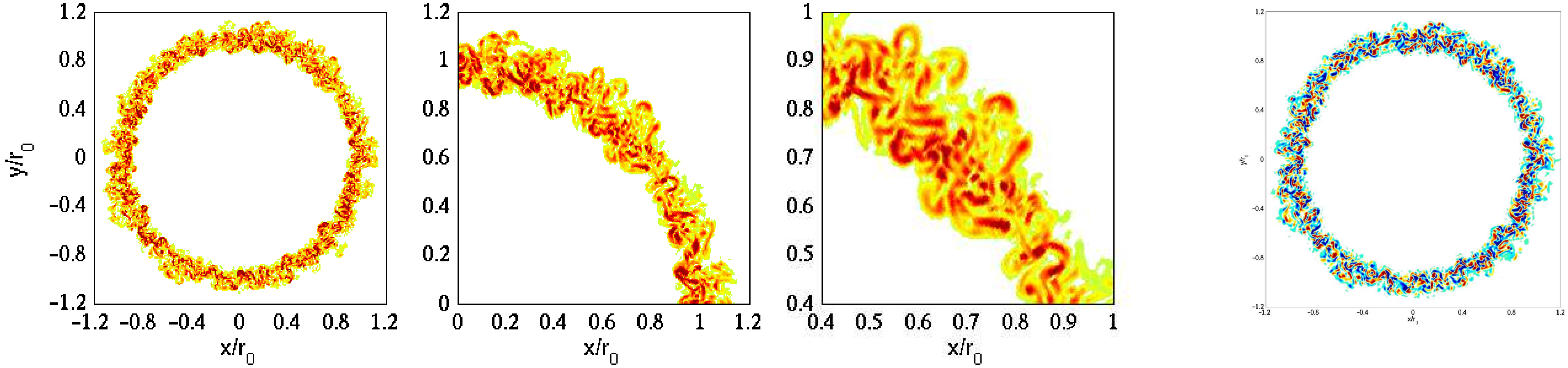

snapshots of vorticity norm ω and ω_z component at $x = r_0$

- Large scales, *i.e.* integral length scales $L^{(\theta)}_{u_i u_i}$, must be well discretized

  $\rightsquigarrow$ mesh grid should be nearly isotropic near the nozzle exit

  Δr, $r_0 \Delta\theta$ and $\Delta z < \delta_\theta / 2$ seems recommended

  $n_r \times n_\theta \times n_z = 256 \times 1024 \times 962$

Bogey *et al.*, *Phys. Fluids* (2011)

- **Work done by the instructors**
  regarding the direct computation of subsonic jet noise
  http://acoustique.ec-lyon.fr

Bogey, C., Bailly, C. & Juvé, D., 2003, *Theoret. Comput. Fluid Dyn.*, 16(4), 273-297
Bogey, C. & Bailly, C., 2006, *Theoret. Comput. Fluid Dyn.*, 20(1), 23-40
Bogey, C. & Bailly, C., 2006, *Phys. Fluids*, 18, 065101, 1-14
Bogey, C. & Bailly, C., 2006, *Comput. & Fluids*, 35(10), 1344-1358
Bogey, C. & Bailly, C., 2007, *J. Fluid Mech.*, 583, 71-97
Bogey, C., Barré, S. & Bailly, C., 2008, *Int. J. Aeroacoustics*, 7(1), 1-22
Bogey, C., Barré, S., Juvé, D. & Bailly, C., 2009, *Phys. Fluids*, 21, 035105, 1-14
Bogey, C. & Bailly, C., 2010, *J. Fluid Mech.*, 663, 507-538
Bogey, C., Marsden, O. & Bailly, C., 2011, *Phys. Fluids*, 23, 035104, 1-20 & 23, 091702
Bogey, C., Marsden, O. & Bailly, C., 2012, *Phys. Fluids*, 24, 105107, 1-24
Bogey, C. & Marsden, O., 2013, *Phys. Fluids*, 25, 055106, 1-27
Bühler, S., Kleiser, L. & Bogey, C., 2014, *AIAA Journal*, 52(8), 1653-1669
Bogey, C. & Marsden, O., 2016, *AIAA Journal*, 54(4), 1299-1312

- Application of the causality method to LES data :
  identification of noise-source mechanisms by establishing direct links between turbulent flow events and emitted sound waves

Experimental works : Siddon & Rackl (1971), Lee & Ribner (1972), Seiner (1974), Hurdle *et al.* (1974), Dahan *et al.* (1978), Schaffar (1979), Richardz (1980), Juvé *et al.* (1980), Panda (2002–2005)

Hileman *et al.* (2001 – 2007)
simultaneous visualizations of the flow and sound waves

- Normalized cross-correlation between **the jet turbulence at** $(\boldsymbol{x}_1, t_0)$ and **the radiated pressure at** $(\boldsymbol{x}_2, t_0 + \tau)$

$$C_{f-p'}(\boldsymbol{x}_1, \boldsymbol{x}_2, t) = \frac{\langle f(\boldsymbol{x}_1, t_0)\, p'(\boldsymbol{x}_2, t_0 + \tau)\rangle}{\langle f^2(\boldsymbol{x}_1, t_0)\rangle^{1/2} \langle p'^2(\boldsymbol{x}_2, t_0)\rangle^{1/2}} \qquad f = u'_i, u'_i u'_j, k, \omega, \ldots$$

- Application to the subsonic jets computed by DNC

  Bogey & Bailly, *J. Fluid Mech.*, 2007, **583**

- **Cross-correlation** between **radiated pressure** at point • ($\theta = 40^o$) and centerline **turbulence** at points +

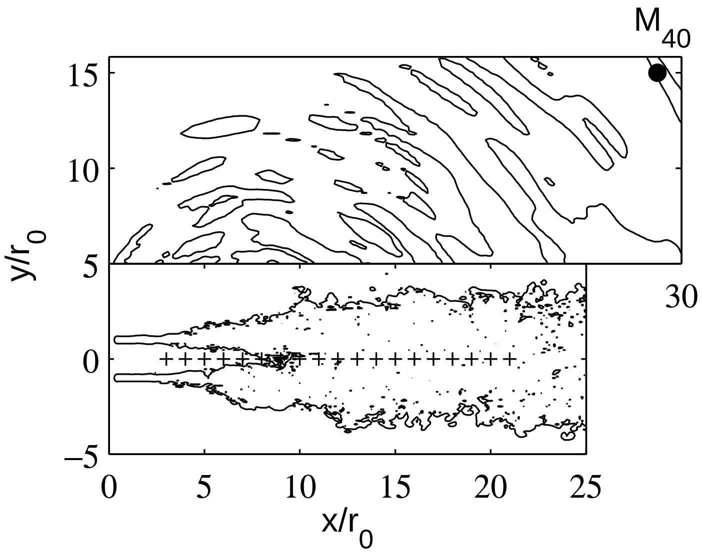

+ $\boldsymbol{x}_1 = (x, 0, 0)$

• $\boldsymbol{x}_2 = \mathrm{M}_{40}$ fixed

$C_{fp}(x/r_0, \tau u_j/D)$

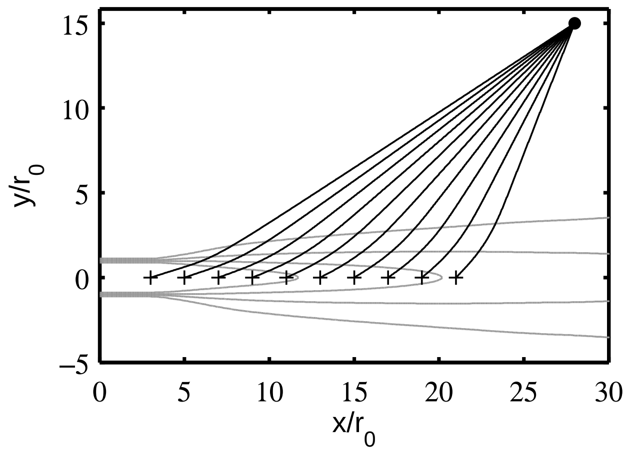

ray tracing for the estimation of the propagation time

$\mathrm{M} = 0.9 \quad \mathrm{Re} = 4 \times 10^5$

$x = x_c$ (end of potential core)

$\cdots$ time τ_{ray} along ray path

$C_{u'-p'}\,(\tau u_j/D)$

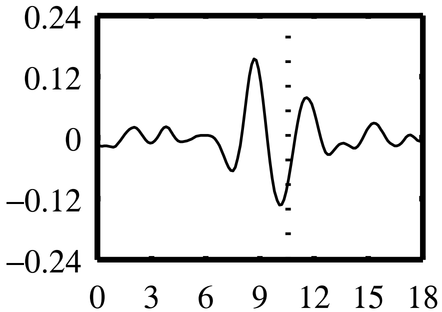

$C_{\omega-p'}\,(\tau u_j/D)$

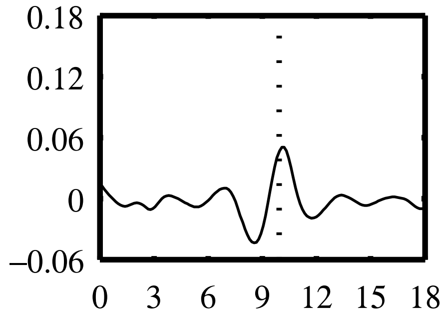

- **Cross-correlation** between **radiated pressure** at point • ($\theta = 40^o$) and centerline **vorticity** norm at points +

—— $\tau = \tau_{ray}(x)$

- - - $\tau(x) = \tau_{ray}(x_c) + \int_x^{x_c} \frac{dx}{u_{conv}(x)}$

.... end of the potential core

color scale : [-0.14 0.14]

Source convected along the jet axis, emission from the region at the end of the potential core (periodic intrusion of vortical structures, passage frequency of large turbulent scales)

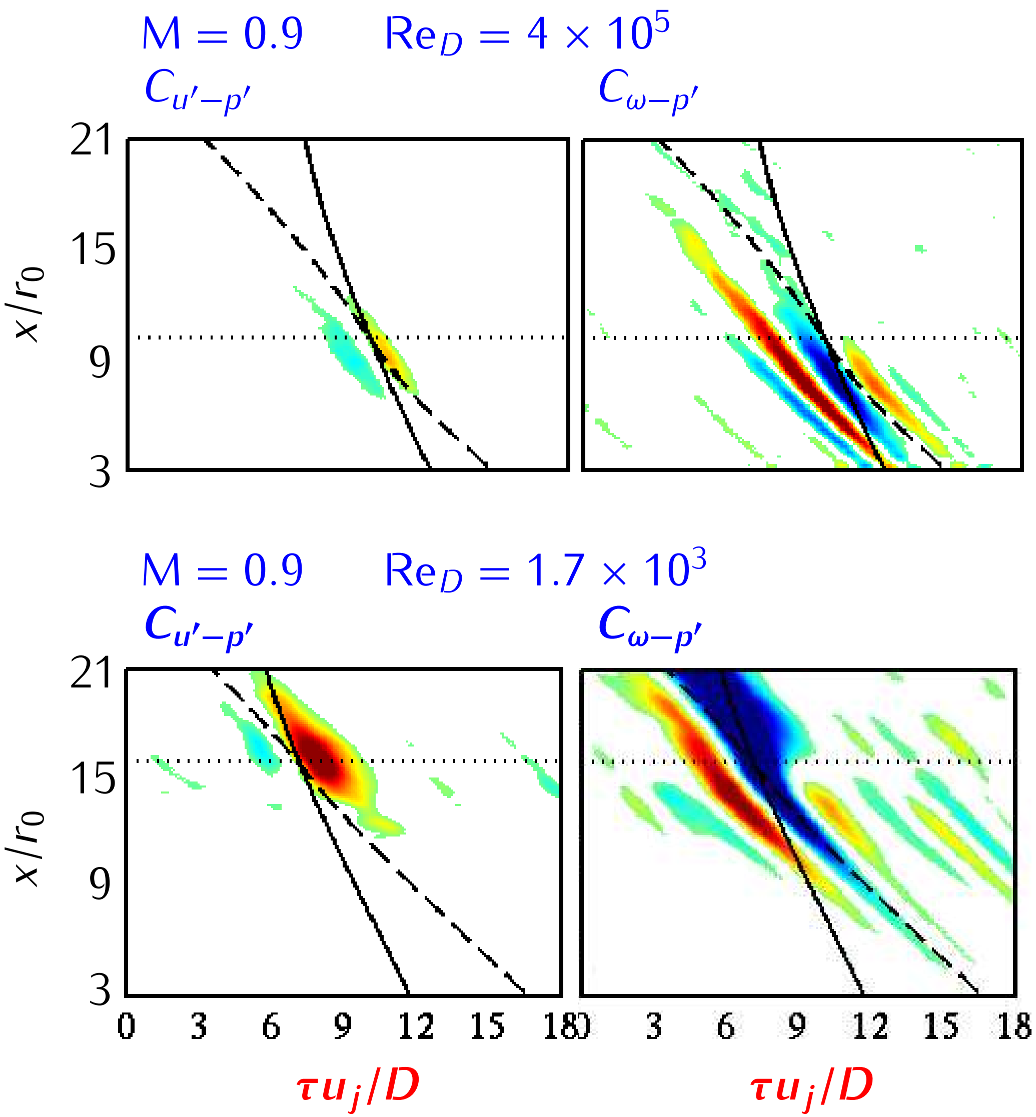

- **Work in progress : simulation of an experiment by Zaman (jfm, 2015)**
  (Bogey & Desjouy, rectangular jet interacting with a flat plate)

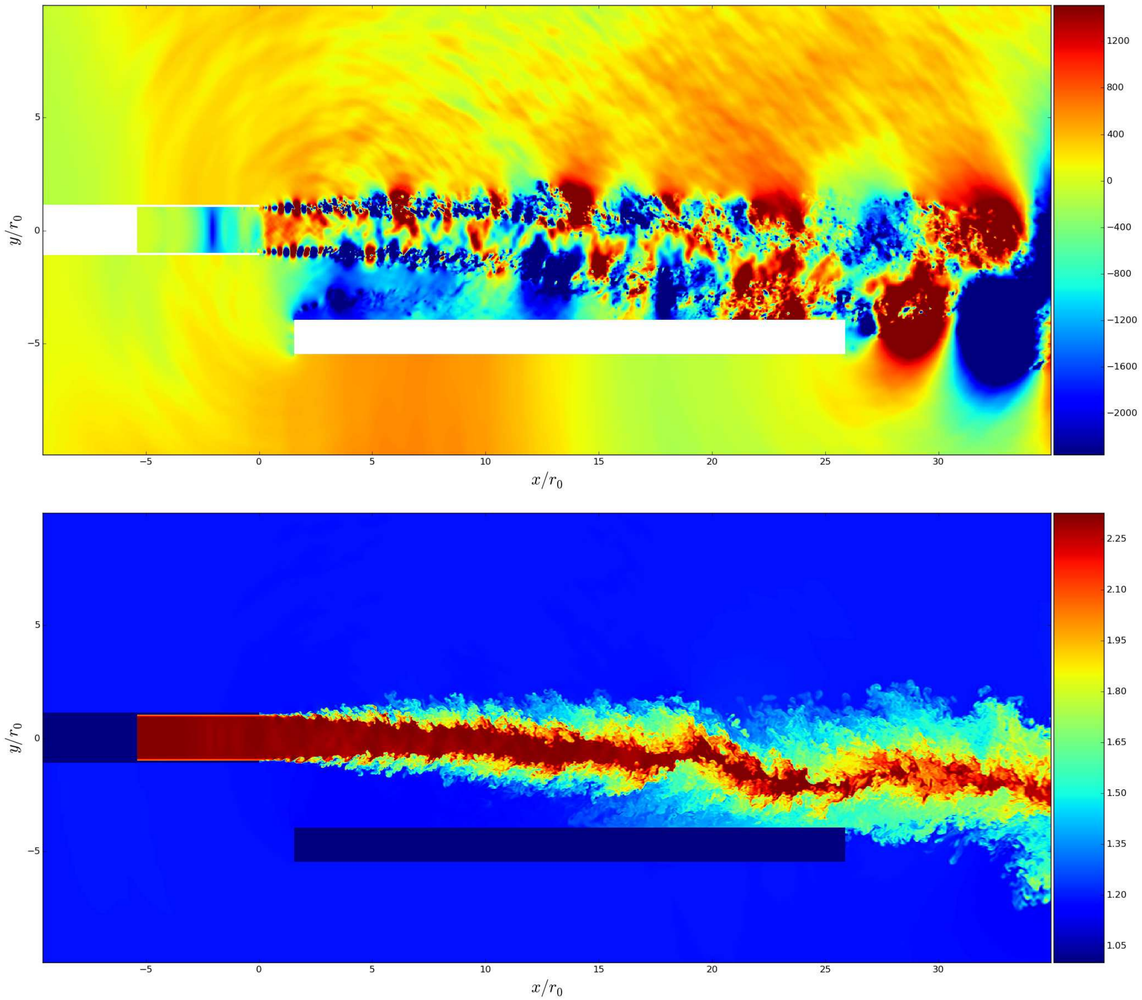

Supersonic jet noise

Bailly, C. & Fujii, K., 2016, High-speed jet noise, *Mechanical Engineering Reviews*, Journals of the Japan Society of Mechanical Engineers, **3**(1)

Supersonic jets

Ariane V ECA – CNES
flight 185 – 41st launch V – 2008

- acoustic environment of space launchers at lift-off and protection of payloads
- military aircrafts (*e.g.* hearing protection of naval crew on aircraft carrier deck)
- broadband shock-associated noise in cruise conditions : cabin noise

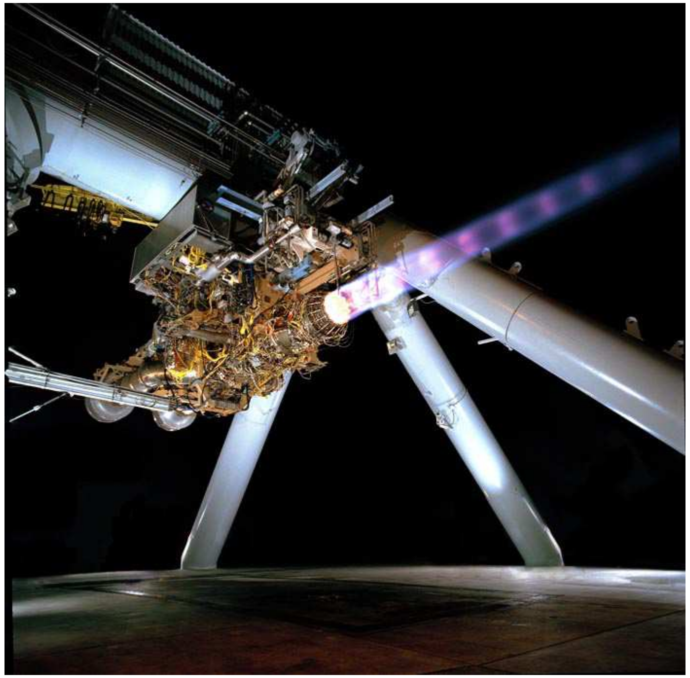

Pratt & Whitney FX631 jet engine (F-35 Joint Strike Fighter)
http://www.jsf.mil

Kleine & Settles, *Shock Waves* (2008)

Take off from aircraft carrier
(noise levels exceed 140 dB)

In aeronautical applications

Secondary flow of a commercial (civil) engine during the climb and cruise phases

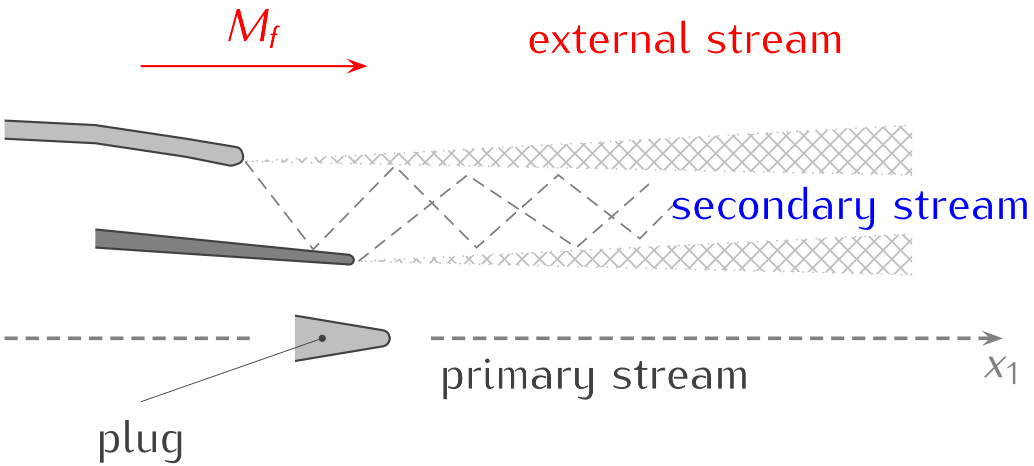

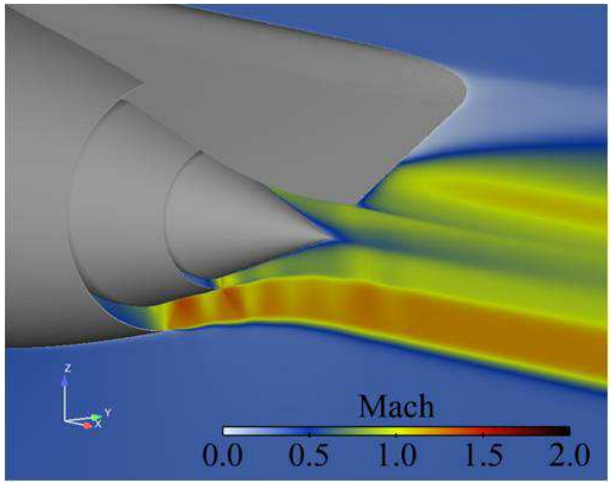

(C. Henry, SNECMA)

Supersonic flow if the NPR $= p_t/p_\infty > [(\gamma+1)/2]^{\gamma/(\gamma-1)}$

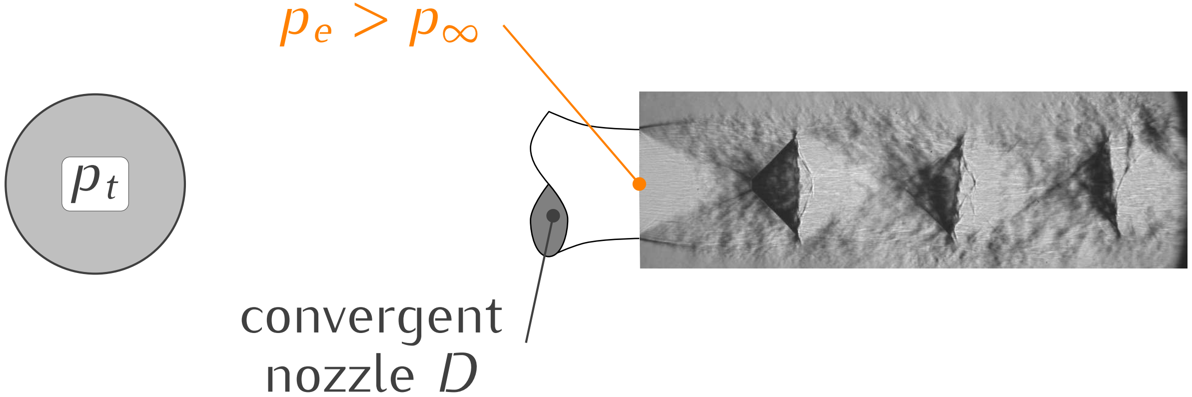

- **Jet at $M_j = 1.35$ – Acoustic spectra**

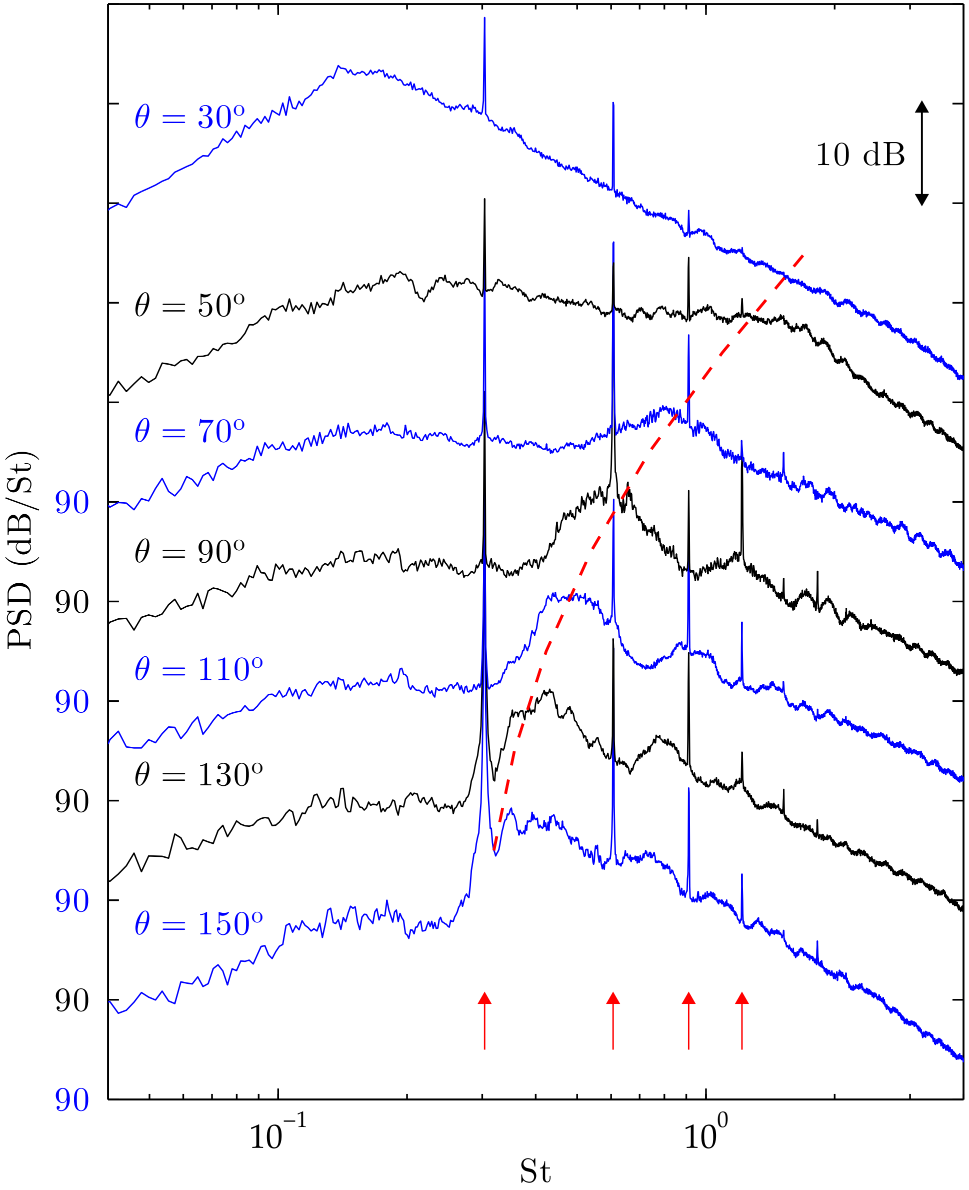

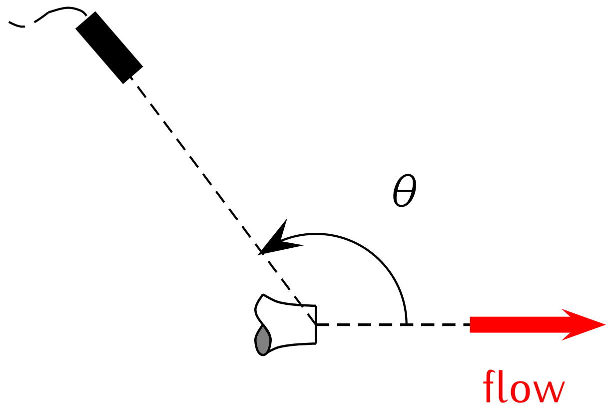

NPR = 2.97, $M_j = 1.356$, $M_d = 1.50$

($r = 53.2D_p$)

André *et al.*, *Phys. Fluids*, **23**, (2011)

- Jet at $M_j = 1.35$ – Acoustic spectrum

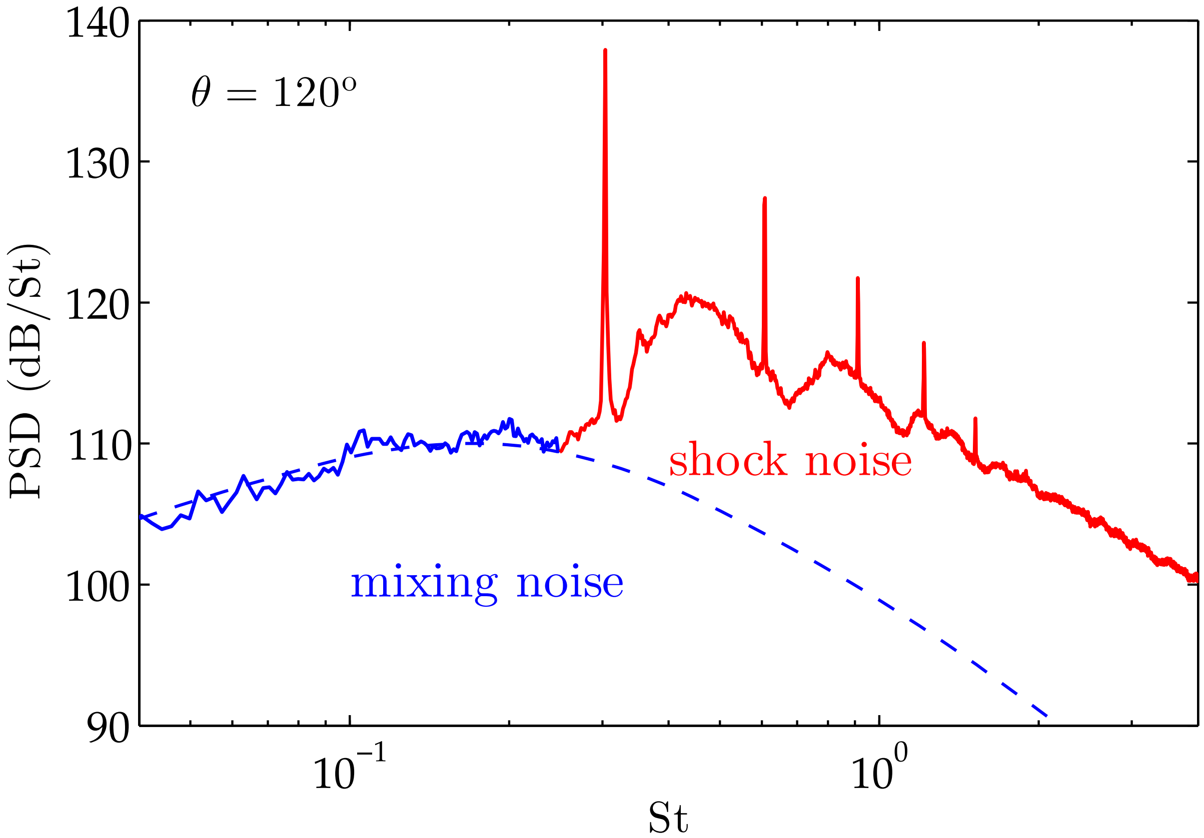

mixing noise (including Mach waves)

broadband shock-associated noise (BBSAN)

screech tones

Quasi-periodic shock-cell structure generated

expansion and compression waves trapped in the jet plume

$M_j = 1.35$ (notched nozzle, no screech)

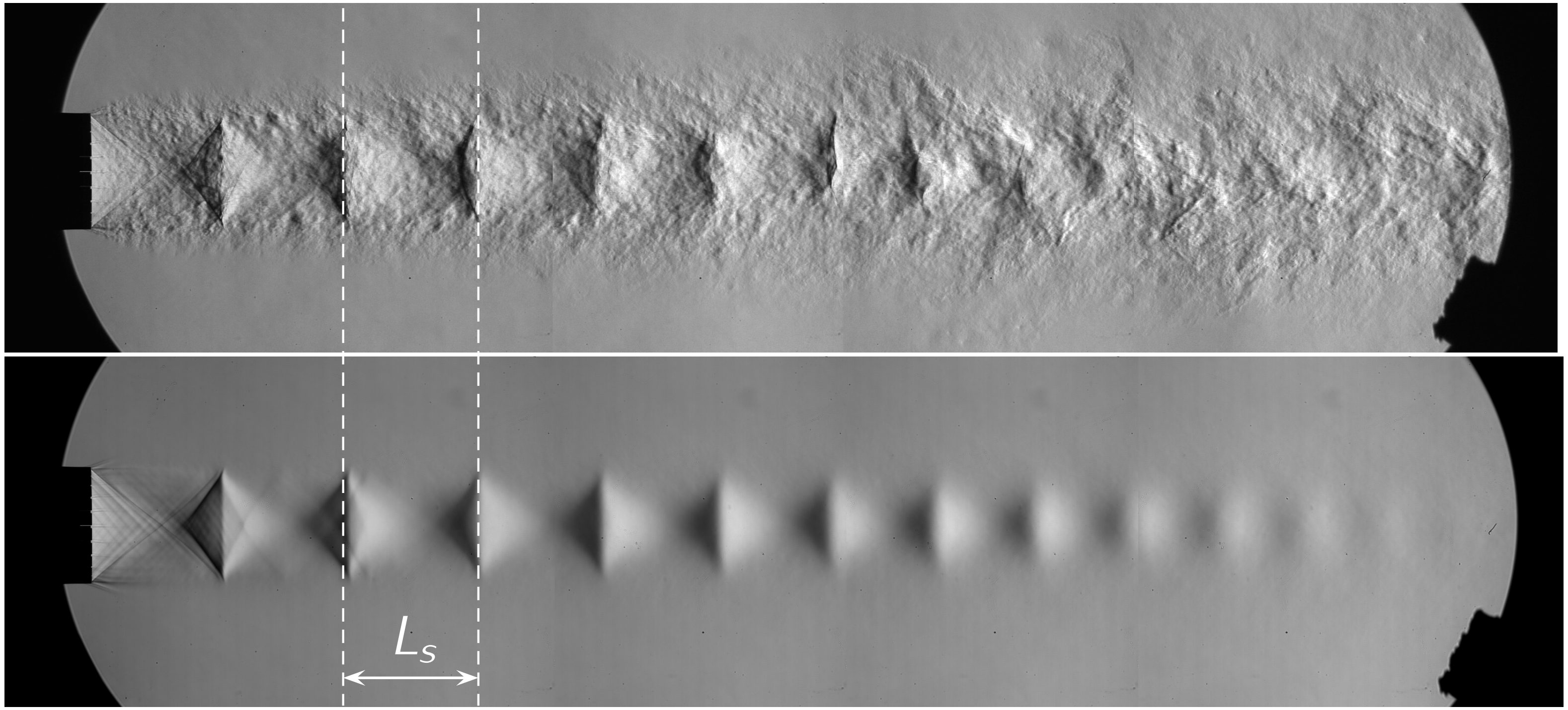

$T_e = 4\mu s$

$T_e \simeq 1 ms$

a shock cell

Z-type schlieren system

High-speed Phantom V12 CMOS camera, frame rate 20 kHz, exposure time 1 μs

& Sigma 120-400 mm lens

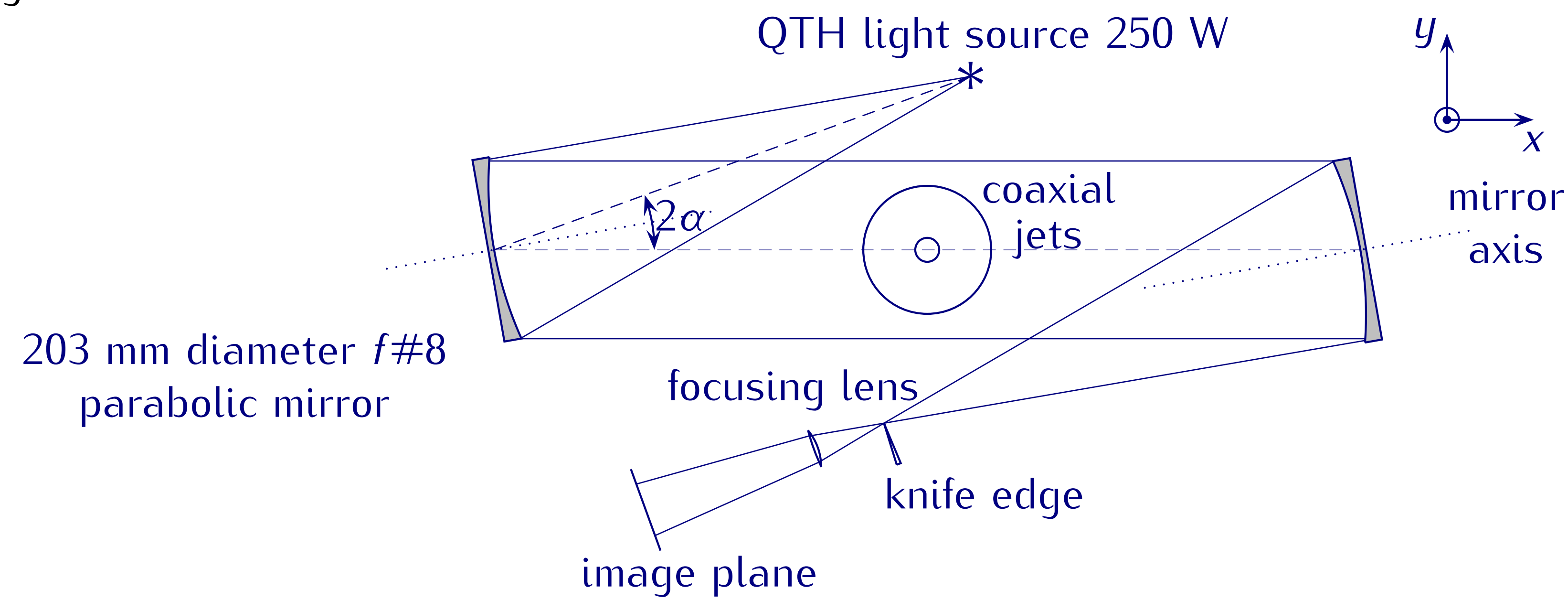

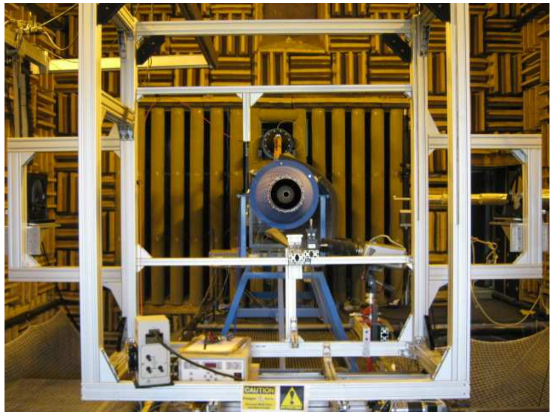

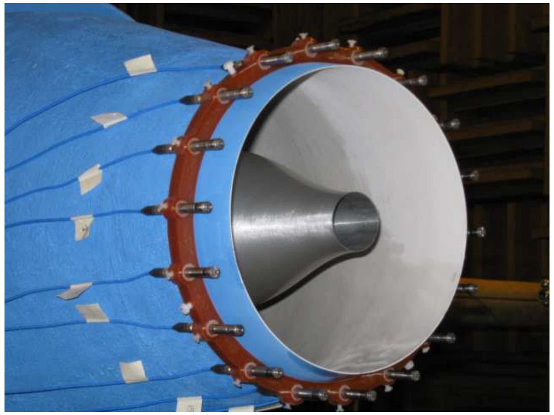

- Spark schlieren pictures (underexpanded screeching jets)

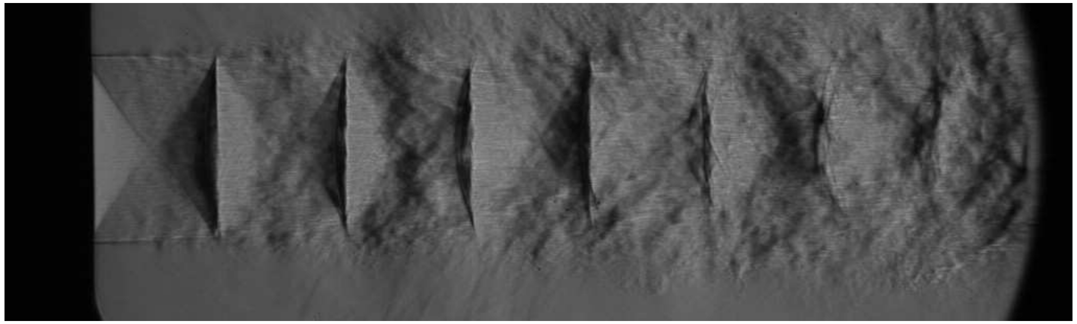

$\mathrm{NPR} = 2.27 \quad M_j = 1.15$

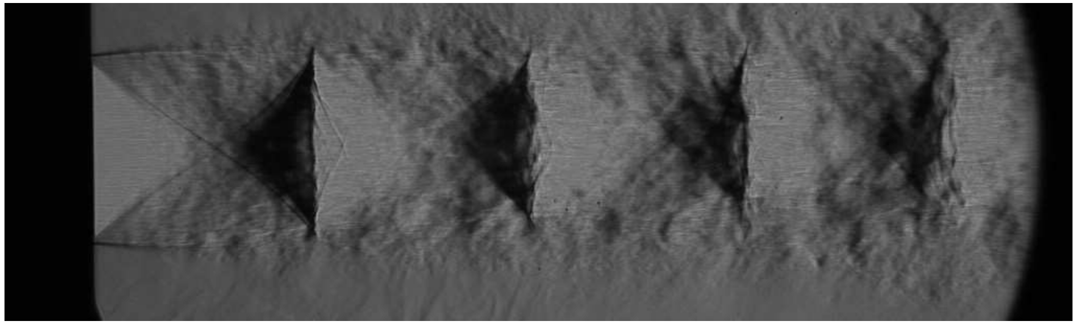

$\mathrm{NPR} = 2.97 \quad M_j = 1.35$

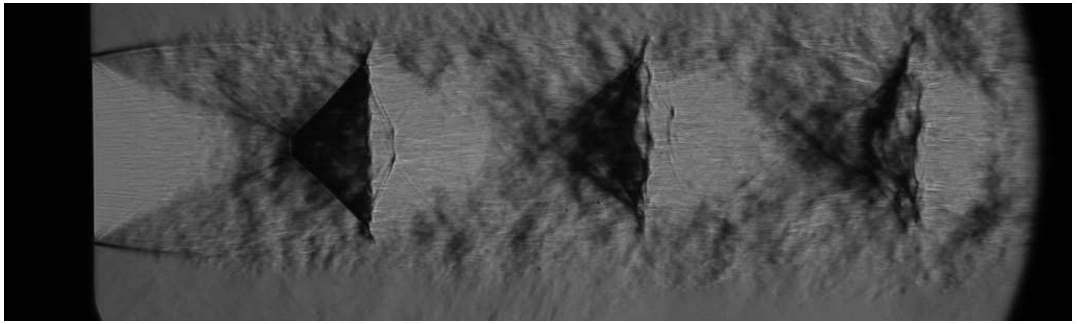

$\mathrm{NPR} = 3.68 \quad M_j = 1.50$

- Time-averaged schlieren images (underexpanded screeching jets)

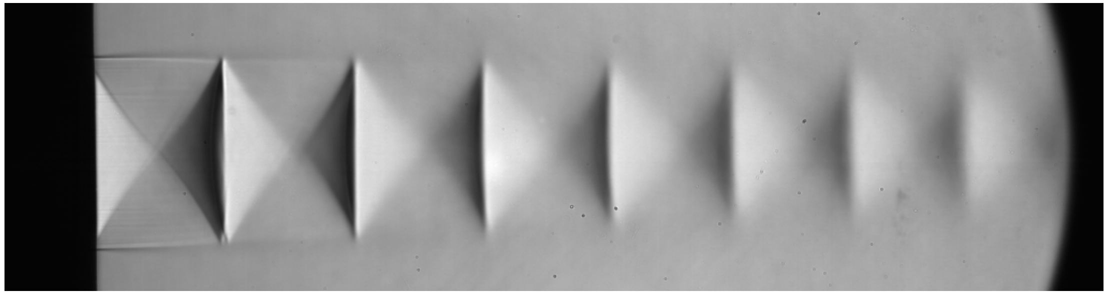

$M_j = 1.15$

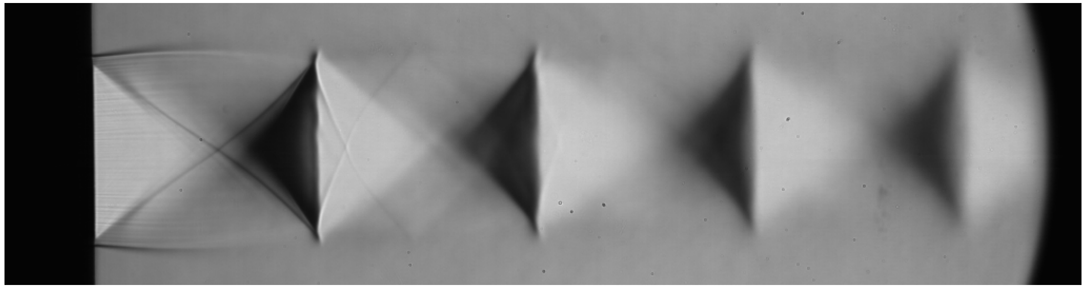

$M_j = 1.35$

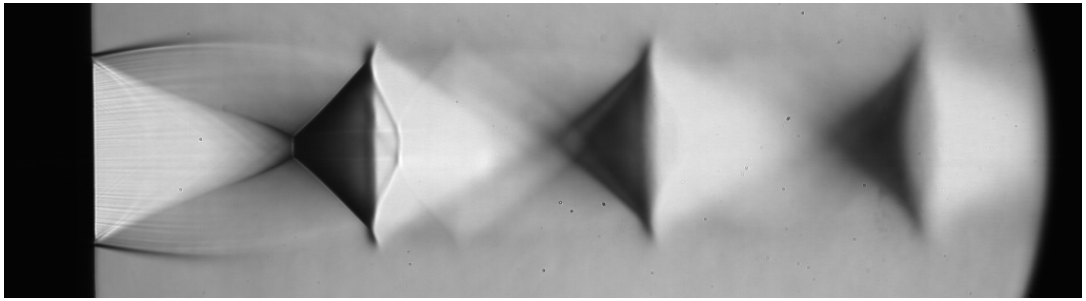

$M_j = 1.50$

- **Broadband shock-associated noise (& turbulence) affected by screech**

Far field acoustic spectra in dB/St

$r/D \simeq 52$, $M_j = 1.30$, $T_t = T_\infty$, $\mathrm{Re}_D = 1.2 \times 10^6$, $\theta = 110^o$

—— convergent nozzle ($M_d = 1$)

—— notched convergent nozzle to remove screech

– – – convergent-divergent nozzle ($M_d = M_j$) to remove shock-cell noise

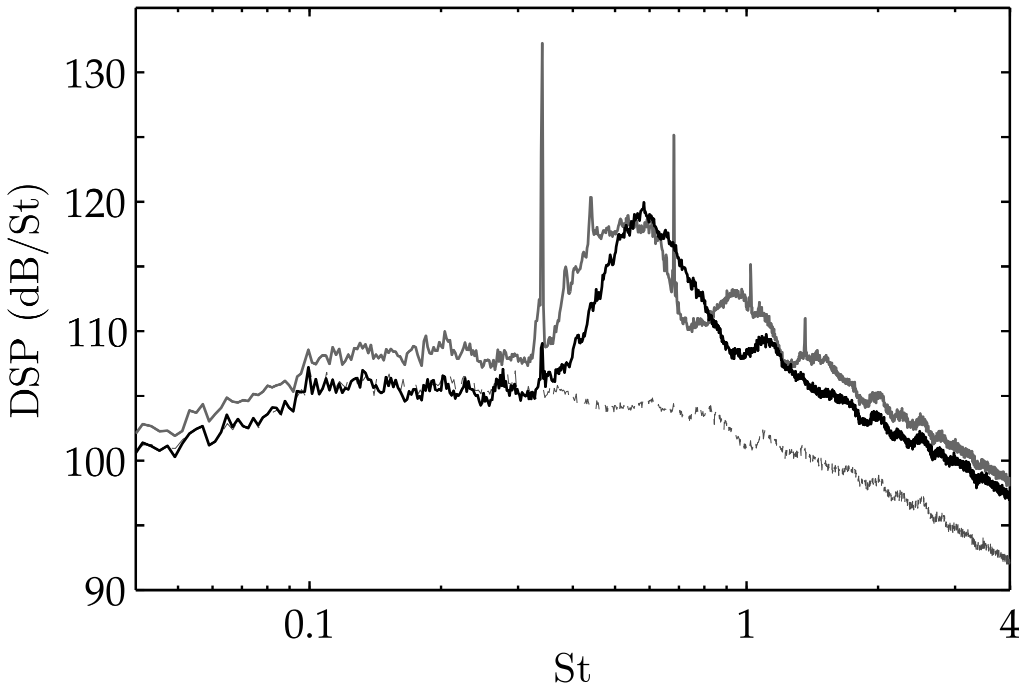

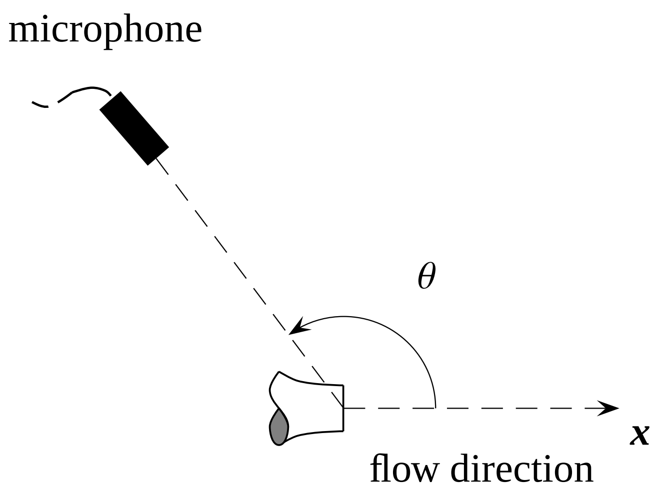

André, Castelain and Bailly (2013)

- **Supersonic mixing noise (perfectly expanded supersonic jet, $M_j = 1.30$)**

  Acoustic spectra measured at ▲ $\theta = 30^o$ and • $\theta = 90^o$

  – – – semi-empirical spectral shapes of Tam, Golebiowski and Seiner (1996)

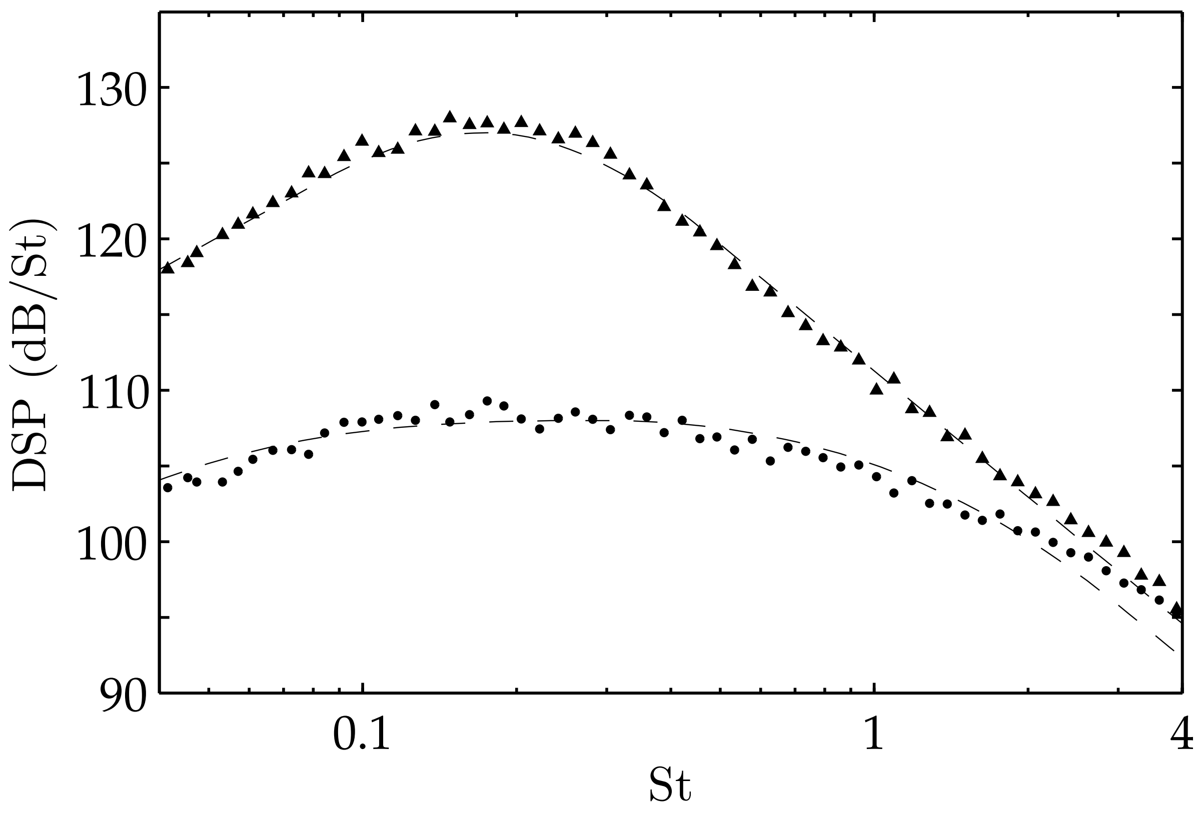

André, Castelain and Bailly (2013)

- **Screech mechanism**

  Screech seen as a self-sustained phenomenon (Powell, Proc. Phys. Soc. 1953)
  Feedback loop consists of (Raman, J. Fluid Mech. 1997)

  1. internal part : growth of vortical disturbances in mixing layer
  2. shock-turbulence interaction
  3. external part : feedback acoustic wave propagate toward nozzle
  4. initial shear layer excitation (*receptivity*)

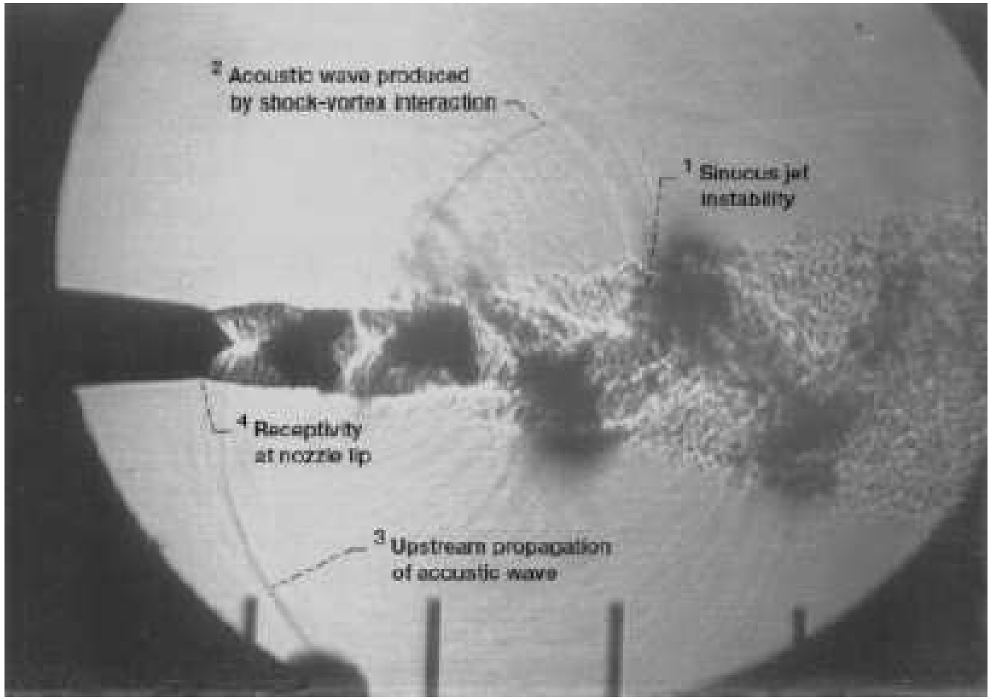

Screech modal behaviour

Modal behaviour of screech has long been identified
(Davies & Oldfield, Acustica 1962, Powell *et al.*, *J. Acous. Soc. Am.* 1992)

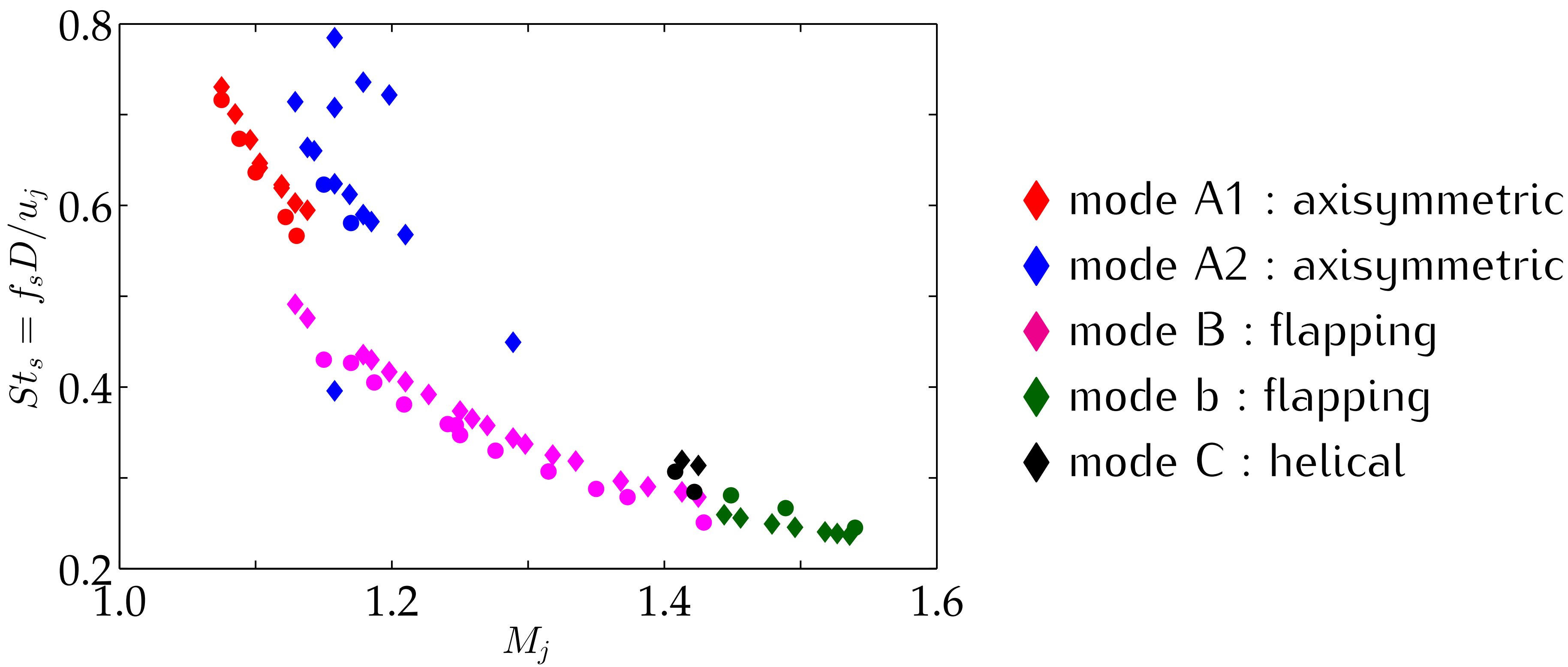

♦ André *et al.*, *Phys. Fluids*, **23**, (2011)
• Mercier *et al.* (EC-Lyon, 2016)

Underexpanded supersonic screeching jets

- **Flight effects : spark Schlieren pictures of the jet plume**

$M_j = 1.5 \;\; M_f = 0.$

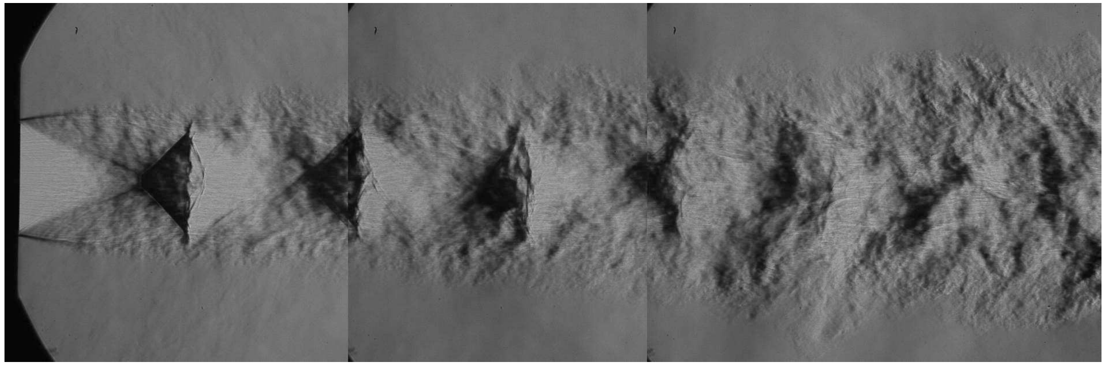

$M_j = 1.5 \;\; M_f = 0.39$ phase average

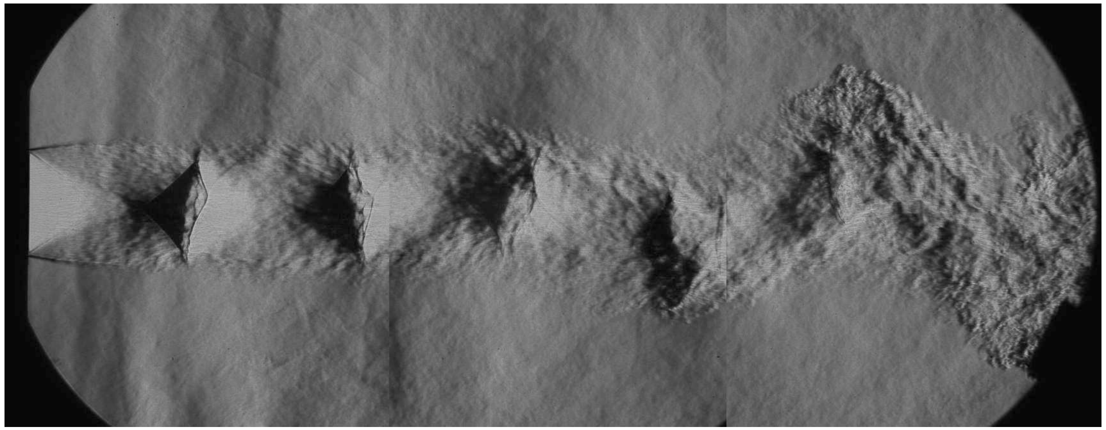

- **Direct link between large scale structures and the radiated noise**
  Large scale structures can be described by instability waves, well-established theoretically and experimentally

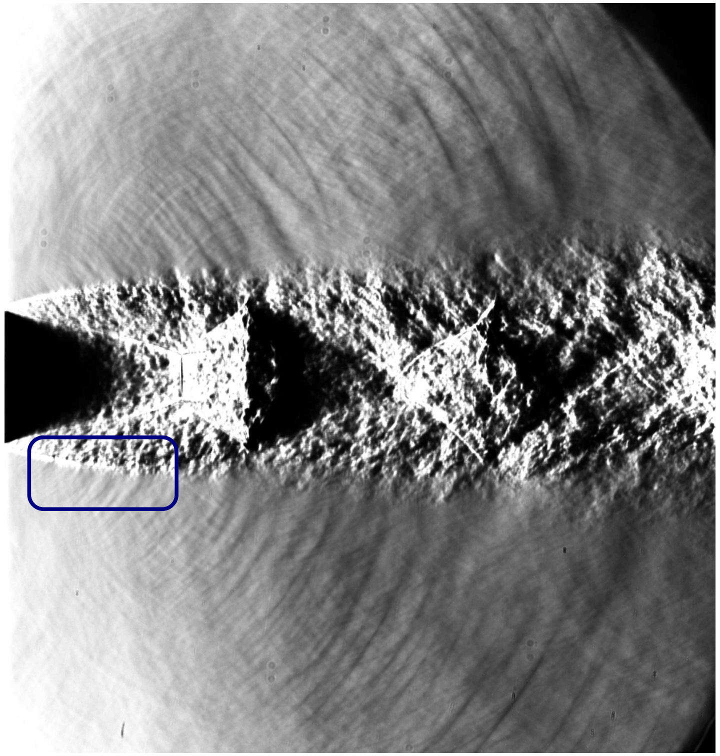

Strioscopy of an underexpanded supersonic jet (convergent nozzle), NPR = 5, $T_t = 293$ K, $D = 22$ mm, exposure time 20 ns.

Courtesy of ONERA DMAE 2008.

Mach wave radiation
(supersonic phase velocity)

$$\cos\theta = c_\infty / u_c = 1/M_c$$

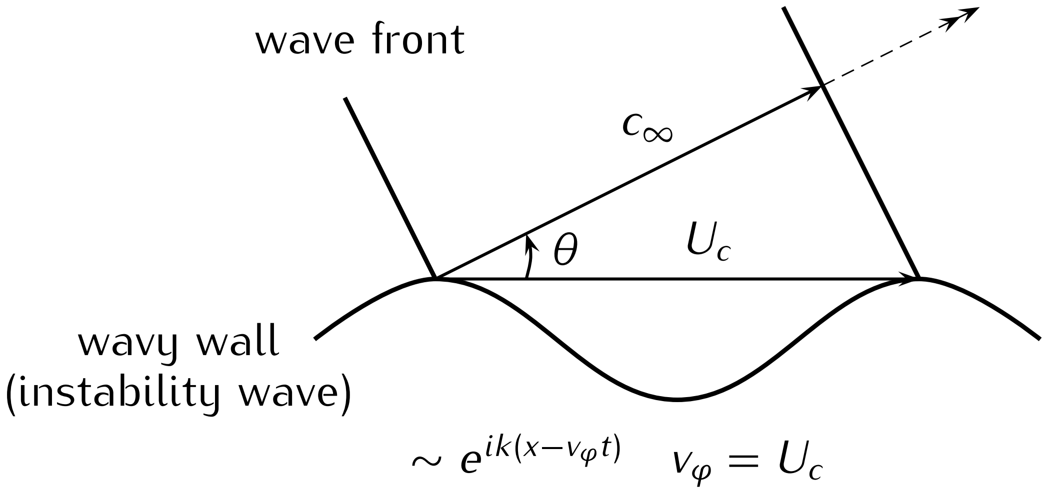

Radiation of instability waves

Tam & Morris (1980), Tam & Burton (1984), Tam & Hu (1990)

- Matching to the near acoustic field (dimensionless variables)

$$p'(z,r,\theta,t) = \int_{-\infty}^{+\infty} \hat{g}\,(\xi)\, H_n^{(1)}\left(i\lambda_\xi r\right) e^{i(\xi z + n\theta - \omega t)}\, d\xi \qquad \lambda_\xi = \sqrt{\xi^2 - \rho_\infty M_j^2 \omega^2}$$

$$\hat{g}\,(\xi) = \frac{1}{2\pi}\int_{-\infty}^{+\infty} A_0 \exp\left\{ i \int_0^z k(\omega, z')\, dz' \right\} e^{-i\xi z} dz \qquad \text{(wave packet)}$$

where k is provided by the (inviscid) stability theory

- Far-field radiation for $\xi \leq \xi_c$, peak noise angle $\cos\theta_p \simeq \xi_{\mathrm{peak}}/(\rho_\infty^{1/2} M_j \omega)$

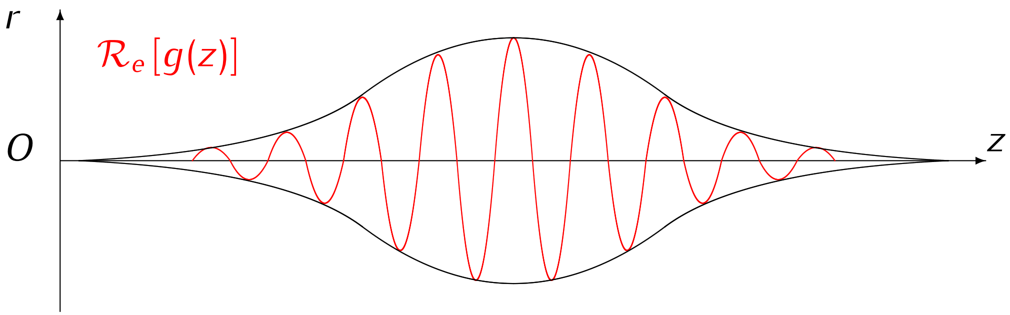

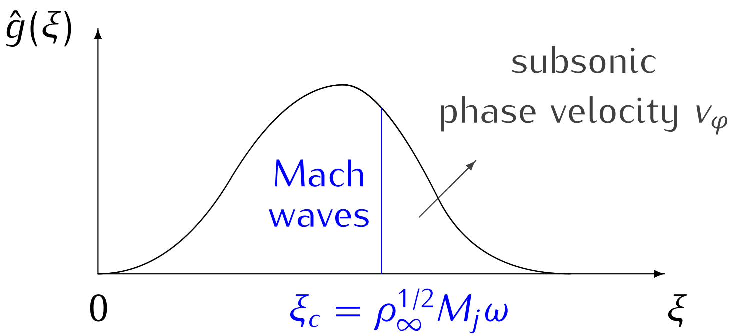

- **Radiation of instability waves by solving linearized Euler's equations**
  Eggers (1966), 3-D jet, M= 2.22, T_j/T_∞, St=0.6/π, $n = 1$

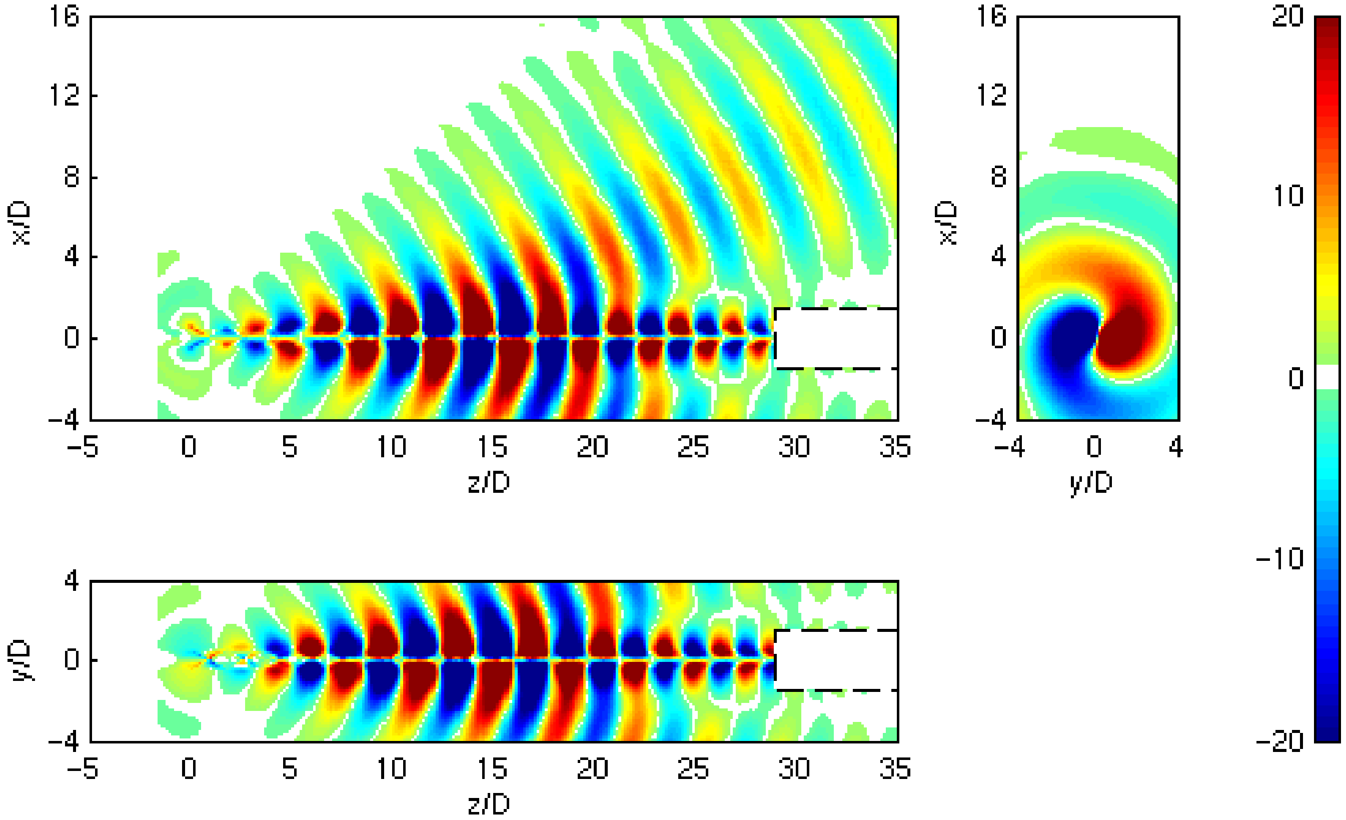

Sprint 3-D - Bailly (2004)

ONERA - ECL, Piot *et al.*, *Int. J. Aeroacoustics* (2006)

Radiation and refraction of sound waves through a 2-D shear layer

(4th CAA workshop, NASA CP-2004-212954)

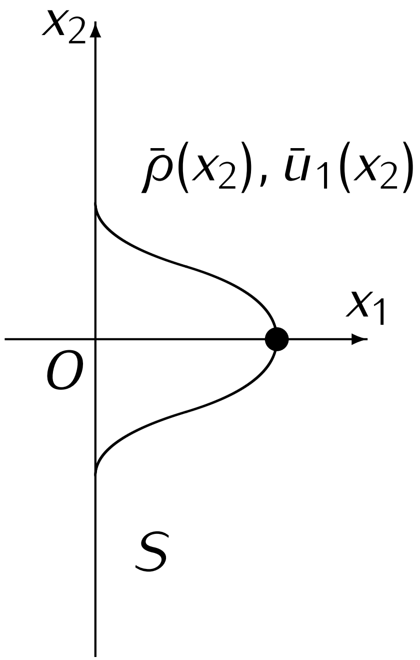

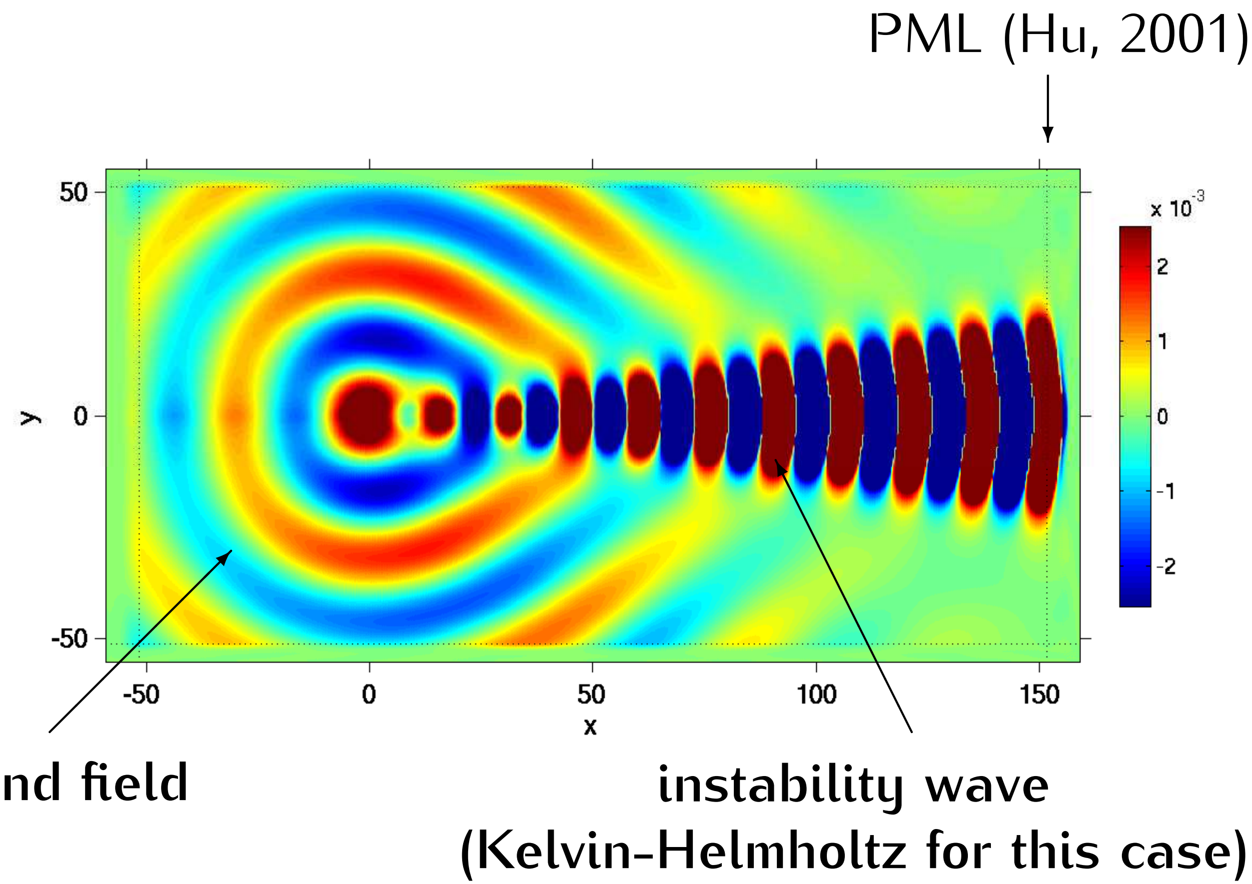

Linearized Euler's Equations

Thomas Emmert - 2004 - Diplomarbeit Technische Universtät München - ECL

- **Interaction between shock-cell structure and instability waves**
  Tam *et al.* (1982, 1985)

  instability waves $u_t \sim e^{i(\alpha x - \omega t)}$ where $\alpha \simeq \omega / U_c$

  periodic shock-cell structure $p_s/p_\infty = \sum_{n=1}^{\infty} A_n \phi_n(r) \cos(k_n x)$ (vortex sheet model, Prandtl 1904 and Pack 1950), that is $u_{sh} \sim \cos(k_{sh} x)$

- Perturbations are given by their product

$$u_t u_{sh} \sim \underbrace{e^{i[(\alpha - k_{sh})x - \omega t]}}_{W^-} + \underbrace{e^{i[(\alpha + k_{sh})x - \omega t]}}_{W^+}$$

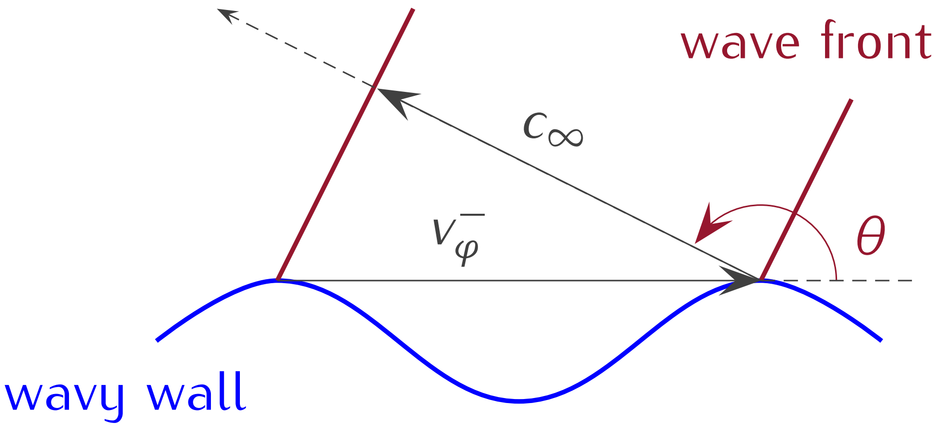

phase velocity of waves W^-
$v_\varphi^- = \omega / (\alpha - k_{sh})$

$k_{sh} \geq \alpha \Longrightarrow v_\varphi < 0, v_\varphi < -c_\infty$
$\cos\theta = c_\infty / v_\varphi^-$

- Narrow-band acoustic spectra in dB/St

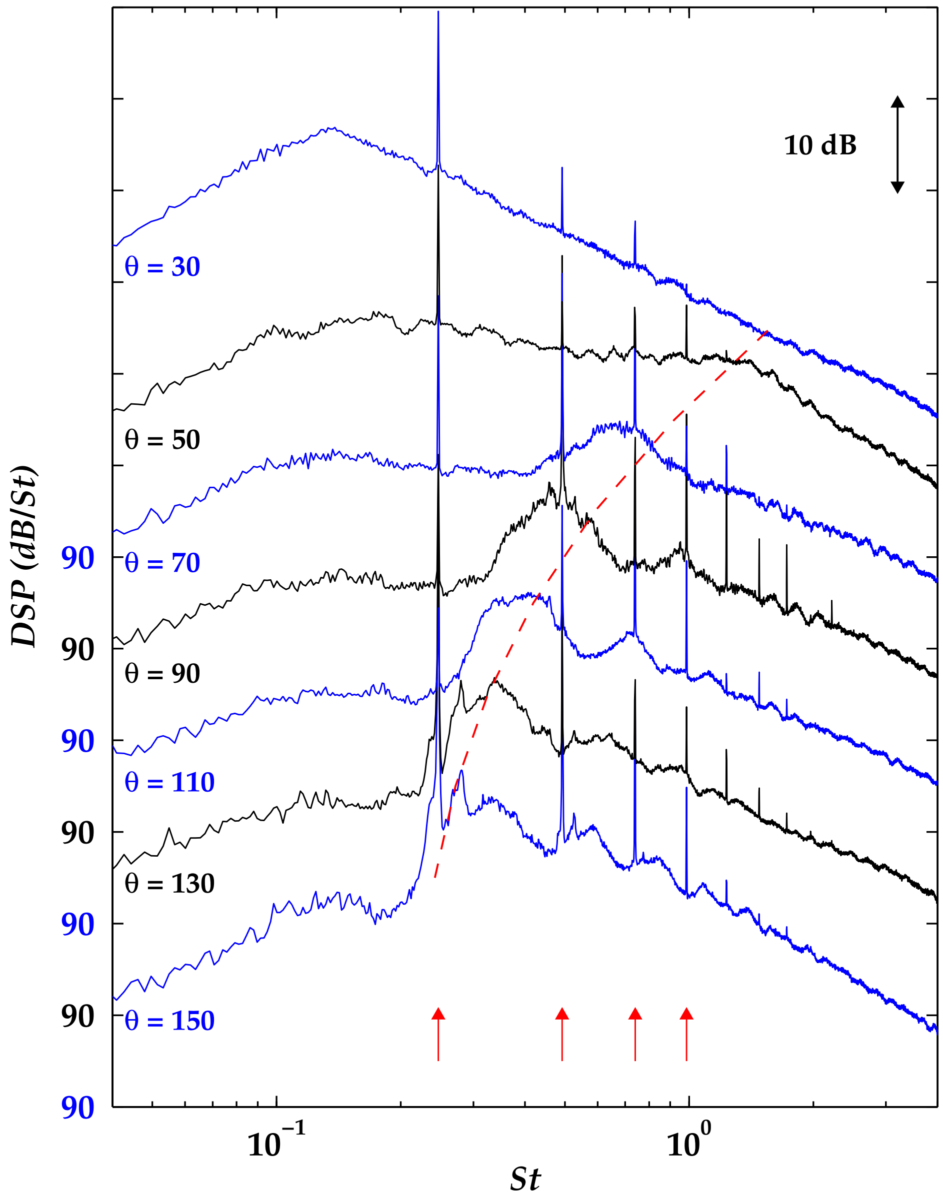

NPR = 3.68 $M_j = 1.50$ $M_d = 1$

$r = 53.2 D_p$

André *et al.* (2011)

↑ harmonics of screech tone

– – – Tam's model for BBSAN

$$\mathrm{St}_e = \frac{u_c (D_e / u_e)}{L_s (1 - M_c \cos\theta)}$$

- **Statistical approaches (RANS)**
  Supersonic underexpanded jet with flight effects
  $M_j = 1.35$ (NPR $= 2.97$, convergent nozzle), $M_f = 0.4$
  elsA solver, $k_t - \omega -$ SST (ONERA)

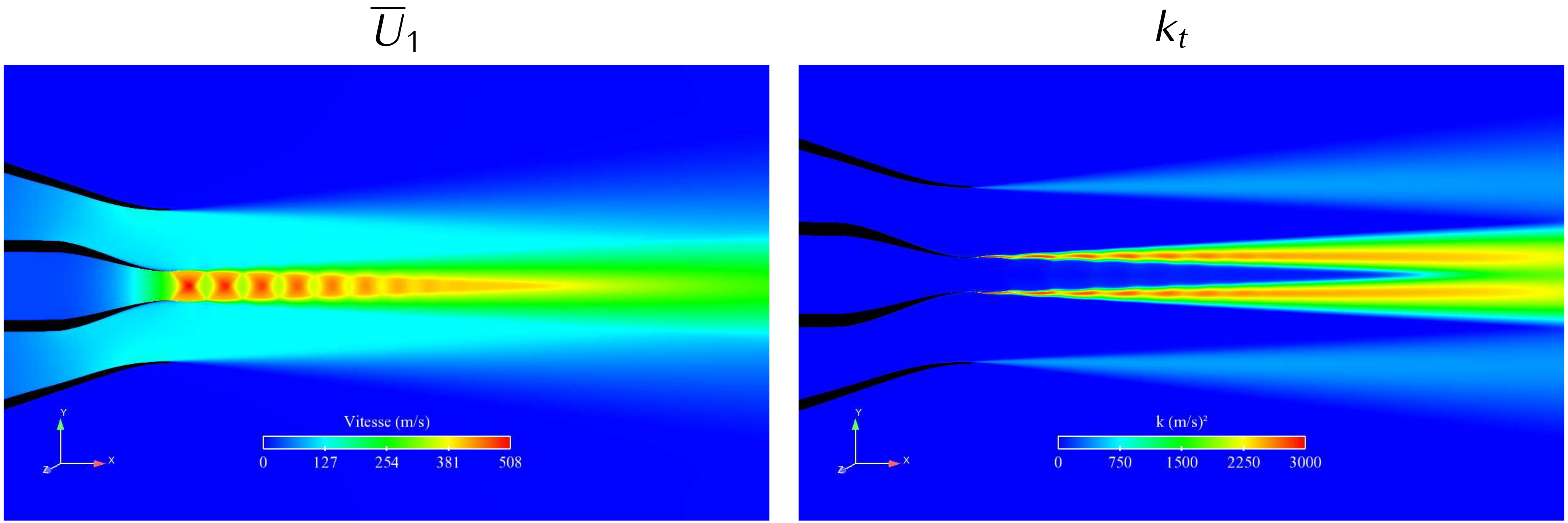

Cyprien Henry, SNECMA (2011)

Morris & Miller, 2010, *AIAA Journal*, **48**(12), 2931-2944
Miller, 2014, *AIAA Journal*, **52**(10), 2143-2164

- DNC of a screeching plane jet

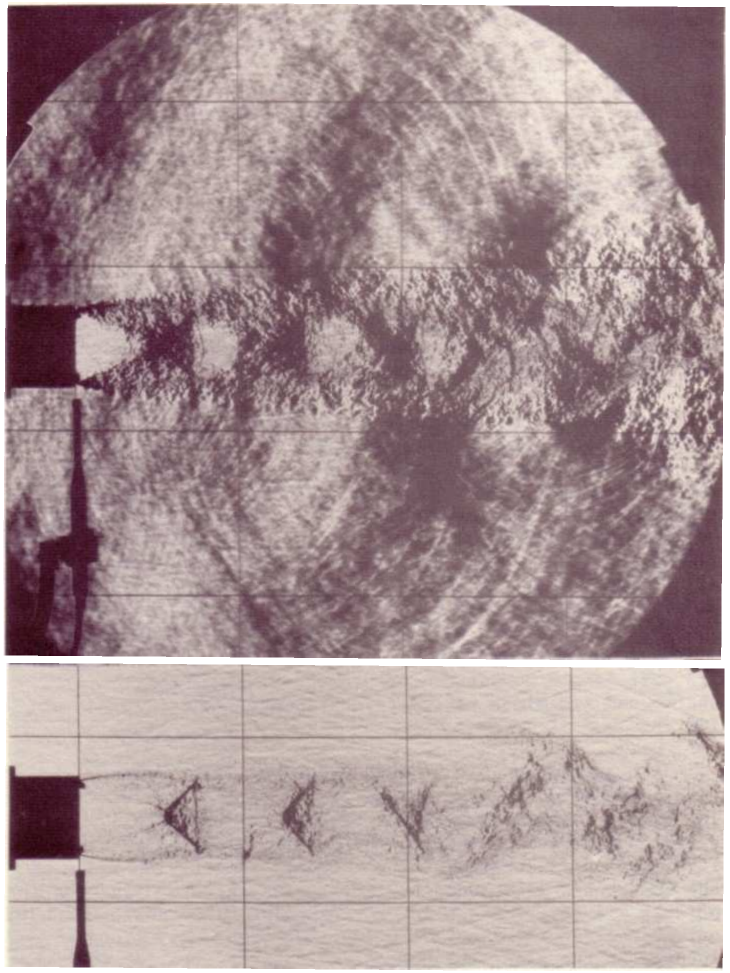

$$p_R/p_\infty = 2.48,\ D = 5.76 \text{ cm}$$
$$p_e/p_\infty = 2.48,\ \mathrm{M}_j = 1.67$$

Westley & Wooley, Prog. Astro. Aero., 43, 1976

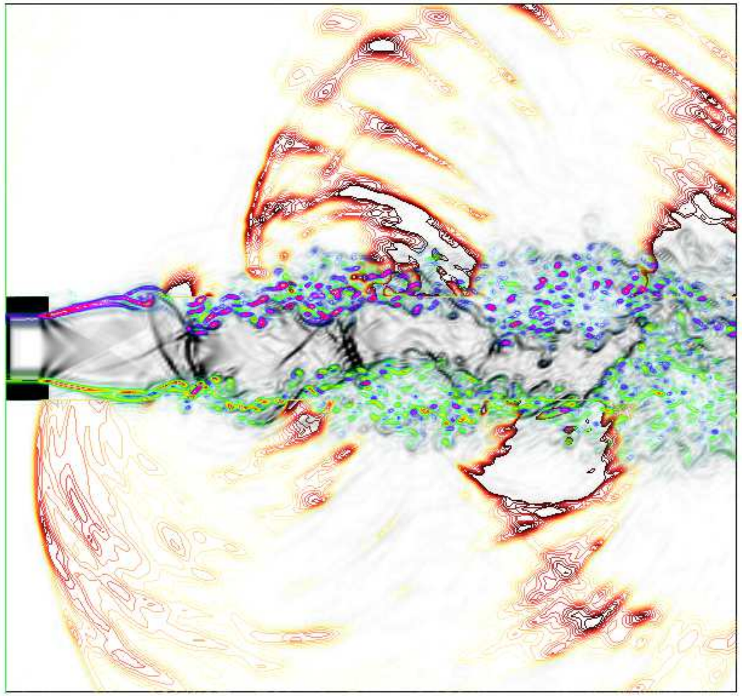

Numerical simulation of screech tones in a underexpanded plane jet

$$M_j = 1.55 \ \&\ Re_h = 6 \times 10^4$$
$$p_e/p_\infty = 2.09$$

Berland, Bogey & Bailly, *Phys. Fluids*, 19, 2007

Concluding remarks : jet noise reduction

(see also lecture notes)

Promoting mixing

... but it does not automatically lead to noise reduction !

High-bypass-ratio nozzle (cfm56 type)
chevrons on the fan and core nozzles
(Loheac *et al.*, SNECMA, 2004)

QTD2 - Boeing - NASA
AIAA Paper 2006-2720

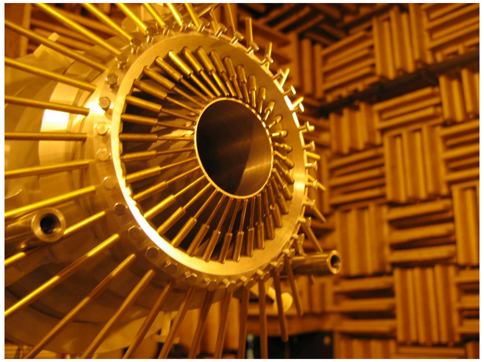

Castelain *et al.*
AIAA Journal, 2008, 45(5)

Saiyed *et al.*, J. E., 2003, *AIAA Journal*
Loheac *et al.*, AIAA Paper 2004-3044
Callender *et al.*, 2005 & 2008, *AIAA Journal*

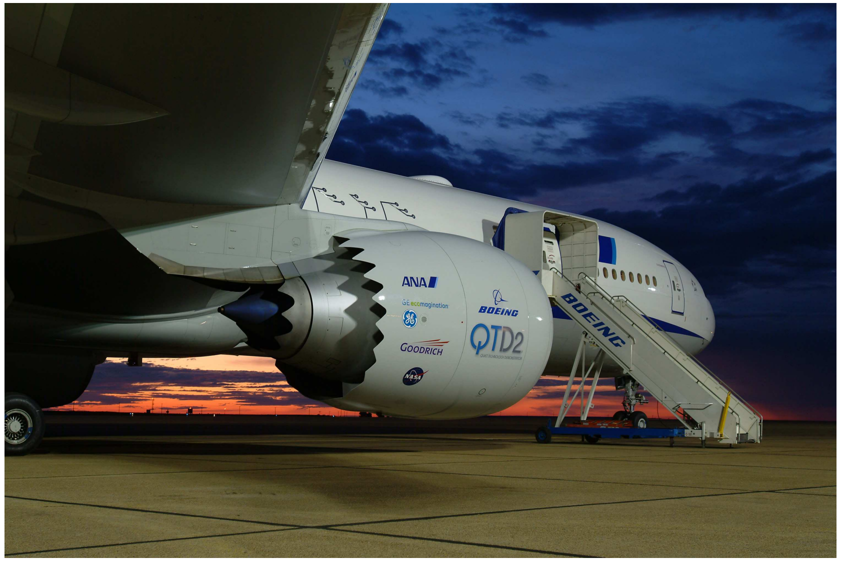

Vortex generators : interpretation

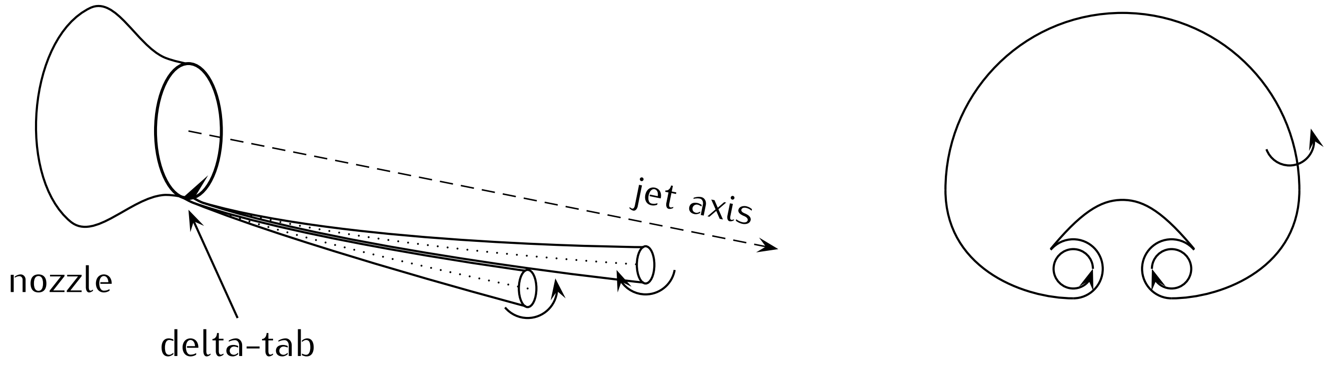

Sketch of the formation of a pair of counter-rotating streawise vortices
from a single delta or triangular tab mounted on a nozzle,
and front view of vorticity field in a cross-section of the jet flow.
Samimy *et al.* (1993), Zaman *et al.* (1994)

- **Variable geometry or smart chevrons**
  Calkins *et al.* (2006)

A GE-115B engine with "smart" metals installed is shown during preparations for flight tests on the Boeing 777-300ER Quiet Technology Demonstrator 2 airplane.

A look at the inner workings of the variable-geometry chevron. Each chevron includes three nickel-titanium actuators.

« ideal scenario »

- Static chevrons used on the core nozzle to reduce cabin noise induced by shock cell structure during cruise conditions without thrust penalty,
- Smart chevrons only immersed into the fan flow during take-off for preserving airport community, and then retracted for thrust performance.

- **Fan chevron versus core chevron**

  Experimental study by SNECMA at CEPRA 19 (2010)

(BPR = 9)

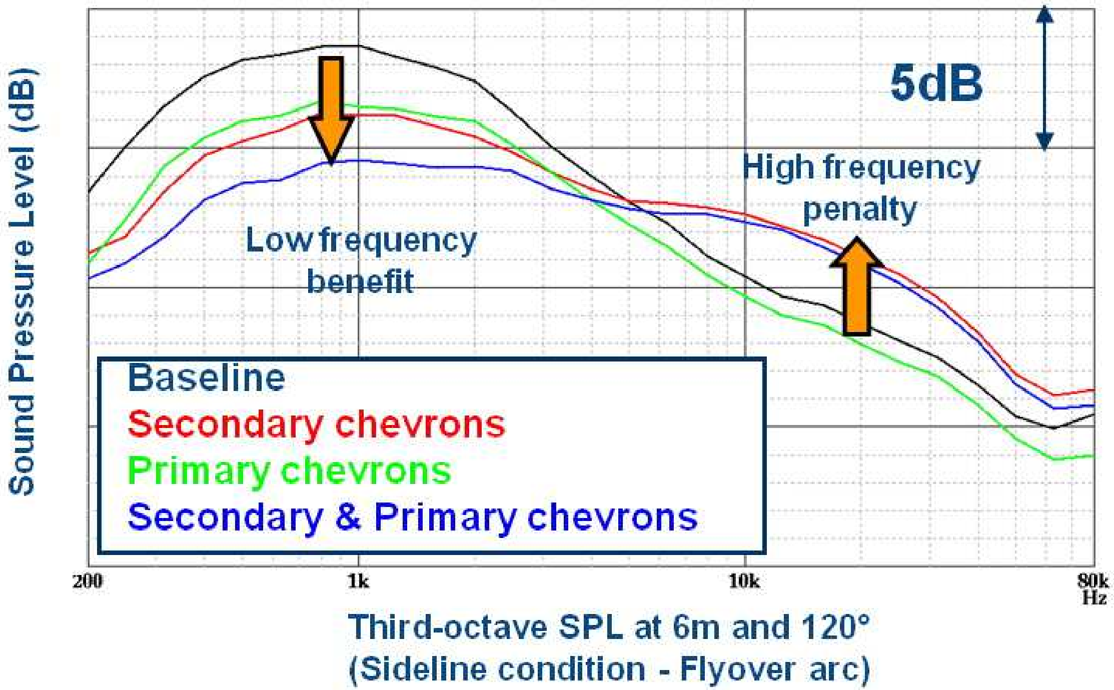

– decrease of low-frequency noise component, but penalty with fan-chevrons in high-frequency range ; balance : gain of $0.7 - 0.9$ EPNdB

– penalty for the nozzle thrust coefficient, $C_T \simeq 0.25\% - 0.30\%$

– shock-cell noise (cabin noise) reduced in cruise conditions with secondary chevrons

B787-8 chevrons

Boeing 787-8, Trent 1000 / GEnx
(Bourget Air Show, June 2011, B. André)

Internal mixer

Close-up of a CFM56-5C engine powering the Airbus A340 airliner.
The fan diameter is 1.85 m, the bypass ratio is about 6.5, and a lobed exhaust ejector / mixer system is used to reduce the core jet speed inside the duct nacelle.
Courtesy of Terence Li, photographer (2008).

- Towards Ultra High Bypass Ratio (UHBR)
  - Improvement in η_p (and thus noise) through increase in BPR (partly induced by optimization of the thermal efficiency)
    from $1 \leq \text{BPR} \leq 2$ in the 1960's to $7 \leq \text{BPR} \leq 9$ in the 1990's

    e.g. CFM International LEAP (LEAP-X, Airbus A320neo) BPR $= 10$
  - Larger fan diameter (limited by ground clearance constraints)

    $\leadsto$ drawbacks : weight of engine and nacelle, nacelle drag, installation effects, other sources ...

    thiner & shorter nacelles, geared turbofan (to come), ...
    BPR ≤ 20
  - Technical innovations (for all the aircraft noise sources)

Counter-rotating open rotor (CROR)

open rotor or propfan : the fan is not within the nacelle !

high flight Mach numbers : CROR (second rotor removes swirl of first rotor)

Boeing 7J7 / GE36 UDF (UnDucted Fan) - 1985 / MD-80 BPR $\simeq$ 35

Antonov An-70 (1994)

Counter-rotating open rotor (CROR)

Clean Sky Project : modern open rotor, BPR $\simeq 60$
drawback : cabin noise (and probably noise for larger aircrafts)

Snecma's SAGE 2 demonstrator is planned for flight testing
on a modified A340-600 in 2016.

- **Blended wing body**

Boeing X-48 Blended Wing Body (Cranfield Aerospace, Boeing, NASA) first flight tests 2007, 8.5 percent scale (7 m), remotely piloted (X48-B, X48-C)

- **Improprobable scenarios**
  - New large supersonic transport (SST)
    environmental concerns, sonic boom (use of supersonic speeds only to the oceans), no propulsion system available today
  - Alternative fuel, hydrogen (cryogenic liquid H_2 would occupy 4 times the volume of kerosene)

Concluding remarks